

Barrier properties of stratum corneum lipid model membranes based on ceramide [AP] and [EOS]

Dissertation

zur Erlangung des akademischen Grades
doctor rerum naturalium (Dr. rer. nat.)

vorgelegt der

Naturwissenschaftlichen Fakultät I
Biowissenschaften

der Martin-Luther-Universität Halle-Wittenberg

von

MSc. Pharm. Michal Ochalek

geboren am 5. März 1984 in Szamocin (Polen)

Gutachter

1. Prof. Dr. Dr. h.c. Reinhard Neubert
2. Prof. Dr. Johannes Wohlrab
3. Prof. Dr. Christel Müller-Goymann

Tag der öffentlichen Verteidigung: 29.08.2012

Table of contents

Chapter 1	Introduction	6
Chapter 2	The stratum corneum – its composition, organization and function....	9
2.1	The organization and function of the human skin.....	9
2.2	The stratum corneum	11
2.2.1	Penetration routes through the stratum corneum	13
2.2.2	The stratum corneum intercellular lipid matrix composition	14
2.2.3	The stratum corneum intercellular lipid matrix organization	17
Chapter 3	Drug delivery into the skin.....	22
3.1	Enhancement of drug penetration into the skin	22
3.2	In vitro diffusion and permeation studies.....	23
Chapter 4	Basic principles of experimental techniques applied	26
4.1	X-ray diffraction	26
4.1.1	Small angle X-ray diffraction (SAXD).....	27
4.2	Vibrational spectroscopy	28
4.2.1	ATR-FTIR diffusion cell	29
4.2.2	Confocal Raman imaging	31
4.3	Environmental scanning electron microscopy	32
4.4	Analytical separation techniques	33
4.4.1	High performance thin layer chromatography.....	33
4.4.2	High performance liquid chromatography	34
4.4.3	Capillary electrophoresis	36
	References	38

Chapter 5	Characterization of lipid model membranes designed for studying impact of ceramide species on drug diffusion and penetration	45
Chapter 6	SC lipid model membranes designed for studying impact of ceramide species on drug diffusion and permeation, Part II: Diffusion and permeation of model drugs.....	64
Chapter 7	SC lipid model membranes designed for studying impact of ceramide species on drug diffusion and permeation, Part III: Influence of penetration enhancer on diffusion and permeation of model drugs	82
Chapter 8	Summary and perspectives	102
Chapter 9	Zusammenfassung und Ausblick	106
	List of Publications	111
	Curriculum Vitae	114

Abbreviations and Symbols

[AP]	α -hydroxy phytosphingosine
ATR	attenuated total reflection
CE	capillary electrophoresis
CZE	capillary zone electrophoresis
Cer	ceramide(s)
Chol	cholesterol
ChS	cholesterol sulfate
d	lamellar repeat distance
d_p	penetration depth
D	diffusion coefficient
e.g.	<i>exempli gratia</i> (“for example”)
EOF	electroosmotic flow
[EOS]	ω -hydroxy sphingosine
ESEM	environmental scanning electron microscopy
FFA	free fatty acid
FT	Fourier transform
HPTLC	high performance thin layer chromatography
i.a.	<i>inter alia</i> (“among other things”)
i.e.	<i>id est</i> (“that is”)
IR	infrared
J	steady-state flux
$K_{m/d}$	partition coefficient between membrane and donor
k_p	permeability coefficient
λ	wavelength
L	membrane thickness (diffusional pathlength)
LPP	long periodicity phase
m/m	mass/mass percentage
MIR	mid-infrared
n	refractive index
NA	numerical aperture

OA	oleic acid
PA	palmitic acid
PBS	phosphate-buffered saline
q	scattering vector
R_f	retention factor
RP-HPLC	reversed-phase HPLC
SAXD	small angle X-ray diffraction
SC	stratum corneum
SEM	scanning electron microscopy
SPP	short periodicity phase
TEM	transmission electron microscopy
T_L	lag-time
θ	scattering angle
u	concentration
UV	ultraviolet
ν	wavenumber
v/v	volume/volume percentage
x	space coordinate

The rest of abbreviations and symbols is explained in relevant chapters.

1 Introduction

The skin is the largest organ of the human body in terms of area and mass. It covers an area of approximately 1.7 m² and constitutes about 10% of the body mass of an average adult person [1]. The skin provides many vital functions. Its principal function is to separate the body fluids and tissues from the external environment and to act as a protective barrier against harmful outside factors like chemicals, pathogens, UV-radiation, temperature, as well as against uncontrolled water loss. It plays also a crucial role in the regulation of body temperature (perspiratory function of sweat glands). The sensing function of the skin (reception of external stimuli such as pressure, pain and heat) is of major importance for the prevention of severe damage of the human body caused by e.g. too long exposure of the skin to the heat source. Some of the minor functions of the human skin are the synthesis of Vitamin D (as a result of a photochemical reaction taking place within the keratinocytes), the elimination of biochemical wastes (in glandular secretions) and the participation in the immune answer of the human body (Langerhans cells present in the skin are an early-warning component of the immune system) [2-4].

The fundamental function of the skin, the skin barrier function, has been of major interest for decades. First, it was discovered that it is provided by the outermost layer of the skin, the stratum corneum (SC), and the barrier properties result from the unique composition and organization of the SC [5]. Later, the SC intercellular lipid fraction was proposed to play a key role in the formation and maintenance of the skin barrier [6]. This discovery led to many studies trying to elucidate the organization of the SC intercellular lipid matrix. As a consequence, a number of theoretical models of the SC lipid matrix organization, along with the most important the *stacked monolayer* model, the *domain mosaic* model, the *sandwich* model, the *single gel phase* model and the most recent *armature reinforcement* model, were suggested [7-12]. However, none of these models clarifies all structural aspects of the human SC organization.

The semipermeable character of the SC is responsible, on the one hand, for the protection against exogenous influences and desiccation, and, on the other hand, limits the penetration of drugs into the skin, both endodermal (the local treatment of skin diseases) and transdermal drugs (the systemic effect, i.e. the drug is taken up by the systemic circulation from the dermis after crossing the SC) [13]. The low ability of drugs to pass the SC barrier constitutes a major problem and, at the same time, a challenge in the

dermal/transdermal administration of drugs. This administration route offers many advantages when compared to other more conventional ways of drug administration (e.g. oral), namely the avoidance of the first pass effect in the liver, the reduction of side effects, etc. In order to facilitate the absorption of topically applied drugs, the skin barrier function needs to be temporarily weakened by the use of physical (e.g. sonophoresis, iontophoresis, electroporation) or chemical (application of penetration enhancers) methods [14]. Nevertheless, the mechanisms of action of the drug penetration enhancement methods, especially modes of action of penetration enhancers, and their impact on the SC structure are still not well understood.

The molecular organization of the SC lipid matrix, as well as the function of each lipid species in the formation and maintenance of the SC barrier, are not yet fully explained. A better comprehension of the SC lipids interactions is crucial for the elucidation of the impact of all SC lipid species, especially ceramides, on the SC barrier properties. In former studies focused on the investigation of the SC lipid organization, native SC lipids isolated from the mammalian skin and lipid model membranes created from the extracted SC lipids were used [15-23]. Since native SC membranes are very complex, the use of such SC systems reduces the possibility to relate the differences in the SC lipid composition to the alterations in the SC molecular organization. A perfect solution to this problem is the use of SC lipid model membranes composed of artificial SC lipids as they offer many advantages over the native ones. First of all, they can help to overcome problems like the limited availability and high inter- and intra-individual variability of native SC membranes [9]. Furthermore, the use of well-defined synthetic SC lipid model membranes offers the possibility to alter their composition systematically, hence it allows to study and elucidate the role of each individual lipid species in the SC intercellular lipid organization and barrier function. In the recent studies, where artificial SC lipid systems were used [11, 12, 24-28], the focus was placed on the investigation of the SC lipid composition–organization relationship. However, no direct information about the relation between the SC lipid composition/organization and the SC barrier function was acquired. This thesis aims at getting a better insight into the SC intercellular lipid matrix composition/organization–barrier function relationship. The purpose is to relate the changes in the organization of the SC lipid model membranes, on a molecular level, to modifications in their barrier function.

In the first part of this thesis, the current status of knowledge on the SC composition and organization will be presented (Chapter 2). In Chapter 3, the methods of drug penetration enhancement into the skin, as well as the use of *in vitro* diffusion and

permeation experiments in the dermal and transdermal drug delivery studies will be discussed. In Chapter 4, the fundamental principles of experimental techniques employed for the purpose of this work will be described.

In the second part, the following objectives of this thesis will be elaborated and discussed:

- (i) Preparation of artificial SC lipid model membranes on a porous substrate to enable the conduct of *in vitro* diffusion and permeation studies of model drugs (Chapter 5).
- (ii) Characterization and standardization of SC lipid model membranes prepared on the porous substrate by means of various analytical techniques, i.a. small angle X-ray diffraction, high performance thin layer chromatography, environmental scanning electron microscopy and confocal Raman imaging (Chapter 5).
- (iii) Diffusion and permeation studies of model drugs through SC lipid model membranes designed for investigating the relation between their composition and the barrier function (Chapter 6).
- (iv) Investigation of the influence of the penetration enhancer on the barrier properties of the SC lipid model membranes (Chapter 7).

2 The stratum corneum – its composition, organization and function

2.1 The organization and function of the human skin

The skin is composed of three distinct layers: the outermost epidermis, the dermis and the innermost hypodermis (the subcutaneous fat layer) [29, 30]. Its structure is presented in Fig. 1.

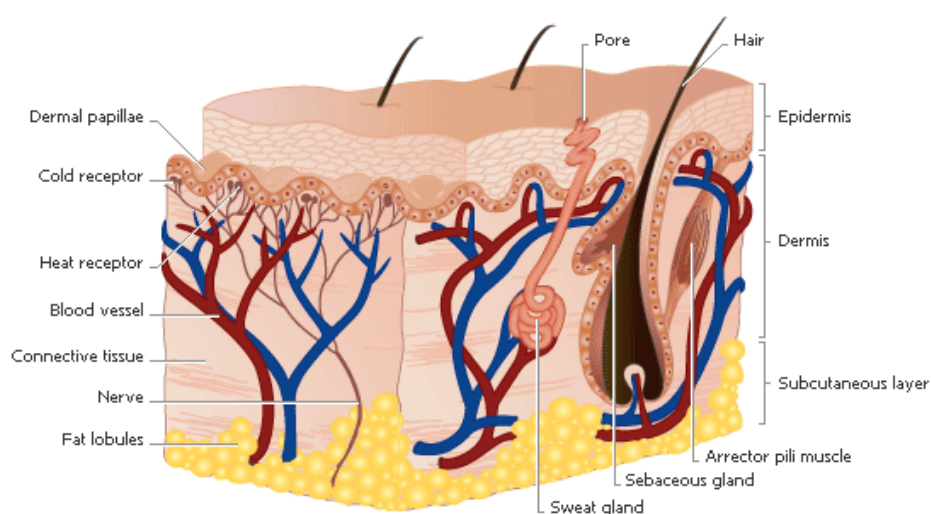


Fig. 1. Structure of human skin (adapted from [31]).

The hypodermis (subcutis) is a connector between the overlying dermis and the body tissues situated underneath. It is typically several millimeters thick and its thickness depends on the number of adipocytes (cells storing fat) located within it. The subcutis provides isolation and, therefore, protection against cold and physical shock. It contains principal blood vessels and nerves, which traverse to the overlying layers of the skin [32].

The next skin layer, lying over the hypodermis, is the dermis (corium). It is 1–5 mm thick [33] and consists of a connective tissue with collagen and elastin fibers embedded in a mucopolysaccharide gel [34]. The collagen fibers provide support to the skin and the elastin ones – flexibility. There are numerous structures embedded within the dermis such as blood and lymphatic vessels, nerve endings, hair follicles, sebaceous and sweat glands.

The outermost layer of the human skin, the epidermis, ranges from about 0.06 mm to about 0.8 mm in thickness (depending on the area of the body). It is a dynamic, self-

renewing tissue layer, where cells that are separated from the surface in consequence of the desquamation process, are replaced by new cells produced in its lowest layer [35]. There are no blood vessels within this skin layer, hence transdermal drugs must permeate through the epidermis in order to get into the systemic circulation [32]. The epidermis can be divided into four histologically distinct layers: starting with the stratum basale at the dermo-epidermal interface, followed by the stratum spinosum, the stratum granulosum and the stratum corneum. A schematic diagram of the epidermal layers as well as a presentation of the changes within the cells undergoing during the cell differentiation are displayed in Fig. 2.

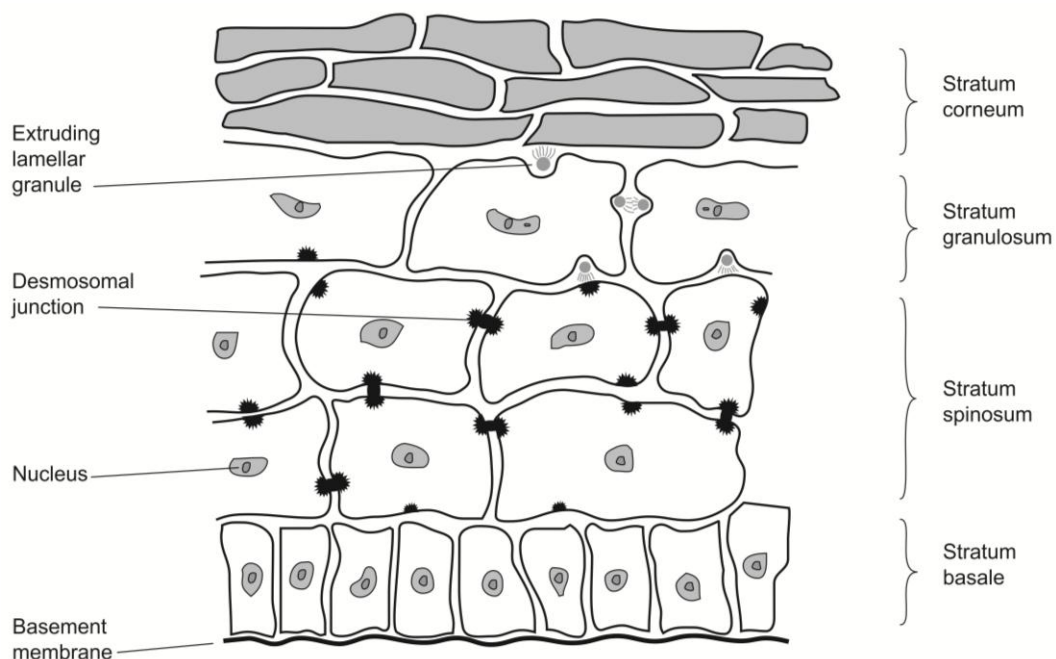


Fig. 2. Schematic representation of the structure of the epidermis and its cell differentiation (adapted from [32]).

The stratum basale, also known as the stratum germinativum or the basal layer, is the innermost epidermal layer. It is composed of a single layer of columnar basal cells (keratinocytes), attached to the basement membrane by hemidesmosomes. Keratinocytes, the major cell type within the viable epidermis, contain all typical cell organelles such as nucleus, mitochondria and ribosomes [36]. A constant mitosis of these cells in the basal layer compensates a loss of cells from the skin surface, causing a renewal of the epidermis. The other cells present in the basal layer are: melanocytes (synthesizing skin pigment melanin), Langerhans cells (antigen-presenting dendritic cells) and Merckel cells (responsible for cutaneous sensation) [3].

The next layer of the epidermis, the stratum spinosum (also referred to as the spinous layer or the prickle cell layer) is made up of 2–6 rows of keratinocytes that start to change their morphology and begin to differentiate. The synthesized keratin filaments tend to aggregate and create tonofilaments. As a result of the condensation of tonofilaments, structures called desmosomes are formed. They act as the connectors between the cell membranes of the adjacent keratinocytes, and hence are responsible for keeping the integrity of the tissue [37, 38]. In the upper layers of the stratum spinosum, the keratinocytes contain two types of intracellular granules: keratohyalin granules and membrane-coated granules (also known as lamellar bodies or Odland bodies [39]). The Odland bodies are composed predominantly of polar lipids (i.e. phospholipids, glucosylsphingolipids, free sterols) and catabolic enzymes (i.e. hydrolases) and their contents are of major importance for the formation of intercellular lipid lamellae within the stratum corneum [40-42].

By the continuation of the cell differentiation process and by moving upward, the keratinocytes reach the stratum granulosum (or the granular layer), which consists of 1–3 layers of highly differentiated cells that start to flatten. Their viable cell constituents (such as nuclei) are degraded by enzymes, and the Odland bodies, containing the lipid precursors for the intercellular lamellae of the SC, migrate to the apical part of the keratinocytes, being ready for a fusion with the cell membrane. As the cells approach the stratum granulosum–SC interface, the contents of the lamellar bodies are secreted via exocytosis to the intercellular space, where hydrolases transform them to ceramides, free fatty acids, cholesterol and cholesterol esters [6, 43].

2.2 The stratum corneum

The outermost layer of the skin, the stratum corneum (SC, also referred to as the cornified layer or the horny layer), is thought to constitute the main penetration barrier for topically administered drugs and other substances, including water [44, 45]. It consists of 10–25 layers of parallel to the skin surface dead, anucleated corneocytes (keratinocytes in a terminal stage of cell differentiation), and ranges from 10 to 15 μm in thickness when dry, however, swells to several times this thickness in a fully hydrated state [46]. The elongated and flat corneocytes are embedded in a lipid matrix. This characteristic organization of the SC is often described as the “brick and mortar” structure

(Fig. 3), where the corneocytes resembling the bricks are embedded in the mortar of the SC intercellular lipid bilayers [47-50].

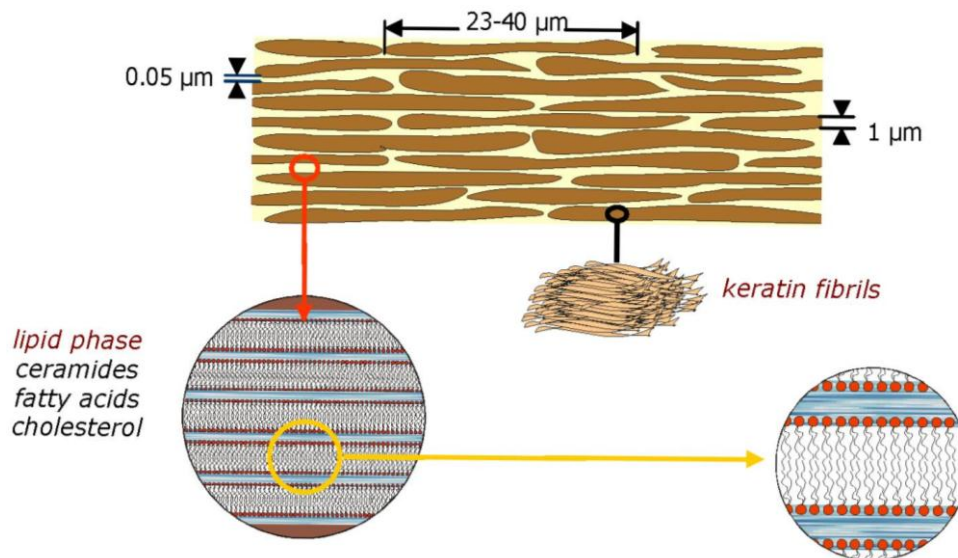


Fig. 3. Organization of the stratum corneum with a characteristic "brick and mortar" structure (adapted from [51]).

The corneocytes, comprising keratin fibrils, are surrounded by a cornified cell envelope, which is formed during the terminal stage of keratinization and is composed predominantly of loricrin, involucrin and cornifine that are cross-linked as a result of the action of calcium dependent transglutaminases [52, 53]. The cornified cell envelope is a rigid structure, highly resistant to proteolytic enzymes and organic solvents. Its proteins (mainly involucrin) are covalently bound to long-chain ω -hydroxyacyl moieties of ceramides of a lipid envelope [54-56]. The interaction between the cornified cell envelope and the lipid envelope stabilizes the SC structure and provides the cohesiveness of corneocytes with the SC intercellular lipids. The corneocytes are kept together by corneodesmosomes, which are enzymatically degraded during the desquamation process [30, 57]. Properly functioning desquamation process is of major importance for the maintenance of the normal skin structure and function. It depends on the hydration state of the SC and the content of cholesterol sulfate in its upper layers. It was found that desquamation is inhibited in the excess of cholesterol sulfate and at low environmental humidity [58]. The mechanism of the inhibition of the cell shedding process is not yet fully explained, however, most probable reason is the reduced activity of desquamatory enzymes at lower water content and/or higher cholesterol sulfate content [59].

Disturbances in the desquamation process lead to the skin disorders like recessive X-linked ichthyosis (caused by a deficiency of a cholesterol sulfatase) [60, 61].

The unique composition of the SC contributes to its barrier function. It consists in 75–85% (the SC dry weight) of proteins, whereas lipids constitute only 5–15% [34]. However, the proteins are mainly to be found in the corneocytes, enzymes and the cornified cell envelope, while the lipids build up the lipid matrix located in the SC intercellular space.

2.2.1 Penetration routes through the stratum corneum

Molecules can penetrate through the normal intact skin using two different penetration routes: the transappendageal route and the transepidermal route (Fig. 4). The former can be divided into the transglandular (via sweat ducts) and the transfollicular (via openings of hair follicles and sebaceous glands) route. It is thought to be less important than the transepidermal route, because of its relatively small area (~ 0.1% of the total skin area) when compared to the latter [62]. However, recent studies point out the importance of the shunt route for the transdermal drug delivery [63–65]. In the case of the transepidermal route, two pathways can be distinguished: the transcellular (also known as intracellular) and the intercellular. The intercellular route is considered to be more preferable pathway for most molecules, although it is tortuous (compounds penetrate through the intercellular lipid lamellae between corneocytes) and, in result, much longer than the transcellular one. The reason for that is a highly impermeable character of the cornified cell envelope, which molecules must pass frequently when using the transcellular pathway [66].

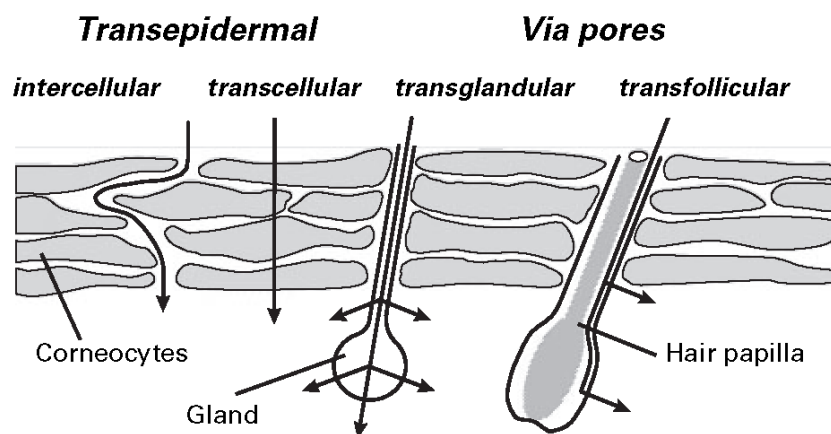


Fig. 4. Penetration routes through the stratum corneum (adapted from [67]).

Because of the lipophilic nature of the SC and the low water content, it is believed that the penetration of hydrophilic compounds is hampered when compared to the penetration of the lipophilic ones. However, recent studies suggest the existence of two distinct penetration pathways within the SC: lipophilic and hydrophilic one.

On the one hand, lipophilic molecules penetrate within the nonpolar tail-group regions of the SC lipid bilayers; on the other hand, hydrophilic molecules penetrate within their polar head group regions using the hydrophilic pathway [68]. Therefore, a further insight into the composition and organization of the SC intercellular lipids is crucial for better understanding of the human skin barrier function.

2.2.2 The stratum corneum intercellular lipid matrix composition

The key role in functioning of the skin barrier plays the lipid part of the SC. Furthermore, the SC barrier function is determined not only by the individual lipid species, but by the organization of different classes of lipid species and corneocytes [69]. As mentioned previously, the SC intercellular lipids originate from Odland bodies. Following the exocytosis of their contents to the intercellular space at the stratum granulosum–SC interface, phospholipids, glucosylsphingolipids and free sterols are enzymatically converted to less polar ceramides, free fatty acids and cholesterol esters that altogether form lipid lamellae [6, 43].

Therefore, ceramides (Cer), cholesterol (Chol) and long-chain free fatty acids (FFA) are the major lipid classes present in the SC intercellular space [70, 71]. Interestingly, the SC does not contain phospholipids, contrary to other biological barriers (e.g. cell membranes). The SC lipid composition varies inter- and intra-individually [9, 72, 73]. Disturbances of the skin barrier function caused by changes in the SC lipid composition can lead to skin diseases. Hence, the knowledge on the role each lipid class plays in the SC lipid barrier function is of great importance.

Ceramides (Cer) are the main constituents of the SC intercellular lipid matrix and are regarded as principal compounds in the formation and maintenance of the SC barrier function [56, 74]. Cer belong to structurally heterogeneous sphingolipids and are composed of a sphingoid base amide-linked to a long chain fatty acid. Only D-forms of Cer are present in the native SC. The results of a recent study indicate the existence of 12 classes of Cer that have been isolated from the human SC [75]. The original nomenclature of Cer was based on their polarity measured by the thin layer chromatography, where each Cer was assigned a number. The higher number of Cer, the more polar molecule

[76]. With the increasing number of identified Cer, this way of Cer labeling appeared to be unsatisfactory. Therefore, nowadays, more preferred and more frequently used classification of Cer is based on their molecular structure [77].

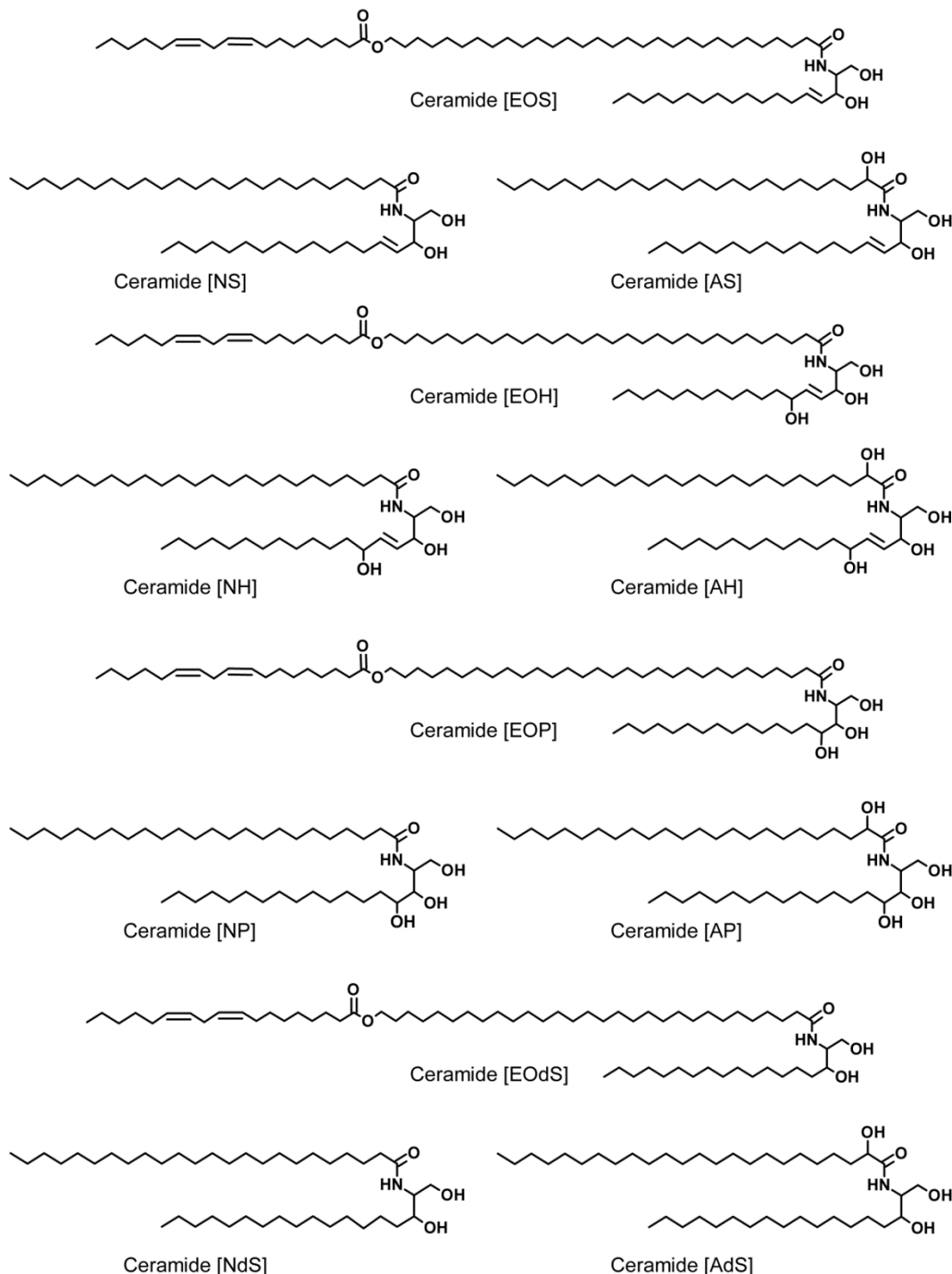


Fig. 5. Chemical structures of ceramides with their nomenclature according to [77].

Individual classes of Cer differ from each other by the type of a sphingoid moiety (sphingosine [S], phytosphingosine [P], 6-hydroxysphingosine [H] or dihydrosphingosine

[dS]) that is bound to a fatty acid moiety, which can be non-hydroxylated [N] or α -hydroxylated [A] with its chain length of mostly 24 to 26 carbon atoms. In the case of acylceramides that have unique, unusually long molecular structures, unsaturated linoleic acid is ester linked to ω -hydroxy fatty acid of 30–34 carbon atoms [EO] [78, 79]. The chemical structures of Cer found in the human SC are displayed in Fig. 5. As indicated above, the Cer have a significant impact on the SC barrier function, however, the role of each Cer class is not yet known or fully explained.

Cholesterol (Chol), which constitutes approx. 25% of the SC lipid mass [13], is the most abundant individual lipid species in the SC. The SC cholesterol is synthesized mainly in the epidermis. Its increased synthesis, as a result of skin barrier function disorders, returns to normal when barrier function is recovered [80], which confirms the importance of Chol for the maintenance of the SC barrier function. Chol molecule fits into the lipid bilayer with its hydrophobic steroid ring and an adjacent short aliphatic chain oriented towards the long hydrocarbon chains of Cer and FFA, while its hydroxyl group is located close to the polar head groups of Cer [81]. Of great importance is the right content of Chol in the SC intercellular lipid matrix. The optimal, for the SC barrier function, concentration of Chol is just under its solubility in the lipid lamellae (~ 30 mol% [82]).

Higher concentrations of Chol may cause the creation of discontinuities within lipid bilayers, as a consequence of the formation of pure domains of crystalline Chol. On the other hand, low content of Chol within lipid bilayers increases their lamellar ordering by promoting the *trans* conformation of hydrocarbon chains and reducing the tilt angle. This effect limits the mobility of the hydrocarbon chains, and hence decreases the permeability of the lipid membrane [83-85].

A minor component, in terms of concentration (typically 2–5% of the SC lipid mass), of the SC intercellular lipids is cholesterol sulfate (ChS). Despite its small content within the SC, it is considered to be a crucial factor in the desquamation process, where ChS is responsible for the inhibition of desquamatory enzymes. As mentioned before, the increased concentration of ChS in the SC, caused by the deficiency of sterol sulfatase, leads to recessive X-linked ichthyosis (a skin disorder with characteristic scaly appearance of the skin) [86, 87]. Interestingly, ChS improves the dissolution of Chol in lipid mixtures (phase separated Chol disappears after addition of ChS to the mixtures of Chol, Cer and FFA) [88].

Free fatty acids (FFA) present in the human SC are predominantly saturated, straight chained and constitute approximately 10% of the SC lipid mass [13]. The chain length of the SC FFA ranges from 16 to 30 carbon atoms with C22, C24 and C26 chains as

the examples of the most abundant species in the SC [73, 89]. The unsaturated FFA found in the SC are: oleic acid (C18:1) and linoleic acid (C18:2). The FFA are the only ionizable molecules, apart from ChS, within the SC, and this might be relevant for the formation of lipid lamellae [90]. The addition of FFA to the lipid mixtures increases the dissolution of Chol in the lamellar phases, as well as the fluidity of the lipids at higher temperatures. The importance of the FFA for the proper SC barrier function was confirmed in the study, where the recovery of the SC barrier was significantly improved after the addition of supplementary FFA [91].

2.2.3 The stratum corneum intercellular lipid matrix organization

The organization of the SC intercellular lipid matrix is of special interest, because of its great importance for the skin barrier function. The freeze fracture electron microscopy studies revealed that the SC intercellular lipids are organized in lamellar structures [92]. In other electron microscopy investigations, it was found that the SC intercellular lipids are arranged in repeat units composed of a broad-narrow-broad sequence of electron lucent bands with a lamellar periodicity of 130 Å [93]. Furthermore, small angle X-ray diffraction studies confirmed the presence of this characteristic phase in murine, pig and human SC [15, 20, 94]. Additionally, these studies revealed the existence of two lamellar phases in the SC intercellular lipid matrix, one with a periodicity of 130 Å (referred to as the long periodicity phase, LPP) and the other with a lamellar repeat distance of 60 Å (known as the short periodicity phase, SPP). The former is suggested to play a significant role in the SC barrier function. The LPP was also found in mixtures composed of isolated or synthetic SC lipids [18, 95]. It is thought that one of the requirements for the formation of the LPP is the presence of the acylceramide, Cer [EOS], in a proper ratio with other Cer, Chol and long-chain FFA [21]. Nevertheless, the results of recent studies show that the LPP was formed only when lipid mixtures consisted of synthetic Cer, Chol and FFA, while in the case of lipid mixtures composed of Cer isolated from the human SC, Chol and FFA, only the presence of the SPP was confirmed [88, 95, 96]. Therefore, the existence of the LPP in human SC *in vivo* is questionable. With the exception of some electron microscopy [7, 93] and small angle X-ray diffraction studies [15, 20, 94], its presence within human SC was not confirmed neither in cryo-transmission electron microscopy studies [97] nor in neutron diffraction studies [98]. Taking these various results into account, it can be assumed that the presence of the LPP within the SC lipid model membranes should not be

regarded as a confirmation of the correct method used for the preparation of the SC lipid model systems and their biological relevance.

Over the years, various theoretical SC models have been developed in order to describe the organization of the SC intercellular lipids. The assumptions of the SC lipid organization on which these models are based, as well as their suitability to explain the organization and processes occurring in the SC *in vivo*, are still vigorously discussed [7-12, 18, 21, 23-25, 27, 99-101]. The most relevant models of the SC lipid matrix organization are the *stacked monolayer* model, the *domain mosaic* model, the *sandwich* model, the *single gel phase* model and the most recent *armature reinforcement* model.

According to the *stacked monolayer* model (displayed in Fig. 6), alkyl chains of Cer in the stretched splayed chain conformation interdigitate, and Chol is uniquely distributed in different layers [7]. Moreover, two adjacent lipid bilayers may form a lipid monolayer by contributing lipid chains. Interestingly, this process is assumed to be reversible, so in result, each monolayer can be expanded into a lipid bilayer.

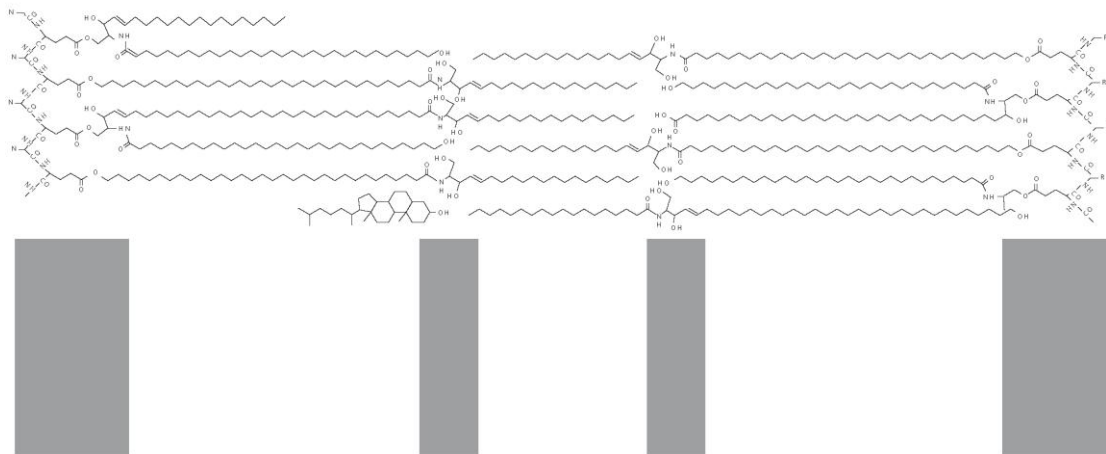


Fig. 6. The *stacked monolayer* model (according to [7]).

As stated in the *domain mosaic* model [8], the SC intercellular lipids create a multilamellar two-phase system with discontinuous lamellar crystalline gel domains embedded in a continuous liquid crystalline phase (see Fig. 7). The gel domains are surrounded by “grain borders” composed of lipids in the liquid crystalline state. This model assumes that the fluid character of these borders enables diffusion of hydrophilic and lipophilic compounds through the skin barrier.

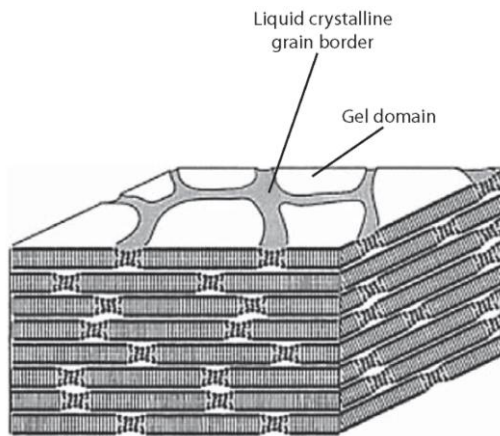


Fig. 7. The *domain mosaic* model (adapted from [10]).

Contrary to the *domain mosaic* model, where the crystalline and liquid domains are situated side by side in one layer, the *sandwich* model (Fig. 8) suggests that these domains are arranged in a trilayer [9]. Such lipid arrangement is in accordance with the broad-narrow-broad sequence of the LPP. A centrally situated liquid layer is formed predominantly by the unsaturated linoleate moieties of the acylceramides (Cer [EOS], Cer [EOH], Cer [EOP], Cer [EOdS]) and Chol. In the two neighboring layers, the crystallinity rises gradually due to the presence of less mobile saturated hydrocarbon chains. Because of a discontinuous character of the fluid phase located in the central unit, the substances permeating through the SC have to pass the crystalline lamellar region and partly diffuse through the more loosely packed lipid regions [100].

The *single gel phase* model (shown in Fig. 9A) differs significantly from the above described models. It suggests that a single and coherent lamellar gel structure, situated in the SC intercellular space, constitutes the skin barrier [10]. Moreover, neither the liquid crystalline and gel phases nor the crystalline phases with hydrocarbon chains arranged in hexagonal and orthorhombic lattice

are separated. The lipid arrangement proposed is also characterized by a low water content, a low degree of mobility and a dense packing of its constituents, which altogether results in a low water permeability. In contrast to the *domain mosaic* and the *sandwich* models, where Cer are organized only in the hairpin (two parallel oriented hydrocarbon chains pointing in the same direction) conformation, in the *single gel phase* model both hairpin and fully extended (hydrocarbon chains point away from a central head group in the opposite directions) conformations are present (Fig. 9B).

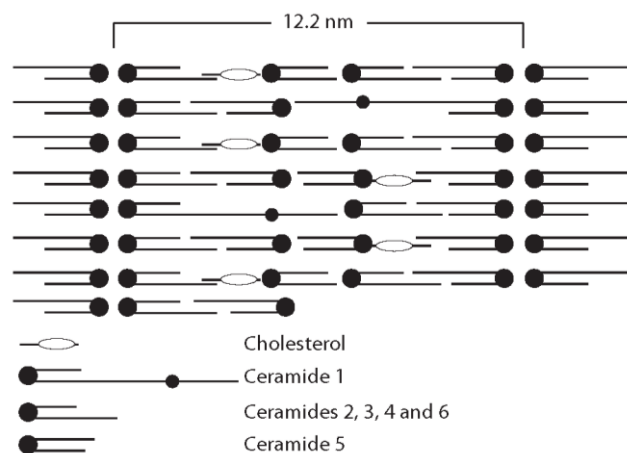


Fig. 8. The *sandwich* model (according to [21]).

All the theoretical models of the SC intercellular lipid matrix organization described above do not explain the changes in the SC lipid matrix after hydration with water excess. The most recent, so-called *armature reinforcement* model [11, 12] explains this phenomenon. In a partly dehydrated state, the bilayer leaflets are in the steric contact (the polar head groups of Cer from the adjacent bilayers are close to each other)

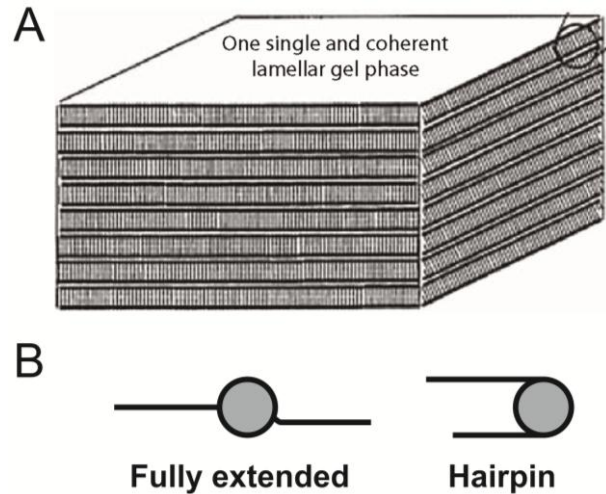


Fig. 9. (A) The *single gel phase* model (adapted from [10]), (B) Fully extended (or splayed chain) and hairpin (or one-sided) conformations of ceramides.

created by the fully extended conformation of the short chain Cer [AP], as presented in Fig. 10. The fully extended conformation of Cer [AP] is of great importance for the formation of a stable structure of the SC intercellular lipid matrix. It keeps together and tightens up the adjacent lipid bilayers and that results in the disappearance of the intermembrane space. Therefore, Cer [AP] can be considered here as an “armature”. An addition of water excess forces Cer [AP] to change its conformation from the fully extended to the hairpin conformation (the so-called chain-flip transition [11, 12]). Simultaneously, the intermembrane space is created between the polar head groups of Cer.

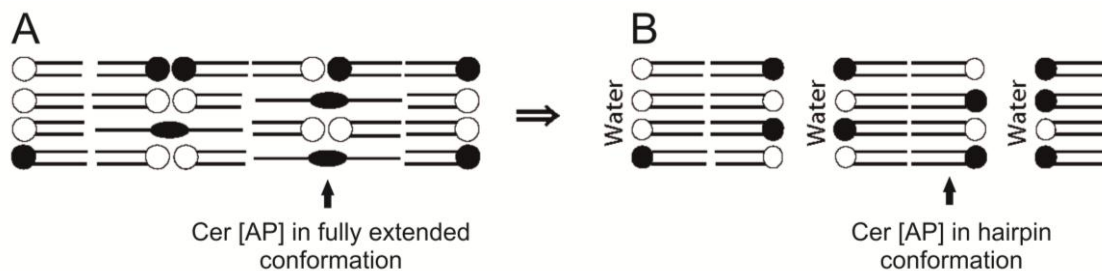


Fig. 10. The *armature reinforcement* model (modified from [12]); (A) partially hydrated membrane, (B) fully hydrated membrane after addition of water excess.

In conclusion, there are several theoretical models of the SC lipid matrix organization. However, the models proposed do not elucidate all structural aspects of the human SC organization. There are still many controversies, regarding this subject, that are

under discussion. A detailed description of the molecular organization of SC lipids, particularly of the function that each Cer species has in the formation and maintenance of the SC barrier, is not yet available. Moreover, a better understanding of the physical properties of the SC lipids and their interactions is crucial for the elucidation of the influence of all SC lipid species (especially each Cer species) on the barrier properties of the SC. In the first studies, native SC lipids isolated from the mammalian skin were used in order to investigate the SC lipid organization [15-19]. The SC lipids used there were only characterized in terms of their head group arrangement and the hydrocarbon chain length distribution. The use of such SC lipid systems limits the possibility to relate the alterations in the SC lipid composition to the changes in the SC molecular organization. Therefore, a new approach with well-defined artificial SC lipid systems produced as oriented multilamellar membranes was introduced [11, 12, 24-28]. The use of such systems can help to overcome obstacles like the ones listed above. Additionally, the impact of the individual lipid species, as well as the influence of external parameters such as temperature, humidity and penetration enhancers, on the SC lipid organization can be investigated on a previously unattainable level. Such approach allows also for a better extrapolation of the *in vitro* obtained results to the *in vivo* situation, including the possibility to study the impact of penetration enhancer molecules on the SC lipid organization on a molecular level, as well as to relate the changes in the SC intercellular lipid organization to a modification in its barrier function.

3 Drug delivery into the skin

3.1 Enhancement of drug penetration into the skin

The highly effective barrier properties of the SC limit the transdermal delivery of drugs. A way to overcome this limitation is the modulation of the drug penetration within the SC. There are a number of mechanisms of the temporary impairment of the SC barrier function. One approach to increase the drug penetration into the skin is the use of physical SC penetration enhancement techniques (i.a. phonophoresis, iontophoresis). The phonophoresis (also referred to as the sonophoresis) uses the ultrasound energy in order to enhance the penetration of drugs [102]. In the case of the iontophoresis, a small electric current is applied to the skin, what results in the facilitation of the drug penetration via electrophoresis, electroosmosis or enhanced diffusion [103]. Additionally to physical methods, a chemical penetration enhancement is of great importance for the modulation of the penetration of drugs after a topical application.

To the group of widely investigated chemical substances promoting the drug penetration into the skin (also known as penetration enhancers) belong water, alcohols (e.g. ethanol), glycols (e.g. propylene glycol), sulfoxides (e.g. dimethylsulfoxide), azone and its derivatives, urea and its derivatives, terpenes and terpenoids (e.g. d-limonene), pyrrolidones (e.g. N-methyl-2-pyrrolidone), cyclodextrins, surfactants (e.g. sodium dodecyl sulfate), fatty acids (e.g. oleic acid) and others (reviewed in [104, 105]). The mechanisms of the action of penetration enhancers are very complex and not yet fully understood. It is suggested that there are two distinct penetration pathways within the SC intercellular lipid matrix, namely hydrophilic one and lipophilic one [105]. The enhancers can influence either the arrangement of polar head groups of the SC lipids (i.e. the hydrophilic pathway) facilitating the penetration of hydrophilic drugs, or the molecular organization of their hydrocarbon chains (i.e. the lipophilic pathway), which results in the enhancement of the penetration of lipophilic drugs. However, the enhancers that affect the hydrophilic pathway, can also influence the ordering of the hydrophobic tails of the SC lipids and vice versa. It explains the improvement of the penetration of either lipophilic or hydrophilic drugs when using the enhancers for the hydrophilic and the lipophilic pathway, respectively [104-108]. Possible modes of the action of penetration enhancers are presented in Fig. 11.

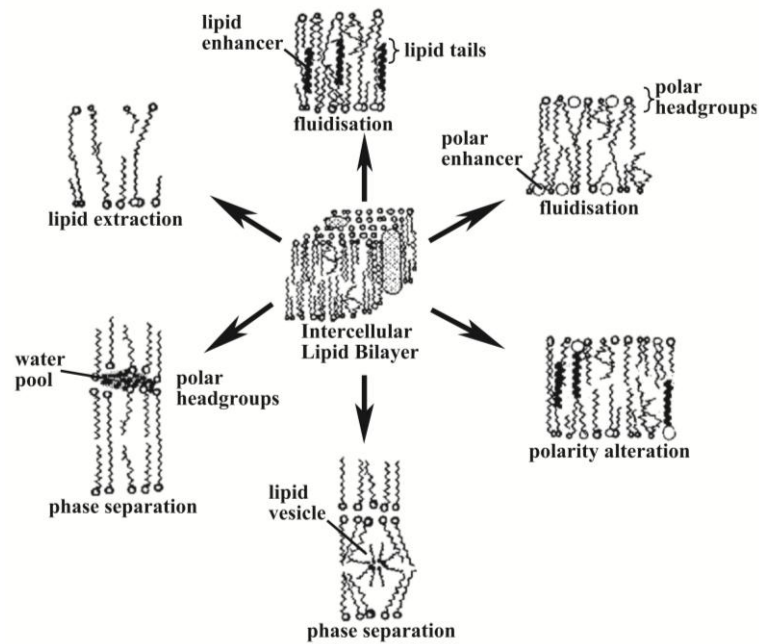


Fig. 11. Mechanisms of action of penetration enhancers on the SC intercellular lipid matrix (modified from [109]).

3.2 In vitro diffusion and permeation studies

In order to acquire information about the barrier properties of the skin, *in vitro* diffusion and permeation studies of model drugs are carried out. The *in vitro* studies are often used to predict the drug transport through the skin *in vivo*. Although the use of native skin samples in such studies offers evident advantages, artificial SC lipid systems have been recently preferred, as the SC intercellular lipid matrix is thought to be the main penetration route for topically applied substances. Besides overcoming problems like the limited availability and the high inter- and intra-variability of native skin samples [13], the use of well-defined SC lipid model membranes allows to investigate the impact of each individual lipid species on the SC lipid organization, and thereby on its barrier function.

Drug transport into the skin is a complex process. Depending on the lipophilicity of a drug, it can either diffuse (hydrophilic substances) or permeate (lipophilic ones) through the SC. In the case of the permeation, after the liberation of the drug from the vehicle, it needs to partition into the SC lipid bilayers before it can diffuse through it. The same situation applies in the case of the SC lipid model membranes. Finally, the drug has to partition from the lipophilic SC into the more hydrophilic viable epidermis and the dermis, where it is absorbed to the systemic circulation. The process of drug diffusion through the SC can be described by the Fick's second law of diffusion [110]:

$$\frac{\partial u}{\partial t} = D \frac{\partial^2 u}{\partial x^2} \quad 0 \leq x \leq L; t \geq 0 \quad (1)$$

where u is the drug concentration, x is the space coordinate, D is the diffusion coefficient and L stands for the diffusional pathlength (taken as thickness of the SC, for simplicity reasons, or the thickness of the SC lipid model membrane). By fitting appropriate initial and boundary conditions to Eq. (1) and using the Laplace transformation or the numerical analysis, one can obtain an estimate for the diffusion coefficient (D). The exact description of the mathematical model used to estimate the D value is presented in the relevant sections in Chapters 5–7. D , as well as other permeability parameters like the steady-state flux (J), the lag-time (T_L) and the permeability coefficient (k_p), are used to describe and compare the diffusion behavior of different drugs. The lag-time occurs at the beginning of the process of diffusion, when the gradient of the drug concentration across the SC is established. It is followed by the steady-state phase, in which the flux of the drug is constant, as long as the permeability of the SC and the drug concentration in the donor compartment (infinite dose) do not change. In order to calculate J and T_L values, the cumulative amount of the permeated drug needs to be plotted as a function of time. The slope of the linear part of the plot is taken as the steady-state flux (J) and its intercept with the time-axis is the lag-time (T_L). The permeability coefficient (k_p) is calculated as a quotient of the flux and the initial drug concentration in the donor compartment [111-113]. There are different types of diffusion cells used in *in vitro* diffusion and permeation studies. The most popular ones are the static Franz-type diffusion cell and the flow-through (also referred to as in-line) diffusion cell [114]. They consist of a donor compartment and an acceptor compartment that are clamped together. A membrane (e.g. the SC sample or the SC lipid model membrane) is placed between them. The main difference between the static and the in-line diffusion cell is the continuous replacement of the acceptor phase when using the latter, whereas in the case of the static cell, the accumulation of the drug in the acceptor phase can influence its flux (by decreasing the gradient of the drug concentration). However, this effect is reduced to minimum by use of relatively large, in terms of volume, acceptor compartments. Therefore, the drug concentration reached in the acceptor phase is relatively low, when compared to its concentration in the donor phase. In result, it has either no or very small impact on the flux. A diagram of the static Franz-type diffusion cell that was used in the diffusion and permeation studies of model drugs is displayed in Fig. 12.

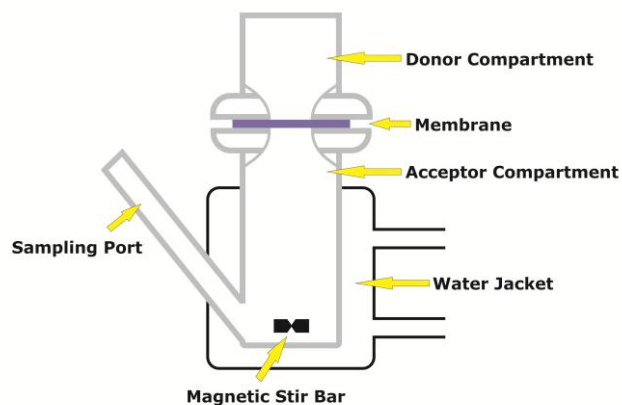


Fig. 12. A schematic representation of a static Franz-type diffusion cell.

An interesting approach in the diffusion and permeation studies is the use of the ATR-FTIR diffusion cell that has been recently introduced [115, 116]. This cell combines the advantages of the Franz-type diffusion cell and the ATR-FTIR technique. The buildup and other characteristics of the ATR-FTIR diffusion cell are described in more detail in section 4.2.1.

4 Basic principles of experimental techniques applied

4.1 X-ray diffraction

X-ray diffraction belongs to the scattering techniques. It is one of the most powerful tools for studying the SC lipid organization. Diffraction occurs when a wave of electromagnetic radiation is deflected after encountering an obstacle on its way. The effect of diffraction is most pronounced when the size of the diffracting objects is of the same order of magnitude as the wavelength of the radiation (0.01–10 nm for X-rays). In the case of the X-ray diffraction, the electromagnetic radiation is scattered by the electron clouds of atoms. The diffraction of electromagnetic waves from three dimensional periodic structures (e.g. atoms in a crystal, lipid lamellar phases) is known as the Bragg diffraction. The condition for the constructive interference of the electromagnetic radiation reflected from successive planes of a crystalline sample is given by the Bragg's law [9]:

$$n\lambda = 2d \sin \theta \quad n = 1,2,3, \dots \quad (2)$$

where λ is the wavelength of the radiation, θ is the angle of incidence, n is an integer (i.e. the order of the diffraction peak) and d is the repeat distance (i.e. distance between two parallel, successive planes). The interference is possible only when the waves coincide. The assumptions of the Bragg's law are shown in Fig. 13.

In the case of the X-ray diffraction, the electromagnetic radiation produced by a source (also referred to as the primary beam) is directed onto a sample. While passing through the sample, a small part of the

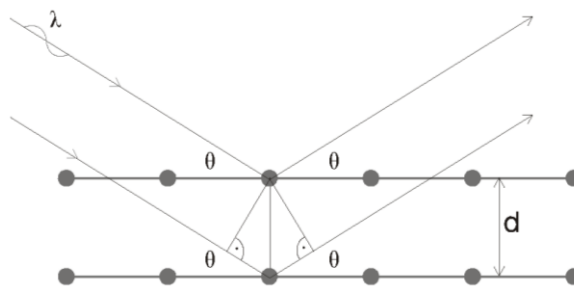


Fig. 13. Explanation of Bragg's law (adapted from [117]).

primary beam is scattered and these scattered X-rays are sent to the detector. The intensity of the scattered X-rays is measured as a function of the scattering angle, θ . However, it is more frequently plotted as a function of the scattering vector, q , which is given by: $q = 4\pi \sin \theta / \lambda$. In the case of samples consisting of lipids organized in a repeating structure (like in the SC lipid model membranes), the scattered intensity is characterized by a series of peaks (i.e. intensity maxima of scattered X-rays). When the scattered intensity is measured at a small angle (typically 0–5°), the technique is referred

to as small angle X-ray diffraction (SAXD). In the case of wide angle X-ray diffraction (WAXD), it is measured at a larger angle (Fig. 14) and this technique provides information about smaller structural units (e.g. lateral packing of lipids forming a lamellar phase). Contrary to WAXD, SAXD gives insight to larger structural units such as the repeat distance (also known as the periodicity) of a lamellar phase [118].

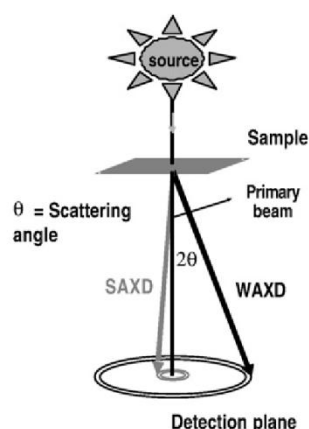


Fig. 14. Diagram presenting the principles of the X-ray diffraction technique (adapted from [118]).

4.1.1 Small angle X-ray diffraction (SAXD)

As stated above, the intensity of the scattered X-rays in the case of organized periodic structures (e.g. a lamellar phase) is characterized by a series of maxima. These diffraction peaks are referred to as the 1st order located at q_1 , 2nd order located at q_2 , 3rd order located at q_3 , etc. As the distance between sequential peaks is the same, the relation between peak positions is given by: $q_3 = 3q_1$, $q_2 = 2q_1$, etc. (see Fig. 15). Using the positions of the diffraction peaks, the repeat distance (d) of a lamellar phase can be calculated by: $d = 2\pi/q_1 = 4\pi/q_2 = 6\pi/q_3$, etc. Interestingly, when the distance between the sequential peaks is smaller, the lamellar repeat distance is larger and vice versa. Furthermore, if the sample contains two lamellar phases (e.g. LPP and SPP), the X-ray diffraction peaks of these phases are additive, which often results in a formation of a broader peak [118].

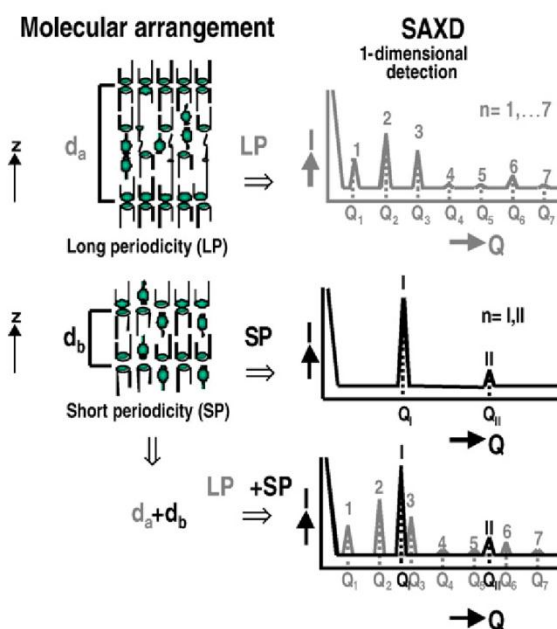


Fig. 15. Small angle X-ray diffraction technique (adapted from [118]). The diffraction patterns of two lamellar phases (LP and SP) are presented separately and together on one diffractogram.

4.2 Vibrational spectroscopy

Infrared (IR) and Raman spectroscopies are referred to as the vibrational spectroscopy, because of the nature of their action. Both techniques provide information about vibrations of atoms of a molecule. In the IR spectroscopy, a beam of IR radiation is directed onto a sample and the amount of incident radiation absorbed at a particular frequency is analyzed. Contrary to the IR spectroscopy (absorption of the electromagnetic radiation by the molecule), Raman spectroscopy is based on the Raman effect which is inelastic scattering of monochromatic light (typically in the visible, near-IR or near-UV range) by the molecule [119]. The energy of this electromagnetic radiation causes excitation of the molecule to the virtual energy state. After emitting a photon, the molecule returns to a different energy state. However, the majority of scattered photons has the same energy as incident ones (Rayleigh scattering). Only a small part of scattered photons has a different, usually lower (Stokes Raman scattering), energy than incident photons [120]. The difference in the energy between the incident and the Raman scattered photon is equal to the energy required for an excitation of a vibrational mode of the molecule. From the position and intensity of vibrational bands characteristic for each bond in the molecule, conformations of atoms and their surroundings, the information about the molecular structure of the sample can be revealed. In the case of the IR spectroscopy, the mid-infrared (MIR, 4000–400 cm^{-1}) region is of most interest, because it corresponds to changes in vibrational energies within atoms of the majority of compounds. IR and Raman spectroscopies are complementary to each other. A vibrational mode of the molecule is IR-active, when it is associated with the change in dipole moment of the molecule. On the other hand, an alteration in the polarizability of the molecule is required for a vibrational mode to be Raman-active [119]. Therefore, IR spectroscopy is generally used to describe polar groups of molecules (strong dipole character), while Raman spectroscopy can be used to characterize the non-polar parts of molecules. In general, two types of vibrational modes of the molecule can be distinguished, namely *stretching* (ν) and *deformation* (δ) modes. The former occurs when atoms move in the direction of their bond, to and from each other, and can be subdivided to *symmetric* (ν_{sym}) and *antisymmetric* (ν_{asym}) *stretching*. In the case of the latter, the angle between two bonds changes. The examples of *deformation* modes are: *scissoring*, *rocking*, *wagging* and *twisting*. Using IR spectroscopy, one can investigate the amount of urea (polar compound) in the acceptor phase of the ATR-FTIR diffusion cell (described in

the next section) based on the characteristic vibrational band $\nu(\text{CN})$ at 1466 cm^{-1} . Raman spectroscopy, as mentioned above, is preferably used to analyze the non-polar parts of molecules. Therefore, it can be used to investigate molecules with long hydrocarbon chains like SC lipids [121]. In confocal Raman imaging (described in section 4.2.2) studies on the distribution of SC lipids within SC lipid model membranes, characteristic vibrational modes of SC lipids occurring at a specific wavelength were chosen. The region between $600\text{--}1300\text{ cm}^{-1}$ contains the alicyclic $\nu(\text{CC})$ vibrations and the $\delta(\text{CH}_2)$ and $\delta(\text{CH}_3)_{\text{asym}}$ vibrations are located in the range $1400\text{--}1470\text{ cm}^{-1}$. The $\nu(\text{C}=\text{C})$ mode can be detected between $1500\text{--}1900\text{ cm}^{-1}$ and the $\nu(\text{CC})$ vibration at about 900 cm^{-1} .

4.2.1 ATR-FTIR diffusion cell

ATR-FTIR diffusion cell is a recently introduced real-time measuring device for the investigation of the transport process of model drugs and other substances of interest across membranes [115, 116]. Its schematic buildup is shown in Fig. 16. The ATR-FTIR diffusion cell combines the advantages of the Franz-type diffusion cell and the ATR-FTIR spectroscopy. It is a non-destructive procedure and requires only very little sample preparation. As in Franz-type diffusion cell, the ATR-FTIR cell consists of two chambers separated by a membrane, namely donor and acceptor compartment. The acceptor phase is in direct contact with the ATR crystal, which is a prerequisite for conducting ATR-FTIR experiments. ATR-FTIR spectroscopy is a widely used analytical technique (e.g. in the field of chemistry, medicine and pharmacy). Attenuated total reflectance (ATR) is a technique used in conjunction with Fourier transform IR (FTIR) spectroscopy.

Nowadays, FTIR spectrometers are frequently used instead of dispersive IR spectrometers. The main advantage of the FTIR over dispersive IR spectrometers is the

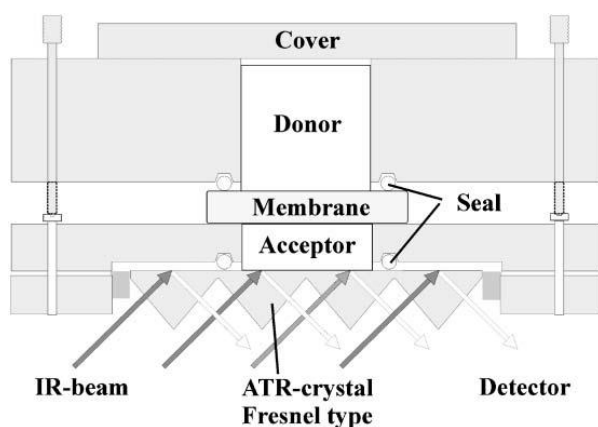


Fig. 14. ATR-FTIR diffusion cell (adapted from [115]).

use of a system called an interferometer (e.g. two-beam Michelson interferometer), instead of a monochromator. It allows collecting the information about the sample at all wavelengths simultaneously, whereas the light at only one wavelength at a time passes

through the sample when using the monochromator. The signal registered by the detector, an interferogram (representing the radiation intensity as a function of the position of the interferometer's movable mirror), is subsequently converted to a spectrum by using a Fourier transform algorithm. By comparison of the sample spectrum and the reference spectrum, the IR transmission spectrum of the sample is acquired. It can be subsequently converted to the absorbance spectrum by taking the negative *common logarithms* of the transmission data points [119].

In ATR technique, the IR beam is directed at a certain angle towards an optically dense crystal with a high refractive index (e.g. ZnSe with $n_1 = 2.4$). A sample with lower optical density n_2 ($n_2 < n_1$) is placed on the surface of the ATR crystal. At the sample-ATR crystal interface, the IR radiation undergoes total internal reflection. Nevertheless, the evanescent wave, which in fact penetrates beyond the surface of the crystal into the sample, is created at the same time (shown in Fig. 17). This is a fundamental principle of the ATR technique. While penetrating through the sample, the radiation is partly absorbed in some regions of the IR spectrum, which results in the attenuation of the evanescent wave in these regions.

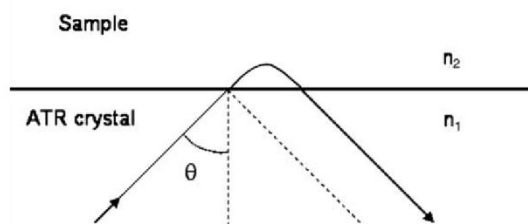


Fig. 15. Principle of the attenuated total reflectance (adapted from [119]).

The penetration depth of the evanescent wave (d_p) depends on the wavelength of IR radiation (λ), its angle of incidence (θ), the refractive indices of the ATR crystal (n_1) and the sample (n_2), and is given by:

$$d_p = \frac{\lambda}{2\pi n_1 \sqrt{\sin^2 \theta - (n_2/n_1)^2}} \quad (3)$$

Of major importance is the angle of incidence, because the internal total reflection occurs only when θ exceeds the value of a critical angle given by: $\theta_c = \arcsin(n_2/n_1)$. The d_p amounts typically to 0.5–5 μm , so the sample must be in direct contact with the ATR crystal. Moreover, the difference in the values of the refractive indices of the ATR crystal and the sample has to be significant. The n_1 value must be larger than n_2 value.

Otherwise, the internal reflection will not occur and the radiation will be rather transmitted through the crystal, than internally reflected.

4.2.2 Confocal Raman imaging

Confocal Raman imaging technique represents a combination of the Raman spectroscopy and the confocal microscopy. It is a powerful tool for a noninvasive chemical imaging of biomaterials. A special feature of Raman imaging is that it provides the information not only about the molecular structure of chemical moieties of a sample, but also about their spatial arrangement. Generally, two types of imaging techniques can be distinguished, namely *direct* (or *parallel*) imaging and *series* imaging (also referred to as *mapping*) [122-125]. The former consists in a global illumination of a sample. A complete two-dimensional (2D) image at a chosen wavelength, characteristic of the vibrational mode of a molecule, is produced immediately. The main advantage of the *direct* imaging technique is relatively short acquisition time, when compared to the *series* imaging method, which results from the reduction of the signal collection time with respect to point illumination (the whole area of the sample is subjected to the laser beam at one time). On the other hand, only a part of spectral information can be acquired at a given time. Moreover, the *direct* imaging technique is characterized by strong background signals (fluorescence, stray light, etc.) and no possibility to benefit from the confocal arrangement (the resolution is strongly influenced by out-of-focus light). The *series* imaging technique is based on the image reconstruction. Individual images are recorded point-by-point and line-by-line by scanning the sample with a finely focused laser beam. Most frequently, it is achieved by the use of a motorized x-y stage. As the sample is moved from point to point, a full spectrum is recorded. Subsequently, an image, corresponding to each spatial location, is reconstructed by selecting vibrational bands of compounds of interest. Because of its nature (collection of a complete set of spatial/spectral data), the *series* imaging technique is very time-consuming and should be applied only to the visualization of a small region of a sample. On the other hand, this method benefits from the concept of the confocal arrangement. Here, the radiation is focused on the sample and the reflected or scattered light is typically collected by the same objective and finally directed through the pinhole to the detector. However, the signal of interest is devoid of blurred signals from out-of-focus planes, because the pinhole ensures that only light originating from the focal plane reaches the detector. Using the confocal microscopy, a significant improvement in the spatial resolution can be

achieved. Instead of the illumination of the whole area of the sample simultaneously, a laser beam is directed onto a very small area of the sample. In result, the intensity of the light scattered by this small fraction of the sample is measured at any one time by the confocal system. Another advantage of the confocal microscopy is that a sample can be analyzed along the optical axis (by means of a motorized z-focus stage), so in result depth profiles or three-dimensional (3D) images can be also generated [125, 126].

4.3 Environmental scanning electron microscopy

In electron microscopy, a beam of electrons is used to illuminate a sample and produce its image. Contrary to light microscopes, electron microscopes are capable of magnifications of up to millions of times. The wavelengths of electrons are approx. five orders of magnitude shorter than the wavelengths of light used in the optical microscopy. Hence, much better resolution (down to the picometer range) can be achieved using the electron microscopy [127]. There can be distinguished two main distinct techniques in the electron microscopy, namely transmission electron microscopy (TEM) and scanning electron microscopy (SEM). In TEM, a high voltage electron beam is transmitted through a very thin sample. While passing through it, the electrons interact with the specimen and these interactions are the basis for the formation of the sample image (the transmitted electrons carry the information about the structure of the specimen). In SEM, on the other hand, images are produced by probing the sample with a focused beam of electrons (with energies typically up to 40 keV) that is scanned across an area of the sample. After the electron–specimen interaction that causes the energy loss of the incident electrons, various signals mainly in form of low-energy secondary electrons, high-energy backscattered electrons, visible light (cathodoluminescence) or X-rays are generated. The signals emerging from the specimen at a specific position are collected by detectors located above the sample. The SEM image is created based on the intensity of these signals that varies from one position to another as the electron–specimen interactions change due to the alterations in the structure of the sample surface [128]. Although SEM is characterized by lower image resolution (when compared to TEM), its ability to yield 3D information from the surface of bulk specimens, over a considerable range of length-scales, makes it an appealing technique for viewing samples especially in materials sciences [127, 129].

Unlike the conventional SEM, which operates in a high vacuum, the environmental scanning electron microscopy (ESEM) technique allows the examination of any specimen in the presence of a gas in the specimen chamber. This eliminates the need for a troublesome sample preparation like e.g. critical point drying or freeze drying, in the case of hydrated specimens that need to be dehydrated in order to be viewed in the high vacuum SEM, as well as coating of non-conductive specimens to avoid charging during the SEM imaging process [130]. To enable observations of specimens under gaseous conditions, changes to conventional SEM microscopes had to be introduced. Namely, two characteristic features of ESEM instruments are the use of a differential pumping, which allows the separation of the gaseous specimen chamber from the electron optics column sustained under the high vacuum, and new detection systems (e.g. gaseous secondary electron detector or GSED). The low-energy secondary electrons emitted by the specimen are selectively accelerated in the small electric field between the sample and the detector. Ionizing collisions between these electrons and gas molecules generate additional electrons causing so-called *cascade of electrons*, which leads to the amplification of the signal before it is collected by the GSED. The positively charged gas ions, resulting from the collisions of secondary electrons with gas molecules, play an essential role in the ESEM. They can balance the accumulation of negative charges on the surface of examined specimens, thus enable imaging of insulators without the need for the use of the conductive coating, which is required in the case of the conventional SEM [127, 129, 130]. Water vapor is one of the most commonly used gases in the specimen chamber as it provides strong signal amplification, as well as it permits the hydrated samples to be observed in their natural state [130, 131], which is of major importance when imaging biological samples (e.g. SC membranes).

4.4 Analytical separation techniques

4.4.1 High performance thin layer chromatography

High performance thin layer chromatography (HPTLC) belongs to commonly used chromatographic separation techniques. It is a robust, simple, rapid and efficient analytical method for the separation, identification and quantification of chemical compounds [132-135]. HPTLC is an enhanced version of thin layer chromatography (TLC). The separation of a mixture of compounds is based on the migration of individual

components at different rates, resulting from their different distributions between a stationary phase (typically glass plates coated with silica gel) and a mobile phase (its movement up the plate is determined by the *capillary action*). A number of enhancements have been introduced to TLC technique in order to improve the sensitivity of the method and the resolution of separated compounds, as well as to allow their quantitative analysis. The procedures used in HPTLC are, on the one hand, very similar to those used in TLC. However, HPTLC is characterized by the use of better quality materials (HPTLC plates with finer particle sizes and narrower size distribution) and more sophisticated methods of a sample introduction, chromatographic separation and detection of substances, when compared to TLC [135]. The steps of the sample application, the plate development and the quantitative analysis have been automated. Samples are applied on the HPTLC plate by means of an automated instrument (e.g. ATS 4 from Camag), which provides the optimum resolution and the reliable quantification. Moreover, the plates can be developed repeatedly using solvents of different elution strength in each run, which leads to the better separation of components with improved resolution. Finally, the quantitative analysis of separated compounds can be performed *in situ* by means of a scanning densitometry (photometric measurement of absorbed light or emitted fluorescence), which provides reliable and reproducible results. In contrast to column chromatography (e.g. HPLC), in HPTLC many substances can be applied and run simultaneously (up to 70 on one HPTLC plate [133]), which makes it a very rapid and efficient method. Furthermore, the detection in HPTLC is separated from the chromatographic step (so-called *static* detection), contrary to HPLC where the detection time of separated compounds, passing through the detection device, is limited by the rate at which they are eluted from the column (so-called *dynamic* detection). It is one of the most important features of HPTLC, because it allows to use various post-chromatographic techniques intended to enhance the sensitivity of detection (e.g. derivatization performed prior to UV or fluorescence detection; wavelength selection), and hence to obtain the optimal response for each examined compound [132]. The procedures of separation and quantification of SC lipids by means of HPTLC were previously reported [136, 137].

4.4.2 High performance liquid chromatography

High performance liquid chromatography (HPLC) is the most popular analytical separation method of a mixture of compounds. HPLC is a form of a liquid

chromatography technique in which a liquid mobile phase is mechanically pumped into and passed through the column containing a densely packed stationary phase [138]. An HPLC instrument consists of an injector (which injects a sample into the column), a pump (which provides the high pressure required to move the mobile phase and sample components through the column), a column (which contains different types of stationary phases) and a detector (typically UV detector). Based on the retention mechanisms of analytes on the column, five major liquid chromatographic methods can be distinguished, namely partition chromatography, adsorption chromatography, ion exchange chromatography, affinity chromatography and size exclusion chromatography [138, 139].

The most frequently used chromatographic mode is the reversed-phase HPLC (also known as RP-HPLC). As the name suggests, RP-HPLC is the reverse of normal-phase HPLC (or NP-HPLC), which involves the use of a polar stationary phase (e.g. silica) and a non-polar mobile phase. In RP-HPLC, a non-polar stationary phase (typically chemically bonded, e.g. silanol groups of silica bonded with a functional group $R(\text{CH}_3)_2\text{SiCl}$, where most commonly R is a straight alkyl chain group such as $-\text{C}_{18}\text{H}_{37}$ or $-\text{C}_8\text{H}_{17}$) and a polar mobile phase are used. As a consequence, more polar compounds are characterized by shorter retention times, while elution of less polar molecules is a slower process. The retention times of examined compounds can be easily modified (increased or decreased) by changing the polarity of the mobile phase. In the case of a hydrophobic substance, the use of the less polar mobile phase results in the decrease of its retention time. The retention mechanism of molecules on chemically bonded, non-polar stationary phases is based on two main effects, so-called *solvophobic* and *partitioning* effects [138]. In the *solvophobic* effect, the retention is mainly related to the hydrophobic effects between the analytes and the mobile phase. The analyte binds to the surface of the stationary phase, which results in the decreased surface area of the analyte exposed to the mobile phase. The adsorption of the analyte on the stationary phase increases with the increasing surface tension of the mobile phase. Hence, by reducing the surface tension of the mobile phase in result of the addition of a less polar solvent to the mobile phase (as in the gradient elution procedure), the retention of the analyte can be decreased (faster elution from the column). While using the gradient elution procedure, the composition of the mobile phase is changed during the separation process, contrary to the isocratic flow procedure, where the composition of the mobile phase remains constant throughout the experiment. The *partitioning* effect, on the other hand, assumes that the molecules of the analyte are fully embedded in the stationary phase chains, hence are partitioned between the mobile phase and the stationary phase. The retention mechanism in RP-HPLC is most

likely the combination of both effects described, with the dominance of the *adsorption* effect when using the stationary phase with shorter chain lengths and the *partitioning* effect in the case of the stationary phase with longer chain lengths.

4.4.3 Capillary electrophoresis

Capillary electrophoresis (CE) is an analytical technique based on the separation of charged components of a mixture under the influence of an electric field in the interior of a capillary filled with an electrolyte [138, 140]. The basic set-up of CE instrumentation is relatively simple (see Fig. 18). It consists of an injection system, a small-diameter capillary (20–100 μm ID), inlet and outlet vials, a high voltage power supply (up to 30 kV and 200–250 μA), electrodes and a detector [141, 142].

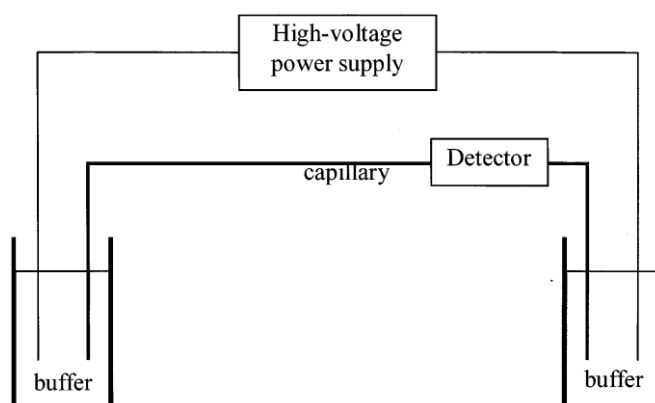


Fig. 16. Schematic presentation of CE system (adapted from [142]).

A sample can be injected into the capillary (most frequently used are fused silica capillaries) by using either hydrodynamic or electrokinetic technique (application of pressure or potential, respectively, while the injection end of the capillary is located in the sample vial). There are several modes of operation in CE that are based on the different separation mechanisms, all of which can be carried out using the same CE instrumentation (by simply changing the electrolyte and/or the capillary). Besides the most simple and widely used mode in CE, namely capillary zone electrophoresis (CZE), other modes of CE such as micellar electrokinetic chromatography (MEKC or MECC), capillary gel electrophoresis (CGE), capillary electrokinetic chromatography (CEC), capillary isotachopheresis (cITP), capillary isoelectric focusing (cIEF) and chiral capillary electrophoresis (chiral CE) are also applied in order to separate investigated compounds [138, 140-142]. In CZE, the separation mechanism is based on mobility differences of

compounds in the electric field that depend on the size and charge-to-mass ratio of analyzed ions. The migration of analytes under the influence of the electric field is characterized by their electrophoretic mobility. The other important factor influencing the movement of the compounds in the capillary is the electroosmotic flow (EOF), which together with the electrophoretic mobility gives the apparent mobility of the analytes. In the case of a fused silica capillary, the acidic silanol groups attached to the interior wall of the capillary dissociate to the silanoate groups at pH values higher than 2. The negatively charged wall of the capillary attracts the positively charged ions, which results in the formation of a double layer of cations inside the capillary (so-called *compact* and *diffuse* layer [138]). When the electric field is applied, the cations from the *diffuse* layer move towards the negatively charged cathode, pulling the bulk solution of the electrolyte along and thus creating the flat flow EOF [138, 140-143]. Typically, the EOF is directed toward the negatively charged cathode, accordingly to the electrolyte flow within the capillary from the inlet to the outlet vial. Since the EOF is generally larger than the electrophoretic flow of the analytes (under the electric field applied, anions are attracted to the positively charged anode, counter to the EOF), all analytes (cations, anions and neutral compounds) migrate with the electrolyte toward the cathode, and hence can be detected [142]. Small multiply charged cations migrate very fast to the detector, unlike small multiply charged anions which are carried along very slowly. The identification and/or quantitation of separated analytes takes place mostly at the end of the capillary by means of various detectors (so-called *on-capillary* detection [140]). Most frequently applied detection techniques in CE are UV absorbance (single- and multi-wavelength, e.g. photodiode array detector, PDA), fluorescence (e.g. laser-induced fluorescence, LIF), electrochemical detection (amperometry, conductivity) and mass spectrometric (MS) detection (*off-capillary* detection by online coupling of CE with MS). The conductivity detection technique is based on the measurement of the solution conductivity by placing a pair of electrodes in the capillary and measuring the current passing between the electrodes as a function of potential. When the analyte passes between the electrodes, the change in the current in the sensing circuit will be observed [138, 140-143].

References

- [1] L. Moore, Y.W. Chien, Transdermal drug delivery: a review of pharmaceuticals, pharmacokinetics, and pharmacodynamics, *Crit. Rev. Ther. Drug Carrier Syst.* 4 (1988) 285-349.
- [2] N. Pimpinelli, M. Santucci, The skin-associated lymphoid tissue-related B-cell lymphomas, *Semin. Cutan. Med. Surg.* 19 (2000) 124-129.
- [3] C.M. Chuong, B.J. Nickoloff, P.M. Elias, L.A. Goldsmith, E. Macher, P.A. Maderson, J.P. Sundberg, H. Tagami, P.M. Plonka, K. Thestrup-Pederson, B.A. Bernard, J.M. Schroder, P. Dotto, C.M. Chang, M.L. Williams, K.R. Feingold, L.E. King, A.M. Kligman, J.L. Rees, E. Christophers, What is the 'true' function of skin?, *Exp. Dermatol.* 11 (2002) 159-187.
- [4] G.L. Flynn, Topical Drug Absorption and Topical Pharmaceutical Systems, in: G.S. Banker, C.T. Rhodes (Eds.) *Modern Pharmaceutics*, Marcel Dekker Inc., New York, 1990, pp. 263-325.
- [5] T. Winsor, G.E. Burch, Differential roles of layers of human epigastric skin on diffusion rate of water, *Arch. Intern. Med.* 74 (1944) 428-436.
- [6] P.M. Elias, D.S. Friend, The permeability barrier in mammalian epidermis, *J. Cell Biol.* 65 (1975) 180-191.
- [7] D.C. Swartzendruber, P.W. Wertz, D.J. Kitko, K.C. Madison, D.T. Downing, Molecular-Models of the Intercellular Lipid Lamellae in Mammalian Stratum-Corneum, *J. Invest. Dermatol.* 92 (1989) 251-257.
- [8] B. Forslind, A domain mosaic model of the skin barrier, *Acta Derm. Venereol.* 74 (1994) 1-6.
- [9] J.A. Bouwstra, F.E. Dubbelaar, G.S. Gooris, M. Ponec, The lipid organisation in the skin barrier, *Acta Derm. Venereol. Suppl.* 208 (2000) 23-30.
- [10] L. Norlen, Skin barrier structure and function: the single gel phase model, *J. Invest. Dermatol.* 117 (2001) 830-836.
- [11] M.A. Kiselev, N.Y. Ryabova, A.M. Balagurov, S. Dante, T. Hauss, J. Zbytovska, S. Wartewig, R.H.H. Neubert, New insights into the structure and hydration of a stratum corneum lipid model membrane by neutron diffraction, *Eur. Biophys. J.* 34 (2005) 1030-1040.
- [12] M.A. Kiselev, Conformation of ceramide 6 molecules and chain-flip transitions in the lipid matrix of the outermost layer of mammalian skin, the stratum corneum, *Crystallogr. Rep.* 52 (2007) 525-528.
- [13] P.W. Wertz, B. van den Bergh, The physical, chemical and functional properties of lipids in the skin and other biological barriers, *Chem. Phys. Lipids.* 91 (1998) 85-96.
- [14] B.W. Barry, Novel mechanisms and devices to enable successful transdermal drug delivery, *Eur. J. Pharm. Sci.* 14 (2001) 101-114.
- [15] S.H. White, D. Mirejovsky, G.I. King, Structure of lamellar lipid domains and corneocyte envelopes of murine stratum corneum. An X-ray diffraction study, *Biochemistry* 27 (1988) 3725-3732.
- [16] B. Ongpipattanakul, M.L. Francoeur, R.O. Potts, Polymorphism in stratum corneum lipids, *Biochim. Biophys. Acta, Biomembranes* 1190 (1994) 115-122.
- [17] T.J. McIntosh, M.E. Stewart, D.T. Downing, X-ray diffraction analysis of isolated skin lipids: reconstitution of intercellular lipid domains, *Biochemistry* 35 (1996) 3649-3653.
- [18] J.A. Bouwstra, G.S. Gooris, K. Cheng, A. Weerheim, W. Bras, M. Ponec, Phase behavior of isolated skin lipids, *J. Lipid Res.* 37 (1996) 999-1011.
- [19] T.J. McIntosh, Organization of skin stratum corneum extracellular lamellae: diffraction evidence for asymmetric distribution of cholesterol, *Biophys. J.* 85 (2003) 1675-1681.
- [20] J.A. Bouwstra, G.S. Gooris, J.A. van der Spek, W. Bras, Structural investigations of human stratum corneum by small-angle X-ray scattering, *J. Invest. Dermatol.* 97 (1991) 1005-1012.
- [21] J.A. Bouwstra, G.S. Gooris, F.E. Dubbelaar, A.M. Weerheim, A.P. Ijzerman, M. Ponec, Role of ceramide 1 in the molecular organization of the stratum corneum lipids, *J. Lipid Res.* 39 (1998) 186-196.

- [22] S.E. Friberg, D.W. Osborne, Interaction of a Model Epidermal Lipid with a Vegetable Oil Adduct, *J. Disper. Sci. Technol.* 8 (1987) 249-258.
- [23] D. Kuempel, D.C. Swartzendruber, C.A. Squier, P.W. Wertz, In vitro reconstitution of stratum corneum lipid lamellae, *Biochim. Biophys. Acta* 1372 (1998) 135-140.
- [24] A. Schroeter, D. Kessner, M.A. Kiselev, T. Hauss, S. Dante, R.H.H. Neubert, Basic nanostructure of stratum corneum lipid matrices based on ceramides [EOS] and [AP]: a neutron diffraction study, *Biophys. J.* 97 (2009) 1104-1114.
- [25] A. Schroeter, M.A. Kiselev, T. Hauss, S. Dante, R.H.H. Neubert, Evidence of free fatty acid interdigitation in stratum corneum model membranes based on ceramide [AP] by deuterium labelling, *Biochim. Biophys. Acta, Biomembranes* 1788 (2009) 2194-2203.
- [26] D. Kessner, M.A. Kiselev, S. Dante, T. Hauss, P. Lersch, S. Wartewig, R.H.H. Neubert, Arrangement of ceramide [EOS] in a stratum corneum lipid model matrix: new aspects revealed by neutron diffraction studies, *Eur. Biophys. J.* 37 (2008) 989-999.
- [27] T. Engelbrecht, T. Hauss, K. Sueß, A. Vogel, M. Roark, S.E. Feller, R.H.H. Neubert, B. Dobner, Characterisation of a new ceramide EOS species: synthesis and investigation of the thermotropic phase behaviour and influence on the bilayer architecture of stratum corneum lipid model membranes, *Soft Matter* 7 (2011) 8998-9011.
- [28] S. Raudenkolb, S. Wartewig, R.H.H. Neubert, Polymorphism of ceramide 6: A vibrational spectroscopic and X-ray powder diffraction investigation of the diastereomers of N-(alpha-hydroxyoctadecanoyl)-phytosphingosine, *Chem. Phys. Lipids* 133 (2005) 89-102.
- [29] R.H.H. Neubert, W. Wohlrab, W. Marsch, *Dermatopharmazie. Vehikel, Wirkstoffe, Pharmakologie*, Wissenschaftliche Verlagsgesellschaft mbH, Stuttgart, 2001.
- [30] G.K. Menon, New insights into skin structure: scratching the surface, *Adv. Drug Deliver. Rev.* 54 Suppl. 1 (2002) S3-S17.
- [31] Encarta. Vol. 2009, Microsoft Inc. 2009.
- [32] A.C. Williams, Structure and function of human skin, in: *Transdermal and Topical Drug Delivery: From Theory to Clinical Practise*, Pharmaceutical Press, London, 2003, pp. 1-25.
- [33] R.T. Woodburne, *Essentials of Human Anatomy*, Oxford University Press, New York, 1965, pp. 6.
- [34] G.L. Wilkes, I.A. Brown, R.H. Wildnauer, The biomechanical properties of skin, *CRC Crit. Rev. Bioeng.* (1973) 453-495.
- [35] H. Baker, A.M. Kligman, Technique for estimating turnover time of human stratum corneum, *Arch. Dermatol.* 95 (1967) 408-411.
- [36] R.L. Eckert, Structure, function, and differentiation of the keratinocyte, *Physiol. Rev.* 69 (1989) 1316-1346.
- [37] I.D.J. Burdett, Aspects of the structure and assembly of desmosomes, *Micron* 29 (1998) 309-328.
- [38] E. Fuchs, S. Raghavan, Getting under the skin of epidermal morphogenesis, *Nat. Rev. Genet.* 3 (2002) 199-209.
- [39] G.F. Odland, A submicroscopic granular component in human epidermis, *J. Invest. Dermatol.* 34 (1960) 11-15.
- [40] R.K. Freinkel, T.N. Traczyk, Lipid composition and acid hydrolase content of lamellar granules of fetal rat epidermis, *J. Invest. Dermatol.* 85 (1985) 295-298.
- [41] P.W. Wertz, D.T. Downing, R.K. Freinkel, T.N. Traczyk, Sphingolipids of the stratum corneum and lamellar granules of fetal rat epidermis, *J. Invest. Dermatol.* 83 (1984) 193-195.
- [42] P.W. Wertz, Epidermal lipids, *Semin. Dermatol.* 11 (1992) 106-113.
- [43] P.W. Wertz, Stratum corneum Lipids and Water, *Exog. Dermatol.* 3 (2004) 53-56.
- [44] I.H. Blank, Transport across the stratum corneum, *Toxicol. Appl. Pharmacol. Suppl.* 3 (1969) 23-29.
- [45] R.J. Scheuplein, I.H. Blank, Permeability of the skin, *Physiol. Rev.* 51 (1971) 702-747.
- [46] J.A. Bouwstra, A. de Graaff, G.S. Gooris, J. Nijse, J.W. Wiechers, A.C. van Aelst, Water distribution and related morphology in human stratum corneum at different hydration levels, *J. Invest. Dermatol.* 120 (2003) 750-758.

-
- [47] A.S. Michaels, S.K. Chandrasekaran, J.E. Shaw, Drug permeation through human skin: Theory and in vitro experimental measurement, *AIChE J.* 21 (1975) 985-996.
- [48] P.M. Elias, Lipids and the epidermal permeability barrier, *Arch. Dermatol. Res.* 270 (1981) 95-117.
- [49] P.M. Elias, Epidermal lipids, barrier function, and desquamation, *J. Invest. Dermatol.* 80 (1983) 44s-49s.
- [50] Z. Nemes, P.M. Steinert, Bricks and mortar of the epidermal barrier, *Exp. Mol. Med.* 31 (1999) 5-19.
- [51] T. Steriotis, G.C. Charalambopoulou, Investigation of Stratum Corneum structural and dynamic properties with neutron techniques, in: *BENSC User's Meeting*, Berlin, 2004.
- [52] C.R. Harding, S. Long, J. Richardson, J. Rogers, Z. Zhang, A. Bush, A.V. Rawlings, The cornified cell envelope: an important marker of stratum corneum maturation in healthy and dry skin, *Int. J. Cosmet. Sci.* 25 (2003) 157-167.
- [53] T. Hirao, Involvement of transglutaminase in ex vivo maturation of cornified envelopes in the stratum corneum, *Int. J. Cosmet. Sci.* 25 (2003) 245-257.
- [54] D.C. Swartzendruber, P.W. Wertz, K.C. Madison, D.T. Downing, Evidence that the corneocyte has a chemically bound lipid envelope, *J. Invest. Dermatol.* 88 (1987) 709-713.
- [55] P.W. Wertz, K.C. Madison, D.T. Downing, Covalently bound lipids of human stratum corneum, *J. Invest. Dermatol.* 92 (1989) 109-111.
- [56] L. Coderch, O. Lopez, A. de la Maza, J.L. Parra, Ceramides and skin function, *Am. J. Clin. Dermatol.* 4 (2003) 107-129.
- [57] A.V. Rawlings, Trends in stratum corneum research and the management of dry skin conditions, *Int. J. Cosmet. Sci.* 25 (2003) 63-95.
- [58] A. Rawlings, C. Harding, A. Watkinson, J. Banks, C. Ackerman, R. Sabin, The effect of glycerol and humidity on desmosome degradation in stratum corneum, *Arch. Dermatol. Res.* 287 (1995) 457-464.
- [59] J. Sato, M. Denda, J. Nakanishi, J. Nomura, J. Koyama, Cholesterol sulfate inhibits proteases that are involved in desquamation of stratum corneum, *J. Invest. Dermatol.* 111 (1998) 189-193.
- [60] E. Zettersten, M.Q. Man, J. Sato, M. Denda, A. Farrell, R. Ghadially, M.L. Williams, K.R. Feingold, P.M. Elias, Recessive x-linked ichthyosis: role of cholesterol-sulfate accumulation in the barrier abnormality, *J. Invest. Dermatol.* 111 (1998) 784-790.
- [61] S.J. Rehfeld, W.Z. Plachy, M.L. Williams, P.M. Elias, Calorimetric and electron spin resonance examination of lipid phase transitions in human stratum corneum: molecular basis for normal cohesion and abnormal desquamation in recessive X-linked ichthyosis, *J. Invest. Dermatol.* 91 (1988) 499-505.
- [62] C.H. Purdon, C.G. Azzi, J. Zhang, E.W. Smith, H.I. Maibach, Penetration enhancement of transdermal delivery--current permutations and limitations, *Crit. Rev. Ther. Drug Carrier Syst.* 21 (2004) 97-132.
- [63] Y.Y. Grams, S. Alaruikka, L. Lashley, J. Caussin, L. Whitehead, J.A. Bouwstra, Permeant lipophilicity and vehicle composition influence accumulation of dyes in hair follicles of human skin, *Eur. J. Pharm. Sci.* 18 (2003) 329-336.
- [64] S. Trauer, A. Patzelt, N. Otberg, F. Knorr, C. Rozycki, G. Balizs, R. Buttemeyer, M. Linscheid, M. Liebsch, J. Lademann, Permeation of topically applied caffeine through human skin--a comparison of in vivo and in vitro data, *Br. J. Clin. Pharmacol.* 68 (2009) 181-186.
- [65] F. Knorr, J. Lademann, A. Patzelt, W. Sterry, U. Blume-Peytavi, A. Vogt, Follicular transport route--research progress and future perspectives, *Eur. J. Pharm. Biopharm.* 71 (2009) 173-180.
- [66] M.L. Williams, P.M. Elias, The extracellular matrix of stratum corneum: role of lipids in normal and pathological function., *Crit. Rev. Ther. Drug Carrier Syst.* 3 (1987) 95-122.
- [67] B.C. Lippold, *Biopharmazie. Eine Einführung zu den wichtigsten Arzneiformen*, VWG Stuttgart. (1984).
- [68] M.R. Prausnitz, S. Mitragotri, R. Langer, Current status and future potential of transdermal drug delivery, *Nat. Rev. Drug Discov.* 3 (2004) 115-124.
- [69] S.E. Friberg, I. Kayali, W. Beckerman, L.D. Rhein, A. Simion, Water permeation of reaggregated stratum corneum with model lipids, *J. Invest. Dermatol.* 94 (1990) 377-380.

- [70] P.W. Wertz, M.C. Miethke, S.A. Long, J.S. Strauss, D.T. Downing, The composition of the ceramides from human stratum corneum and from comedones, *J. Invest. Dermatol.* 84 (1985) 410-412.
- [71] N.Y. Schurer, G. Plewig, P.M. Elias, Stratum corneum lipid function, *Dermatologica* 183 (1991) 77-94.
- [72] M.A. Lampe, A.L. Burlingame, J. Whitney, M.L. Williams, B.E. Brown, E. Roitman, P.M. Elias, Human stratum corneum lipids: characterization and regional variations, *J. Lipid Res.* 24 (1983) 120-130.
- [73] A. Weerheim, M. Ponc, Determination of stratum corneum lipid profile by tape stripping in combination with high-performance thin-layer chromatography, *Arch. Dermatol. Res.* 293 (2001) 191-199.
- [74] W.M. Holleran, M.Q. Man, W.N. Gao, G.K. Menon, P.M. Elias, K.R. Feingold, Sphingolipids are required for mammalian epidermal barrier function. Inhibition of sphingolipid synthesis delays barrier recovery after acute perturbation, *J. Clin. Invest.* 88 (1991) 1338-1345.
- [75] J. van Smeden, L. Hoppel, R. van der Heijden, T. Hankemeier, R.J. Vreeken, J.A. Bouwstra, LC/MS analysis of stratum corneum lipids: ceramide profiling and discovery, *J. Lipid Res.* 52 (2011) 1211-1221.
- [76] P.W. Wertz, D.T. Downing, Ceramides of pig epidermis: structure determination, *J. Lipid Res.* 24 (1983) 759-765.
- [77] S. Motta, M. Monti, S. Sesana, R. Caputo, S. Carelli, R. Ghidoni, Ceramide composition of the psoriatic scale, *Biochim. Biophys. Acta* 1182 (1993) 147-151.
- [78] M.W. de Jager, G.S. Gooris, I.P. Dolbnya, M. Ponc, J.A. Bouwstra, Modelling the stratum corneum lipid organisation with synthetic lipid mixtures: the importance of synthetic ceramide composition, *Biochim. Biophys. Acta, Biomembranes* 1664 (2004) 132-140.
- [79] M.W. de Jager, G.S. Gooris, I.P. Dolbnya, W. Bras, M. Ponc, J.A. Bouwstra, Novel lipid mixtures based on synthetic ceramides reproduce the unique stratum corneum lipid organization, *J. Lipid Res.* 45 (2004) 923-932.
- [80] G.K. Menon, K.R. Feingold, A.H. Moser, B.E. Brown, P.M. Elias, De novo sterologenesi in the skin. II. Regulation by cutaneous barrier requirements, *J. Lipid Res.* 26 (1985) 418-427.
- [81] D. Kessner, M.A. Kiselev, T. Hauss, S. Dante, S. Wartewig, R.H.H. Neubert, Localisation of partially deuterated cholesterol in quaternary SC lipid model membranes: a neutron diffraction study, *Eur. Biophys. J.* 37 (2008) 1051-1057.
- [82] R. Lieckfeldt, J. Villalain, J.C. Gomez-Fernandez, G. Lee, Diffusivity and structural polymorphism in some model stratum corneum lipid systems, *Biochim. Biophys. Acta* 1150 (1993) 182-188.
- [83] T.J. McIntosh, The effect of cholesterol on the structure of phosphatidylcholine bilayers, *Biochim. Biophys. Acta* 513 (1978) 43-58.
- [84] S. Bhattacharya, S. Haldar, Interactions between cholesterol and lipids in bilayer membranes. Role of lipid headgroup and hydrocarbon chain-backbone linkage, *Biochim. Biophys. Acta, Biomembranes* 1467 (2000) 39-53.
- [85] J. Czub, M. Baginski, Comparative molecular dynamics study of lipid membranes containing cholesterol and ergosterol, *Biophys. J.* 90 (2006) 2368-2382.
- [86] M.L. Williams, P.M. Elias, Stratum corneum lipids in disorders of cornification: increased cholesterol sulfate content of stratum corneum in recessive x-linked ichthyosis, *J. Clin. Invest.* 68 (1981) 1404-1410.
- [87] P.W. Wertz, D.T. Downing, Cholesteryl sulfate: the major polar lipid of horse hoof, *J. Lipid Res.* 25 (1984) 1320-1323.
- [88] J.A. Bouwstra, G.S. Gooris, F.E. Dubbelaar, A.M. Weerheim, M. Ponc, pH, cholesterol sulfate, and fatty acids affect the stratum corneum lipid organization, *J. Invest. Dermatol. Symp. Proc.* 3 (1998) 69-74.
- [89] L. Norlen, I. Nicander, A. Lundsjo, T. Cronholm, B. Forslind, A new HPLC-based method for the quantitative analysis of inner stratum corneum lipids with special reference to the free fatty acid fraction, *Arch. Dermatol. Res.* 290 (1998) 508-516.
- [90] P.W. Wertz, The nature of the epidermal barrier: biochemical aspects, *Adv. Drug Deliver. Rev.* 18 (1996) 283-294.

-
- [91] M. Mao-Qiang, P.M. Elias, K.R. Feingold, Fatty acids are required for epidermal permeability barrier function, *J. Clin. Invest.* 92 (1993) 791-798.
- [92] A.S. Breathnach, T. Goodman, C. Stolinski, M. Gross, Freeze-fracture replication of cells of stratum corneum of human epidermis, *J. Anat.* 114 (1973) 65-81.
- [93] K.C. Madison, D.C. Swartzendruber, P.W. Wertz, D.T. Downing, Presence of intact intercellular lipid lamellae in the upper layers of the stratum corneum, *J. Invest. Dermatol.* 88 (1987) 714-718.
- [94] J.A. Bouwstra, G.S. Gooris, W. Bras, D.T. Downing, Lipid organization in pig stratum corneum, *J. Lipid Res.* 36 (1995) 685-695.
- [95] M.W. de Jager, G.S. Gooris, I.P. Dolbnya, W. Bras, M. Ponec, J.A. Bouwstra, The phase behaviour of skin lipid mixtures based on synthetic ceramides, *Chem. Phys. Lipids* 124 (2003) 123-134.
- [96] M.W. de Jager, G.S. Gooris, M. Ponec, J.A. Bouwstra, Lipid mixtures prepared with well-defined synthetic ceramides closely mimic the unique stratum corneum lipid phase behavior, *J. Lipid Res.* 46 (2005) 2649-2656.
- [97] A. Al-Amoudi, J. Dubochet, L. Norlen, Nanostructure of the epidermal extracellular space as observed by cryo-electron microscopy of vitreous sections of human skin, *J. Invest. Dermatol.* 124 (2005) 764-777.
- [98] G.C. Charalambopoulou, T.A. Steriotis, T. Hauss, A.K. Stubos, N.K. Kanellopoulos, Structural alterations of fully hydrated human stratum corneum, *Physica B: Condensed Matter* 350 (2004) E603-E606.
- [99] J.A. Bouwstra, F.E. Dubbelaar, G.S. Gooris, A.M. Weerheim, M. Ponec, The role of ceramide composition in the lipid organisation of the skin barrier, *Biochim. Biophys. Acta* 1419 (1999) 127-136.
- [100] J.A. Bouwstra, P.L. Honeywell-Nguyen, Skin structure and mode of action of vesicles, *Adv. Drug Deliv. Rev.* 54 Suppl 1 (2002) S41-55.
- [101] A. Ruettinger, M.A. Kiselev, T. Hauss, S. Dante, A.M. Balagurov, R.H.H. Neubert, Fatty acid interdigitation in stratum corneum model membranes: a neutron diffraction study, *Eur. Biophys. J.* 37 (2008) 759-771.
- [102] S. Mitragotri, Healing sound: the use of ultrasound in drug delivery and other therapeutic applications, *Nat. Rev. Drug Discov.* 4 (2005) 255-260.
- [103] Y.N. Kalia, A. Naik, J. Garrison, R.H. Guy, Iontophoretic drug delivery, *Adv. Drug Deliver. Rev.* 56 (2004) 619-658.
- [104] A.C. Williams, B.W. Barry, Penetration enhancers, *Adv. Drug Deliver. Rev.* 56 (2004) 603-618.
- [105] H. Trommer, R.H.H. Neubert, Overcoming the stratum corneum: the modulation of skin penetration. A review, *Skin Pharmacol. Physiol.* 19 (2006) 106-121.
- [106] J. Kalbitz, R.H.H. Neubert, W. Wohlrab, Modulation of drug penetration in the skin, *Pharmazie* 51 (1996) 619-637.
- [107] R.B. Walker, E.W. Smith, The role of percutaneous penetration enhancers, *Adv. Drug Deliver. Rev.* 18 (1996) 295-301.
- [108] B.M. Magnusson, K.A. Walters, M.S. Roberts, Veterinary drug delivery: potential for skin penetration enhancement, *Adv. Drug Deliv. Rev.* 50 (2001) 205-227.
- [109] G.K. Menon, S.H. Lee, Ultrastructural effects of some solvents and vehicles on the stratum corneum and other skin components: evidence for an "extended mosaic-partitioning model of the skin barrier", in: M.S. Roberts, K.A. Walters (Eds.) *Dermal Absorption and Toxicity Assessment*, Marcel Dekker, New York, 1998, pp. 727-751.
- [110] J. Crank, *The mathematics of diffusion*, 2 ed., Oxford, 1975.
- [111] S. Hansen, A. Henning, A. Naegel, M. Heisig, G. Wittum, D. Neumann, K.-H. Kostka, J. Zbytovska, C.-M. Lehr, U.F. Schaefer, In-silico model of skin penetration based on experimentally determined input parameters. Part I: Experimental determination of partition and diffusion coefficients, *Eur. J. Pharm. Biopharm.* 68 (2008) 352-367.
- [112] L. Duracher, L. Blasco, A. Abdel Jaoued, L. Vian, G. Marti-Mestres, Irradiation of skin and contrasting effects on absorption of hydrophilic and lipophilic compounds, *Photochem. Photobiol.* 85 (2009) 1459-1467.
- [113] D. Groen, G.S. Gooris, M. Ponec, J.A. Bouwstra, Two new methods for preparing a unique stratum corneum substitute, *Biochim. Biophys. Acta, Biomembranes* 1778 (2008) 2421-2429.

- [114] OECD, (2004), Guidance Document for the Conduct of Skin Absorption Studies, OECD Series on Testing and Assessment, No. 28, OECD Publishing. doi: 10.1787/9789264078796-en.
- [115] M. Hartmann, B.D. Hanh, H. Podhaisky, J. Wensch, J. Bodzenta, S. Wartewig, R.H.H. Neubert, A new FTIR-ATR cell for drug diffusion studies, *Analyst* 129 (2004) 902-905.
- [116] U. Guenther, M. Hartmann, S. Wartewig, R.H.H. Neubert, Diffusion of urea through membranes, *Diffusion Fundamentals* 4 (2006) 4.1-4.5.
- [117] R. Jenkins, R.L. Snyder, *Introduction to X-ray powder diffractometry*, Wiley, New York, 1996.
- [118] J.A. Bouwstra, M. Ponc, The skin barrier in healthy and diseased state, *Biochim. Biophys. Acta, Biomembranes* 1758 (2006) 2080-2095.
- [119] S. Wartewig, R.H.H. Neubert, Pharmaceutical applications of Mid-IR and Raman spectroscopy, *Adv. Drug Deliv. Rev.* 57 (2005) 1144-1170.
- [120] R. Singh, C. V. Raman and the Discovery of the Raman Effect, *Physics in Perspective (PIP)*. 4 (2002) 399-420.
- [121] R. Mendelsohn, C.R. Flach, D.J. Moore, Determination of molecular conformation and permeation in skin via IR spectroscopy, microscopy, and imaging, *Biochim. Biophys. Acta* 7 (2006) 923-933.
- [122] J. Barbillat, *Raman imaging*, Academic, 1996, pp. 175-200.
- [123] A. Whitley, F. Adar, Confocal spectral imaging in tissue with contrast provided by Raman vibrational signatures, *Cytometry, Part A* 69A (2006) 880-887.
- [124] P.J. Treado, M.D. Morris, Infrared and Raman spectroscopic imaging, *Appl. Spectrosc. Rev.* 29 (1994) 1-38.
- [125] B. Gotter, W. Faubel, R.H.H. Neubert, FTIR microscopy and confocal Raman microscopy for studying lateral drug diffusion from a semisolid formulation, *Eur. J. Pharm. Biopharm.* 74 (2010) 14-20.
- [126] T. Dieing, O. Hollricher, High-resolution, high-speed confocal Raman imaging, *Vib. Spectrosc.* 48 (2008) 22-27.
- [127] A. Bogner, P.H. Jouneau, G. Thollet, D. Basset, C. Gauthier, A history of scanning electron microscopy developments: Towards "wet-STEM" imaging, *Micron* 38 (2007) 390-401.
- [128] R. Reichelt, *Scanning Electron Microscopy Science of Microscopy*, in: P.W. Hawkes, J.C.H. Spence (Eds.), Springer New York, 2007, pp. 133-272.
- [129] D.J. Stokes, Recent advances in electron imaging, image interpretation and applications: environmental scanning electron microscopy, *Philos. Trans. R. Soc. London, Ser. A* 361 (2003) 2771-2787.
- [130] S.E. Kirk, J.N. Skepper, A.M. Donald, Application of environmental scanning electron microscopy to determine biological surface structure, *J. Microsc.* 233 (2009) 205-244.
- [131] A.M. Donald, Environmental scanning electron microscopy for the study of "wet" systems, *Curr. Opin. Colloid Interface Sci.* 3 (1998) 143-147.
- [132] D.C. Fenimore, C.M. Davis, High performance thin-layer chromatography, *Anal. Chem.* 53 (1981) 252A-254A, 256A, 258A, 262A, 265A-266A.
- [133] J. Sherma, Thin layer chromatography in environmental analysis, *Rev. Anal. Chem.* 14 (1995) 75-142.
- [134] T.H. Jupille, J.A. Perry, High-Performance Thin-Layer Chromatography: A Review of Principles, Practice, and Potential, *C R C Critical Reviews in Analytical Chemistry* 6 (1977) 325-359.
- [135] B. Aldhubaib, K. Mueen Ahmed, M. Attimarad, S. Harsha, High-performance thin layer chromatography: A powerful analytical technique in pharmaceutical drug discovery, *Pharmaceutical Methods* 2 (2011) 71-75.
- [136] A. Opitz, M. Wirtz, D. Melchior, A. Mehling, H. Kling, R.H.H. Neubert, Improved Method for Stratum Corneum Lipid Analysis by Automated Multiple Development HPTLC, *Chromatographia* 73 (2011) 559-565.
- [137] H. Farwanah, R.H.H. Neubert, S. Zellmer, K. Raith, Improved procedure for the separation of major stratum corneum lipids by means of automated multiple development thin-layer chromatography, *J. Chromatogr. B: Anal. Technol. Biomed. Life Sci.* 780 (2002) 443-450.
- [138] A. Weston, P.R. Brown, *HPLC and CE: Principle and Practice*, Academic, 1997.
- [139] V.R. Meyer, Introduction, in: *Practical High-Performance Liquid Chromatography*, John Wiley & Sons, Ltd, 2010, pp. 5-16.

-
- [140] H. Whatley, Basic principles and modes of capillary electrophoresis, Humana Press Inc., 2001, pp. 21-58.
- [141] F. Tagliaro, G. Manetto, F. Crivellente, F.P. Smith, A brief introduction to capillary electrophoresis, *Forensic Sci. Int.* 92 (1998) 75-88.
- [142] C.M. Boone, J.C.M. Waterval, H. Lingeman, K. Ensing, W.J.M. Underberg, Capillary electrophoresis as a versatile tool for the bioanalysis of drugs - a review, *J. Pharm. Biomed. Anal.* 20 (1999) 831-863.
- [143] W.G. Kuhr, Capillary electrophoresis, *Anal. Chem.* 62 (1990) 403R-414R.

Chapter 5

Characterization of lipid model membranes designed for studying impact of ceramide species on drug diffusion and penetration

M. Ochalek ^a, S. Heissler ^b, J. Wohlrab ^c, R.H.H. Neubert ^a

^a *Institute of Pharmacy, Martin Luther University, Halle (Saale), Germany*

^b *Institute of Functional Interfaces, Karlsruhe Institute of Technology, Eggenstein-Leopoldshafen, Germany*

^c *Department of Dermatology and Venereology, Martin Luther University, Halle (Saale), Germany*

(adapted from *Eur. J. Pharm. Biopharm.* 81 (2012) 113–120)

Abstract

The stratum corneum (SC) intercellular lipid matrix plays a crucial role in the skin barrier function. In the present study, lipid model membranes mimicking its phase behavior were prepared and characterized using different analytical techniques (i.a. SAXD, HPTLC, ESEM, confocal Raman imaging, ATR-FTIR spectroscopy) in order to obtain well-standardized model membranes for diffusion and penetration studies. The lipid model membranes should be used in the future for studying the impact of each ceramide species on the diffusion and penetration of drugs. The SAXD study confirmed that the lipids within artificial lipid systems are arranged similarly to the lipids in the human SC. The polarization microscopic and ESEM images showed the homogenous deposition of lipids on the polycarbonate filter. Both the HPTLC and confocal Raman imaging studies proved the homogenous distribution of individual lipid classes within the lipid model membranes. First *in vitro* diffusion experiments (performed using an ATR-FTIR diffusion cell) of the hydrophilic compound, urea, revealed that the lipid model membrane represents even stronger diffusion barrier than the human SC.

1. Introduction

The main penetration barrier for topically administered drugs and other substances (e.g. water) is formed by the outermost layer of the skin, the stratum corneum (SC) [1]. It consists of 10–25 layers of parallel to the skin surface corneocytes embedded in a lipid matrix and ranges from 10 to 15 μm in thickness in a dry state, however, swells to several times this thickness in a fully hydrated state [2]. Of special interest is the organization of the SC intercellular lipid matrix, since the intercellular route of transport through the normal intact SC is thought to be the most preferable one [3]. Unlike other biological membranes, the SC does not contain phospholipids. In return, the SC intercellular lipid matrix is enriched in ceramides, free fatty acids, cholesterol and its derivatives organized in lamellar phases [4]. One of its main components are ceramides, which are regarded as fundamental compounds in functioning of the SC barrier [5]. Recent reports indicate the existence of 12 classes of ceramides that have been isolated from the human SC [6]. As found in the former studies, a crucial role in the internal membrane structure formation plays ceramide [AP] due to its headgroup polarity [7-9]. It is assumed that the other constituent of the SC intercellular lipid matrix, which influences to a high degree the lipid assembly and the barrier properties of the SC, is the acylceramide, ceramide [EOS] [10]. To deliver insight into the role of each individual lipid species on the functioning and maintaining of the SC barrier, well-defined artificial SC lipid systems have been produced as oriented multilamellar membranes [8, 11, 12]. Similar approach was also presented in other studies [13-16], however, lipid systems used there were much more complex.

In the present study, basic lipid model membranes composed of only 4 constituents (including Cer [AP] and Cer [EOS]) were prepared on porous substrates. Use of such elementary systems helps to elucidate the impact of each lipid compound, particularly the different ceramide species, on the diffusion and penetration of drugs and other substances of interest. This routine is complementary to the previous studies on the influence of each lipid component on the nanostructure of the SC intercellular lipid matrix [10-12, 17]. Therefore, it is very important to characterize and to standardize such lipid model membranes. The lamellar organization of the prepared lipid model membranes and distribution of lipids within them were examined using various analytical techniques, including small angle X-ray diffraction, high performance thin layer chromatography and microscopic methods (i.a. environmental scanning electron microscopy and confocal Raman imaging). The barrier properties of these systems were investigated by means of a comparison of diffusion of the hydrophilic compound, urea, through lipid model

membranes and the human SC isolated from the full thickness skin. The diffusion experiments were conducted using the ATR-FTIR diffusion cell with online detection of the diffusing and penetrating agents, constructed by the technical department of our institute.

2. Materials and methods

2.1. Materials

Synthetic Cer [EOS] and Cer [AP] were generously provided by Evonik Goldschmidt (Essen, Germany). Palmitic acid, sodium cholesteryl sulfate and urea were purchased from Sigma-Aldrich Chemie GmbH (Steinheim, Germany) and cholesterol from Sigma Chemical CO. (St. Louis, USA). Methanol, ethanol, chloroform, acetone, ethyl acetate and n-hexane were obtained from Merck (Darmstadt, Germany). Nuclepore polycarbonate membrane filters (diameter 25 mm, pore size 50 nm) were purchased from Whatman (Kent, UK). Solvents used for the sample preparation, extraction and the high performance thin layer chromatography procedure were of analytical grade.

2.2. Preparation of model lipid membranes

Two used quaternary lipid mixtures were composed of: Cer [AP]/Chol/PA/ChS (55/25/15/5, m/m), referred to as Membrane I, and Cer [AP]/Cer [EOS]/Chol/PA (10/23/33/33, m/m), referred to as Membrane II. Chemical structures of these lipids are presented in Fig. 1. Appropriate quantities of individual lipids were dissolved in a mixture of chloroform/methanol (2/1, v/v). Because of the incompatibility of chloroform and Nuclepore polycarbonate filters, the organic solvents were evaporated under a stream of nitrogen, and the lipids were re-dissolved in a mixture of n-hexane/ethanol (2/1, v/v). A total lipid concentration was 5 mg/ml. Afterward, the lipid mixtures were applied onto the filter using Automatic TLC Sampler 4 (Camag, Muttenz, Switzerland) with a specially built holder, at a very low flow rate (80 nl/s) and under the stream of nitrogen. It resulted in an immediate evaporation of organic solvents from the filters and a fast arrangement of lipid bilayers. The sprayed area was a square with dimensions 13 x 13 mm (i.e. area of 169 mm²), and the volume of lipid solution used was 100 or 200 μ l. The prepared membranes were subjected to an annealing procedure, which consisted of heating the samples at 80 °C or 70 °C (Membrane I and Membrane II, respectively) for a period of 30

min and a subsequent cooling down step (to room temperature, 25 °C). It enhanced the multilamellar orientation of lipids and decreased the mosaicity of samples.

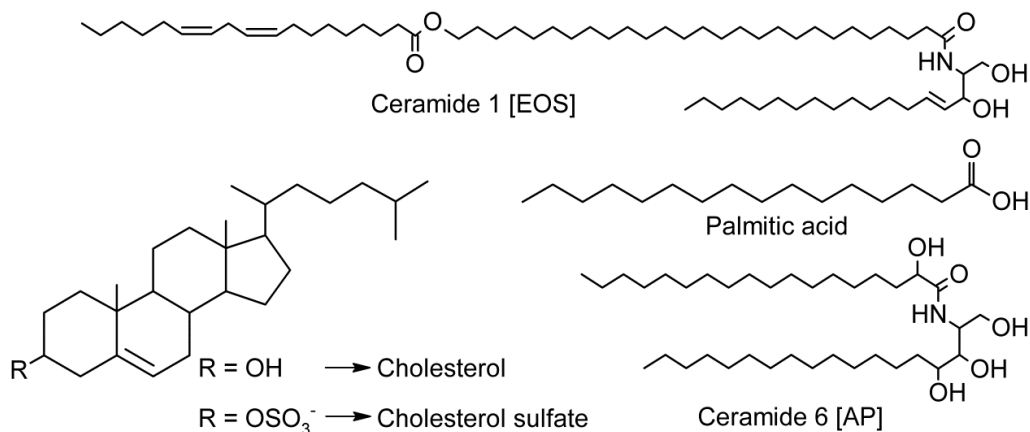


Fig. 1. Chemical structures of constituents of lipid model membranes.

2.3. Small angle X-ray diffraction studies

The lamellar organization of artificial lipid membranes was investigated using small angle X-ray diffraction (SAXD). The X-ray diffraction experiments were carried out using the Stoe Stadi MP Powder diffraction system (STOE & Cie GmbH, Darmstadt, Germany) in the Bragg–Brentano mode with the linear PSD detector. The measurements were taken at standard ambient temperature (25 °C), by placing a sample in vertical position. The intensity of the scattered X-rays (in arbitrary units) was plotted as a function of the scattering vector q (in \AA^{-1}). Its relation to the scattering angle is given by the equation: $q = (4\pi \sin \theta)/\lambda$, where θ is the scattering angle and λ is the wavelength of the primary beam. Each diffraction pattern consists of a series of equidistant peaks. The lamellar repeat distance (or lamellar periodicity, d) is calculated by using the equation: $d = 2n\pi/q_n$, where n is a diffraction order of the peak and q_n gives its location [18].

2.4. High performance thin layer chromatography studies

The distribution of lipids within the synthetic model lipid membranes was examined using high performance thin layer chromatography (HPTLC) technique. Membrane I and Membrane II were divided into five parts by cutting out five pieces (Area 1 = 16.6 mm², Area 2 = 31.2 mm², Area 3 = 20.1 mm², Area 4 = 37.8 mm² and Area 5 = 63.3 mm²) using a

puncher (Fig. 2A). Next, an extraction of lipids was conducted by shaking the samples for 60 min in n-hexane/ethanol 2/1 (v/v) mixture. Afterward, the solvents were evaporated under a stream of nitrogen, and the lipids were re-dissolved in chloroform/methanol 2/1 (v/v). The samples prepared in this manner were then applied on the HPTLC plate using ATS 4 (Camag, Muttenz, Switzerland). Next, the plate was developed using AMD 2 device (Camag, Muttenz, Switzerland). The principle of this procedure is that the HPTLC plate is developed repeatedly (in successive runs) in the same direction, and each successive run uses a solvent of lower elution strength than that of the one used before, so in result a stepwise gradient elution takes place. In this study, the HPTLC plates were developed in 16 runs (Fig. 2B). After the development, the plates were immersed in 10% CuSO_4 solution and charred for 20 min at 150 °C (derivatization). Finally, the densitometric evaluation was performed using TLC Scanner 3 (Camag, Muttenz, Switzerland). Integration of peaks' areas and quantification of lipids' amounts in each area of the lipid membrane were performed using CATS software (Camag). A similar HPTLC procedure was previously described by Farwanah et al. [19] and Opitz et al. [20].

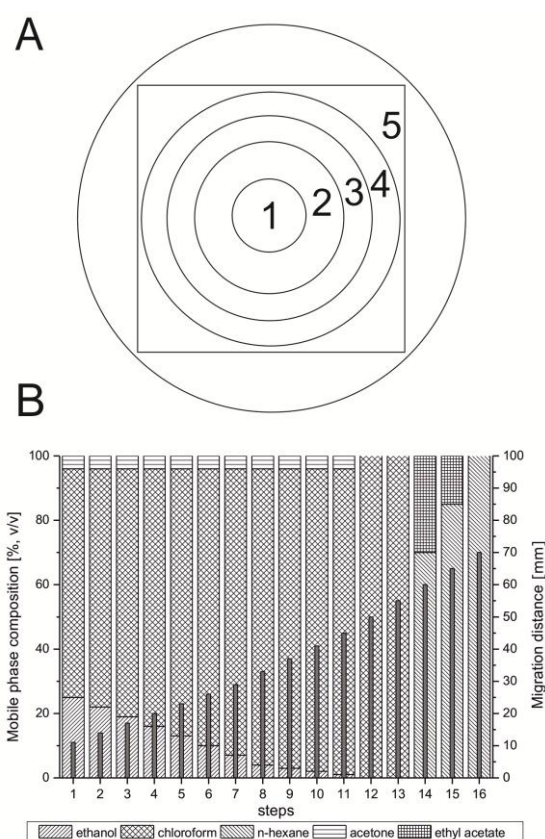


Fig. 2. (A) Graphical description of a lipid model membrane deposited on a filter marked with 5 areas used in HPTLC studies. (B) HPTLC elution system composed of 16 gradient steps.

2.5. Microscopic studies

The arrangement and deposition of lipids on the filters were also determined by using three different microscopic techniques, namely: polarization microscopy, environmental scanning electron microscopy (ESEM) and confocal Raman imaging.

The images of lipid model membranes were obtained using a polarizing microscope Axiolab (Carl Zeiss, Goettingen, Germany).

The ESEM measurements were performed using Philips ESEM XL30 FEG (FEI, Hillsboro, USA) equipped with a unique gaseous secondary electron detector (GSED). The samples were measured in so-called WET-Mode and at a voltage of 12 kV. The ESEM technique is characterized by a very high spatial resolution (2 nm) and a possibility of the observation of samples under dynamic conditions (at different pressures and temperatures). Use of water vapor as a standard gas in the microscope chamber allows to examine hydrated specimens in their natural state.

Raman imaging experiments were conducted using confocal Raman microscope Senterra (Bruker Optics, Ettlingen, Germany). A diode laser (785 nm, 100 mW) was used as an excitation source. Its beam was sent through a 20x Olympus MPlan LD objective (NA = 0.4). The backscattered radiation collected and collimated by the same objective was focused through a 25 μm pinhole onto CCD (charge-coupled device) detector. Since only light originating from the focal plane has its focus within the pinhole and thereby reaches the detector, one can obtain a signal of interest without blurred signals from out-of-focus planes. It is an essential feature of confocal imaging techniques. The Raman spectra were taken in the range 75-3200 cm^{-1} with a spectral resolution of 9 cm^{-1} . The integration times of the Raman spectra amounted to 120 s (each point was measured twice). In order to investigate the distribution of individual lipid species within the surface of the lipid model membranes, areas of 0.107 mm^2 and 0.126 mm^2 in the case of Membrane I and Membrane II, respectively, comprising 64 measuring points were scanned. The Raman data evaluation was performed using the OPUS software (Bruker Optics, Ettlingen, Germany).

2.6. Diffusion studies

Diffusion experiments were carried out using Vertex 70 FTIR spectrometer (Bruker Optics, Ettlingen, Germany) with a built-in ATR-FTIR diffusion cell constructed by the technical department of our institute. Its special features are diffusion area of 0.18 cm^2

and maintenance of the constant temperature (32 °C) throughout the whole experiment. An ATR crystal, ZnSe ($n = 2.4$, $d = 20$ mm), was horizontally oriented with an angle of incidence of 45°. Each IR spectrum consisted of 32 scans taken in the range 680–4000 cm^{-1} with a resolution of 2 cm^{-1} . The ATR-FTIR diffusion cell combines the advantages of the ATR-method with the Franz-type diffusion cell. It is a non-destructive procedure, which provides online detection of permeating agents (“in situ”) and enables monitoring of multiple species simultaneously. Other characteristics and a precise buildup of the ATR-FTIR diffusion cell were reported previously [21-23]. As model membranes, human SC and artificial lipid system, Membrane I (Cer [AP]/Chol/PA/ChS = 55/25/15/5, m/m) with thickness of 3 μm , were used. The SC was isolated from the full thickness human skin (two female donors; samples taken from back, abdomen and thigh), which was acquired after cosmetic surgery. Prior to the isolation of the SC, the subcutaneous fat tissue was removed from the skin samples. The protocol of this study was approved by the Ethics Committee of the Martin Luther University Halle-Wittenberg (Germany). The isolation procedure was in accordance with a method depicted by Kligman and Christophers [24]. After separation of the SC from the epidermis (incubation in 0.1% trypsin solution in PBS buffer, pH 7.4, for 12–24 h at 32 °C), the SC samples were stored at –26 °C until use. As model drug, 10% (m/m) water solution of urea was used and the acceptor compartment was filled with 50 μl of distilled water. Before adding the donor solution into the donor chamber, a membrane (human SC or Membrane I) was mounted in the diffusion cell and equilibrated for a period of 15 min. All diffusion experiments were conducted under occlusive conditions. Permeability parameters were obtained from plotting the cumulative permeated amount per cm^2 versus time. Diffusion coefficients were acquired by fitting the normalized diffusion data using Eq. (1), which was derived from the Fick’s second law of diffusion by fitting appropriate initial and boundary conditions and using the Laplace transformation:

$$C = C_0 \times \operatorname{erfc} \left(\frac{a}{\sqrt{t}} \right) \quad (1)$$

where $a = l/(2\sqrt{D})$, C is the concentration of urea in the acceptor phase, C_0 is the initial concentration of urea, D is the diffusion coefficient and l is the diffusional pathlength. A partition coefficient between the membrane and the donor solution, $K_{m/d}$, was calculated using equation: $k_p = K_{m/d} \times D/l$, where k_p is the permeability coefficient.

3. Results and discussion

3.1. Lamellar organization of lipid model membranes

The lamellar arrangement of lipid model membranes plays a key role in the SC barrier function. To check the organization of lipids within lipid model membranes, SAXD studies were carried out. The X-ray diffraction patterns of Membrane I are presented in Fig. 3. In the case of both membranes (for both used lipid mixture volumes), two lamellar phases were present, one with shorter lamellar repeat distance (referred to as the small phase) and one with longer periodicity (referred to as the main phase). Membrane I (spraying of 100 μl of the lipid mixture) showed the main phase with a periodicity of $46.53 \pm 0.06 \text{ \AA}$, of which the 1st, 2nd, 3rd, 4th, 6th, 7th and 8th diffraction peaks were detected at $q = 0.14, 0.28, 0.41, 0.55, 0.81, 0.95, 1.09 \text{ \AA}^{-1}$, and the small phase with the lamellar repeat distance of $41.73 \pm 0.13 \text{ \AA}$, of which the 1st, 2nd, 3rd, 5th and 6th diffraction peaks were located at $q = 0.16, 0.31, 0.46, 0.76$ and 0.91 \AA^{-1} . Use of 200 μl of the lipid mixture (Membrane I) resulted in the similar lamellar organization, that is the main phase with the periodicity of $46.50 \pm 0.03 \text{ \AA}$ (1st, 2nd, 3rd, 4th, 6th, 7th and 8th diffraction peaks at $q = 0.13, 0.27, 0.41, 0.55, 0.81, 0.95$ and 1.08 \AA^{-1}) and the small phase with the lamellar spacing of $41.37 \pm 0.06 \text{ \AA}$ (1st, 2nd, 3rd, 5th and 6th diffraction reflections at $q = 0.15, 0.30, 0.45, 0.76$ and 0.91 \AA^{-1}). Membrane II (100 μl) showed the main phase with the periodicity of $45.62 \pm 0.71 \text{ \AA}$, of which the 1st, 2nd, 3rd and 4th diffraction peaks were situated at $q = 0.14, 0.28, 0.41, 0.53 \text{ \AA}^{-1}$ and the small phase with the lamellar repeat distance of $41.90 \pm 0.06 \text{ \AA}$, of which the 1st, 2nd and 3rd diffraction reflections were located at $q = 0.15, 0.30$ and 0.45 \AA^{-1} . The diffraction pattern of Membrane II (200 μl) was also characterized by the presence of the main phase with the lamellar spacing of $45.77 \pm 0.47 \text{ \AA}$ (1st, 2nd, 3rd and 4th diffraction peaks at $q = 0.14, 0.28, 0.41$ and 0.53 \AA^{-1}) and the small phase with the periodicity of $42.21 \pm 0.06 \text{ \AA}$ (1st, 2nd and 3rd diffraction peaks at $q = 0.15, 0.30$ and 0.45 \AA^{-1}). In addition, in the case of both lipid model membranes, two reflections of phase separated crystalline cholesterol were present at $q = 0.18$ and 0.36 \AA^{-1} . As can be deduced from the above listed results, the periodicity of the main phase for Membrane II was slightly shifted to a lower value, approx. 45.70 \AA , when compared to Membrane I ($d_{\text{main phase}} \sim 46.50 \text{ \AA}$). On the other hand, the lamellar repeat distance of the small phase was reduced in the case of Membrane I and amounted to approx. 41.55 \AA (for Membrane II $d_{\text{small phase}} \sim 42.05 \text{ \AA}$). The next interesting features of X-ray diffraction patterns of both lipid membranes were the number of diffraction orders and the intensity of diffraction reflections. The

diffraction pattern of Membrane I showed eight peaks of the main phase and six peaks of the small phase, except for the 5th and the 4th peak of the main and the small phase, respectively, where the intensities were too low to make these reflections detectable. Membrane II showed only four peaks assigned to the main phase and three peaks assigned to the small phase. The intensity of diffraction reflections was much higher for Membrane I (by few factors when compared to Membrane II). Moreover, the difference in the peaks' intensities for Membrane I prepared using 100 μl and 200 μl was also apparent, namely Membrane I prepared using bigger volume of the lipid mixture showed diffraction reflections with higher intensity. For Membrane II, the intensity of the diffraction peaks was similar for both systems prepared using different volumes of the lipid solution. Additionally, the level of the phase separated cholesterol was similar in the case of both lipid model membranes.

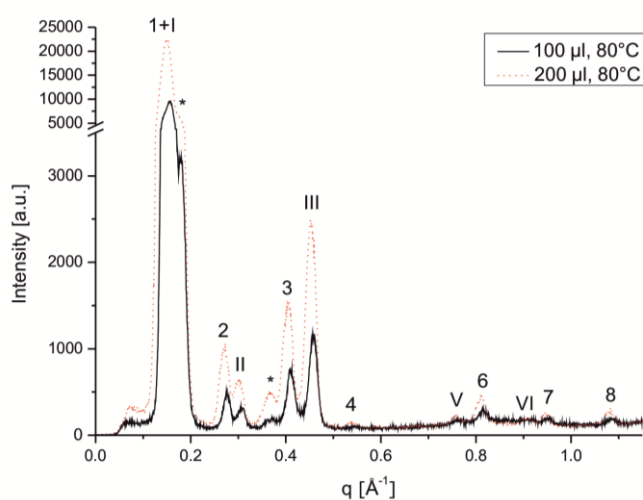


Fig. 3. X-ray diffraction patterns of Membrane I (100 μl and 200 μl of a lipid mixture). Arabic and Roman numbers denote orders of diffraction of the main and the small phase, respectively. Asterisks stand for phase separated crystalline cholesterol.

The aim of this study was to investigate the lamellar organization of artificial lipid membranes and thereby to standardize the preparation of the model membranes and to confirm the similarity of the structure of these model systems to the native SC. Both Membrane I and Membrane II were characterized by the presence of two phases, the main and the small phase. In terms of the lamellar periodicity, the differences between those phases were statistically significant. Similar phase behavior of the lipid membrane consisting of Cer [AP]/Chol/PA/ChS (55/25/15/5, m/m) was previously reported by Ruettinger et al. [25], where $d = 45.6 \text{ \AA}$. In the basic membranes used in this study, no

long periodicity phase (LPP) was observed. The reason of the absence of the LPP might be the simplicity of the model lipid membranes used in this project, which were composed of only four individual lipid species and/or the absence or too low concentration of Cer [EOS] within Membrane I and Membrane II, respectively. From previous studies, it is known that Cer [EOS] plays a crucial role in the formation of the LPP [10]. Groen et al. [16] used equimolar mixtures of Chol:synthCer:FFA and have reported the presence of the LPP with the lamellar spacing of ~ 120 Å. However, in their study, the synthCer fraction was a mixture of six different ceramides and FFA fraction was composed of seven different free fatty acids. In the present study, it was proven that the lipid membrane consisting in 55% (m/m) of Cer [AP] created a stable lamellar structure with a small amount of the phase separated crystalline Chol, which appearance can be ascribed to the limited solubility of Chol in the lipid phase. Lipids within Membrane II that main characteristics were the following: lower concentration of Cer [AP] (10%, m/m), the presence of Cer [EOS] (23%, m/m) and the absence of ChS, formed similarly lamellar structures. Crystalline Chol domains were also present, only here the reflections assigned to the main and the small phase were much weaker and were not that numerous. It indicates that in the case of Membrane II, smaller fraction of the lipids contributed to the organization of the lamellar phases.

3.2. Lipid distribution within lipid model membranes

The HPTLC procedure was performed to investigate the distribution of individual lipid species within lipid model systems. Lipids extracted from all five parts of the lipid model systems were separated and quantitatively analyzed by means of a comparison with separated lipids from the control sample (i.e. lipid mixture used for the preparation). All lipid species were present in all five parts of the lipid model membranes (Fig. 4A and B). Individual lipid species were identified by comparing their retention factor (R_f) values to the R_f of standard lipids. The retention factors of ChS, Chol and PA amounted to 0.11, 0.74 and 0.81, respectively. Cer [AP] was separated into two stereoisomers, namely D- and L-isomers with retention factors of 0.26 and 0.31. The R_f of Cer [EOS] amounted to 0.49. The quantification of lipid amounts was based on the densitometric evaluation. The calibration curves of all lipids were not linear and were fitted using the Michaelis–Menten function [19]. The quantitative results are presented in Fig. 4A and B. The distribution of lipids within Membrane I is shown in Fig. 4A. The quantities of lipids per mm^2 evaluated in all parts of Membrane I amounted to 2.94 ± 0.46 μg , 1.08 ± 0.24 μg , 0.80 ± 0.22 μg and

$0.27 \pm 0.05 \mu\text{g}$ (MEAN \pm SD, $n = 4$) for Cer [AP], Chol, PA and ChS, respectively. The analysis of variance (ANOVA) with *post hoc* comparison made using Tukey's test proved that the means of the amount/area of all lipid species, within first three areas (total area of 67.9 mm^2), were not significantly different ($\alpha = 0.05$). Fig. 4B shows the distribution of lipids within Membrane II. The amounts of lipids per mm^2 evaluated in all parts of Membrane II amounted to $0.48 \pm 0.04 \mu\text{g}$, $0.63 \pm 0.06 \mu\text{g}$, $1.16 \pm 0.13 \mu\text{g}$ and $1.29 \pm 0.07 \mu\text{g}$ (MEAN \pm SD, $n = 4$) for Cer [AP], Cer [EOS], Chol and PA, respectively. The ANOVA (with Tukey's test) proved that the means of the amount/area of Cer [AP], within first four areas (total area of 105.7 mm^2) and in the case of other lipids in all five areas (total area of 169 mm^2), were not significantly different ($\alpha = 0.05$).

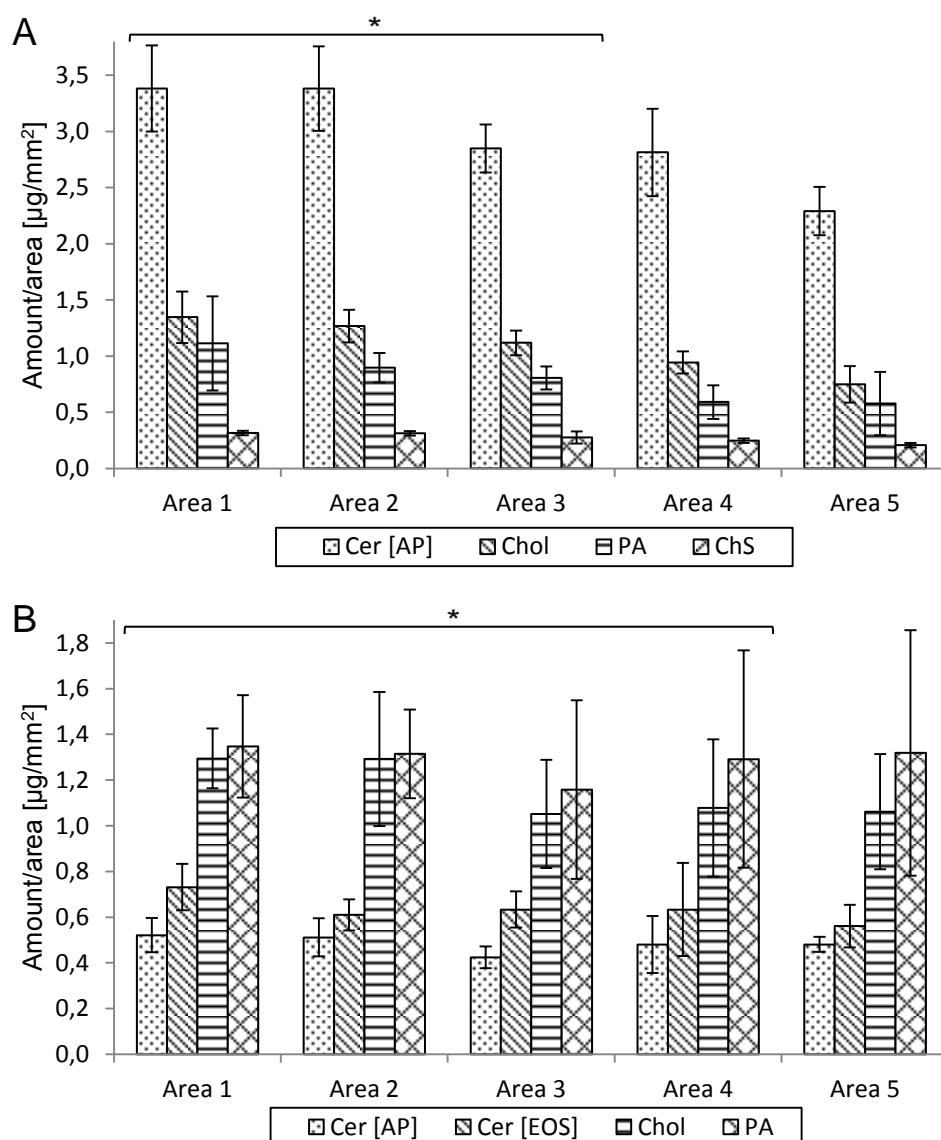


Fig. 4. Distribution of lipids within (A) Membrane I and (B) Membrane II - the amount of lipids per mm^2 (data represent MEAN \pm SD, $n = 4$; * indicates no significant difference at $p < 0.05$).

The aim of this study was to examine the distribution of lipids within lipid model systems. To interpret the data properly, it has to be taken into account that only a small part of the lipid membrane took part in the further diffusion studies. In the case of the ATR-FTIR diffusion cell, it was an area of only 18.1 mm². Therefore, it can be assumed that in terms of the diffusion studies, the most important role plays the central part of the artificial lipid system. Both Membrane I and Membrane II showed the homogenous distribution of individual lipid species within the central part of the lipid membrane. The total area of homogeneously distributed lipid species within the lipid membrane amounted to 67.9 mm² and 105.7 mm² in the case of Membrane I and Membrane II, respectively. It can be concluded that the lipid model membranes used in this study could have been prepared in a standardized way in terms of the lipid distribution and, therefore, were suitable model membranes to be tested and to be compared with the human SC in the diffusion and penetration studies.

The deposition of lipids on the polycarbonate filters was investigated using microscopic techniques: polarization microscopy and ESEM. The microscopic images of Membrane I and Membrane II obtained by a polarizing microscope are shown in Fig. 5A–C and D–F, respectively. Fig. 6 displays electron micrographs of Membrane I (A), Membrane II (B) and a polycarbonate filter not covered with lipids (C and D). The polarization microscopic and ESEM images complement one another. One can obtain the information about the surface of the lipid membrane on both the macro- (polarization microscopy) and the micro-scale (ESEM). Images shown in Fig. 5 confirm the homogenous deposition of lipids on the polycarbonate filter. The lipids formed continuous layer with no areas not covered with the lipid mixture. Moreover, the images show only a small number of crystals originating from phase separated Chol. In the case of the ESEM images, the difference in the surface appearance between the lipid membrane and the membrane filter not covered with lipids is presented. In Fig. 6C and D, the pores of the filter can be seen as small dark spots with white rings. On the other hand, Fig. 6A and B shows the surface of the continuous structure composed of the lipid mixture with no apparent pores. The surfaces of Membrane I and Membrane II differ from each other (clearly visible in polarization microscopic and ESEM images). It might be caused by the different composition of the lipid membranes (the presence of Cer [EOS] in Membrane II), resulting in the distinctive phase behavior (confirmed earlier by the SAXD).

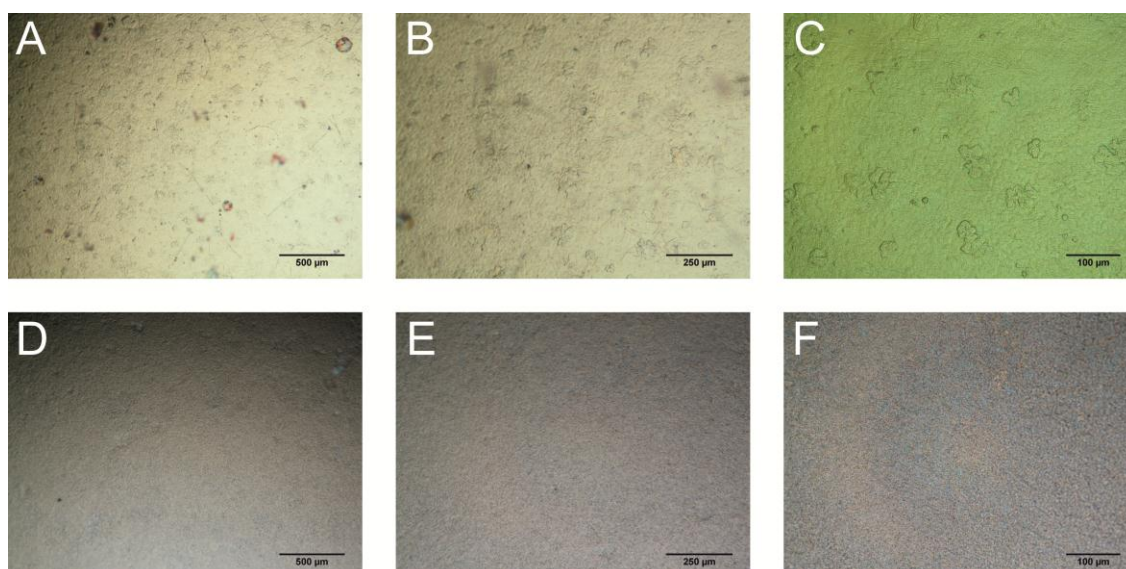


Fig. 5. Microscopic images of lipid model systems: Membrane I (A–C) and Membrane II (D–F) acquired by a polarizing microscope.

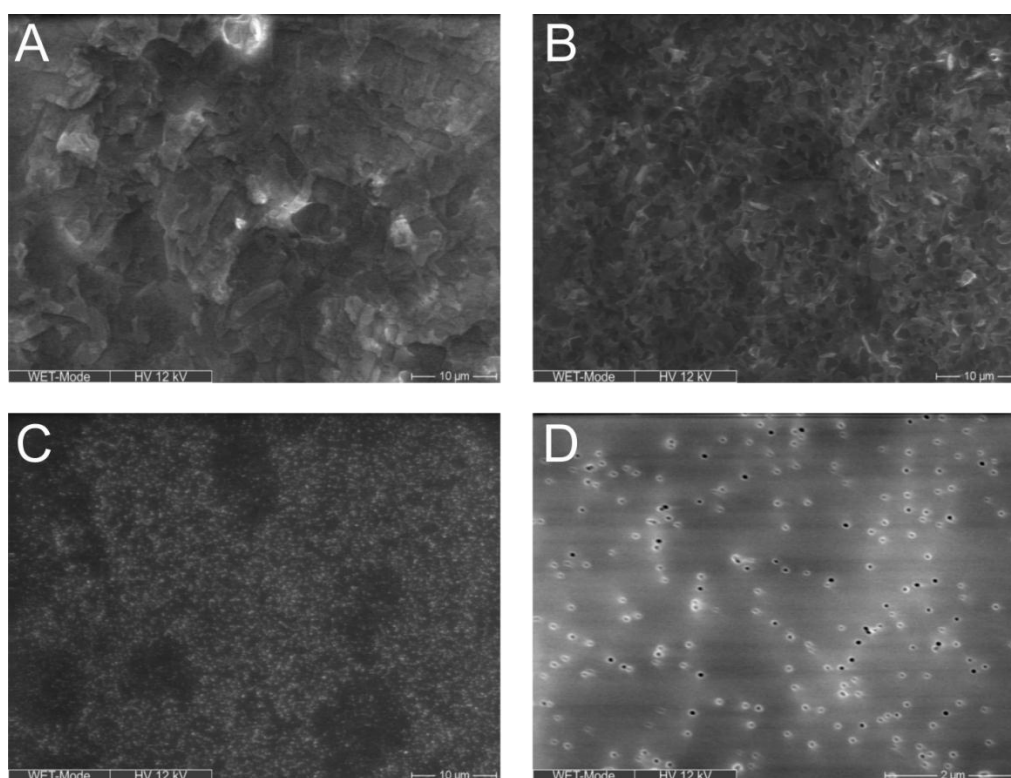


Fig. 6. Electron micrographs of Membrane I (A), Membrane II (B) and a polycarbonate filter not covered with lipids (C and D).

The distribution of lipids within lipid model membranes was also examined using confocal Raman imaging technique. The Raman spectra with indicated characteristic peaks of individual components of lipid model membranes are given in Fig. 7.

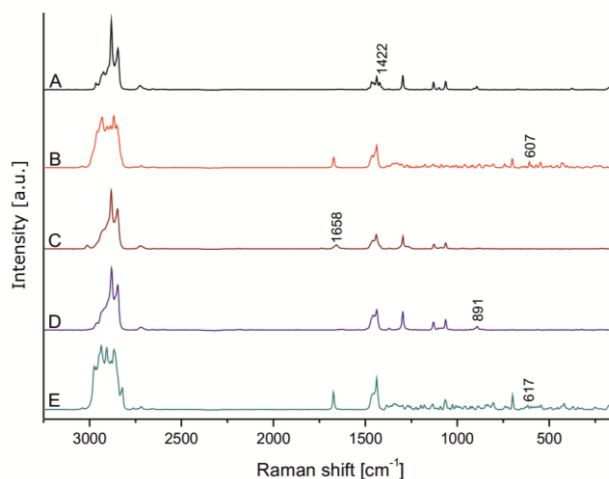


Fig. 7. Raman spectra of components of lipid model membranes: (A) PA, (B) Chol, (C) Cer [EOS], (D) Cer [AP] and (E) ChS. Wavenumbers presented on the graph indicate characteristic peaks used for the evaluation of individual lipid species.

The spectra of Chol and ChS show the peaks that can be assigned to the alicyclic stretching vibrations at 607 cm⁻¹ and 617 cm⁻¹, respectively. The $\delta(\text{CH}_2)$ and $\delta(\text{CH}_3)_{\text{asym}}$ vibrations of PA are located around 1422 cm⁻¹, and the $\nu(\text{C}=\text{C})$ band of Cer [EOS] can be found at 1658 cm⁻¹. In the case of Cer [AP], the characteristic peak is located at 891 cm⁻¹ and can be assigned to the $\nu(\text{CC})$ vibration. These characteristic bands were used for the integration procedure and thereby the evaluation of the amount of the lipid species within the surface of the lipid model membranes. The results of the evaluation procedure are presented in Fig. 8A and B. This figure contains Raman images (contour maps) displaying the distribution of individual lipid species within lipid model membranes. Fig. 8A shows the distribution of Cer [AP], Chol, PA and ChS within Membrane I, and Fig. 8B demonstrates the distribution of Cer [AP], Cer [EOS], Chol and PA within Membrane II. A normalized integrated intensity of lipids' specific bands is reflected by means of a color scale (starting with black = 0 and ending with red = 1). Raman images confirm the results of the polarization microscopy and ESEM experiments. The whole area of the polycarbonate filter is covered with lipid systems. Individual lipids are distributed homogeneously, with single spots characterized by bigger amounts of lipids. It has to be taken into account that the color scale reflects the normalized intensity. Therefore, the amounts of different lipids are relative. One can obtain only the information about the distribution of lipids, not about their absolute quantities.

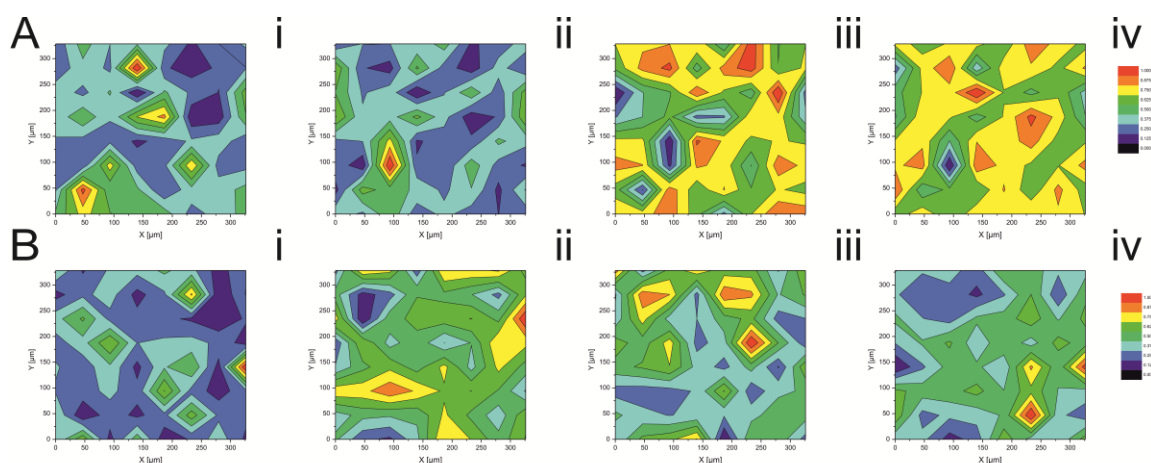


Fig. 8. Raman images (contour maps) displaying the distribution of constituents of (A) Membrane I: (i) Cer [AP], (ii) Chol, (iii) PA and (iv) ChS; and (B) Membrane II: (i) Cer [AP], (ii) Cer [EOS], (iii) Chol and (iv) PA. A normalized integrated intensity of lipids' specific bands is color-coded.

3.3. Diffusion of urea examined using the ATR-FTIR diffusion cell

Fig. 9 shows the ATR-FTIR spectra of the water solution of urea in the range 1350–1900 cm^{-1} acquired in the time course of the diffusion process with indicated urea-specific IR band at 1466 cm^{-1} , i.e. $\nu(\text{CN})$. At the beginning of the diffusion process, the IR spectrum of the pure acceptor phase (distilled water) was observed. With the elapsing time of the experiment, the absorbance of the urea-specific IR bands increased. A concentration of urea in the acceptor phase was calculated using the multivariate analysis Quant2 OPUS software in the spectral range from 1017 to 3718 cm^{-1} . The diffusion profiles of urea are presented in Fig. 10. As can be clearly seen in this figure, the diffusion profiles of urea through the isolated human SC and Membrane I are not alike. In the case of the artificial lipid membrane, the diffusion was much slower with a well indicated lag time.

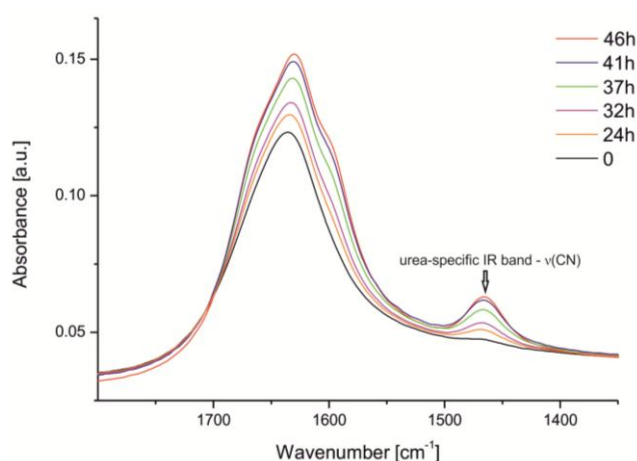


Fig. 9. IR spectra of the water solution of urea in the range 1350–1900 cm^{-1} with indicated urea-specific IR band at 1466 cm^{-1} . The spectra were acquired in the time course of the diffusion process.

The physical properties and permeability parameters of urea are summarized in Table 1. The lag time (T_L) in the case of the native SC was much shorter than the T_L value of Membrane I, whereas the steady state flux (J_{ss}) and the permeability coefficient (k_p) of the model membrane were two times lower than the corresponding values in the case of the SC. The values of the diffusion coefficient (D) of urea for the native and the model membrane differed significantly. The D value of urea in the case of the human SC was higher than the D of urea for Membrane I by a factor of 100 and was lower than the D values of urea for the human SC reported by Guenther et al. [23] and Hartmann et al. [21] by a factor of 23 and 55, respectively. The differences in the D values in the case of the human SC are most likely caused by high inter- and intra-variability of the human SC samples [1]. The low D values, both for the SC and Membrane I, show that the diffusion of urea (small hydrophilic molecule) through the lipophilic membranes is a slow process. Both membranes represent a strong diffusion barrier for small hydrophilic substances, such as urea. From all permeability results, it can be concluded that the artificial lipid membrane, i.e. Membrane I, represents the stronger diffusion barrier than the native SC. It has to be stressed once more that the model lipid membranes used in this study were very simple systems when compared to the SC. It seems that the artificial lipid membrane containing Cer [AP] had tighter structure than the human SC and, therefore, showed very strong barrier properties for hydrophilic compounds, such as urea.

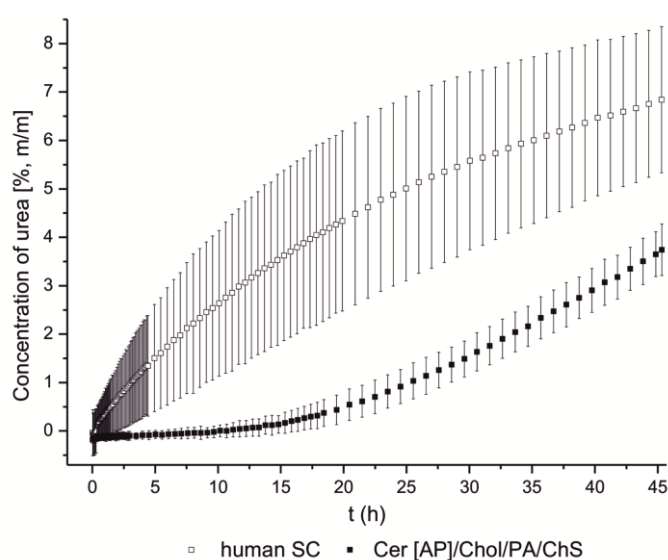


Fig. 10. Concentration of urea permeated through the human SC (two female donors; samples taken from abdomen, thigh and back) and Membrane I. Error bars show the standard deviation ($n = 3$).

Table 1 Physical properties and permeability parameters of urea – *in vitro* study.

Parameter	Urea	
	human SC	Cer [AP]/Chol/PA/ChS
Molar mass [g/mol]		60.06
$\log P$		-2.11
pK_a (25°C)		0.18
J_{ss} [$\mu\text{g}/(\text{cm}^2\text{h})$]	7.90 ± 4.97 (E+02)	3.77 ± 0.47 (E+02)
T_L [h]	2.95 ± 0.88 (E-01)	1.84 ± 0.34 (E+01)
k_p [cm/h]	7.90 ± 4.97 (E-03)	3.77 ± 0.47 (E-03)
D [cm^2/h]	4.40 ± 2.56 (E-08)	4.04 ± 0.64 (E-10)
$K_{m/d}$	1.62 ± 0.36 (E+02)	2.86 ± 0.60 (E+03)

Permeability data represent MEAN \pm SD (n = 3).

4. Conclusions

To sum up, it has been shown in this study that the lipid model membranes prepared using a described preparation method are reproducible and of good quality. The microscopic techniques confirmed that the lipids deposited on the polycarbonate filter formed a continuous lipid layer covering the whole sprayed area of the filter. The HPTLC and confocal Raman imaging experiments confirmed the uniform distribution of the individual lipid species on the filter. From the SAXD results, it can be concluded that the lipids formed the lamellar structure with two present lamellar phases. The diffusion studies using small hydrophilic compound (i.e. urea) revealed that the artificial lipid system used in the experiment (i.e. Membrane I) showed very strong barrier properties, even stronger than the isolated human SC, which can be ascribed to its very simplistic composition, when compared to a very complex structure of the native SC. Proposed approach with simple lipid model systems can be used in the future to study the impact of the different ceramide species on the diffusion and penetration of drugs and other substances of interest.

Acknowledgements

A scholarship granting for Michal Ochalek by the “Graduiertenförderung des Landes Sachsen-Anhalt” is gratefully appreciated. The authors would like to thank Frank Syrowatka for his cooperation and support with the ESEM measurements.

References

- [1] P.W. Wertz, B. van den Bergh, The physical, chemical and functional properties of lipids in the skin and other biological barriers, *Chem. Phys. Lipids* 91 (1998) 85-96.
- [2] J.A. Bouwstra, A. de Graaff, G.S. Gooris, J. Nijssse, J.W. Wiechers, A.C. van Aelst, Water distribution and related morphology in human stratum corneum at different hydration levels, *J. Invest. Dermatol.* 120 (2003) 750-758.
- [3] M.L. Williams, P.M. Elias, The extracellular matrix of stratum corneum: role of lipids in normal and pathological function, *Crit. Rev. Ther. Drug Carrier Syst.* 3 (1987) 95-122.
- [4] N.Y. Schurer, G. Plewig, P.M. Elias, Stratum corneum lipid function, *Dermatologica* 183 (1991) 77-94.
- [5] L. Coderch, O. Lopez, A. de la Maza, J.L. Parra, Ceramides and skin function, *Am. J. Clin. Dermatol.* 4 (2003) 107-129.
- [6] J. van Smeden, L. Hoppel, R. van der Heijden, T. Hankemeier, R.J. Vreeken, J.A. Bouwstra, LC/MS analysis of stratum corneum lipids: ceramide profiling and discovery, *J. Lipid Res.* 52 (2011) 1211-1221.
- [7] S. Raudenkolb, S. Wartewig, R.H.H. Neubert, Polymorphism of ceramide 6: A vibrational spectroscopic and X-ray powder diffraction investigation of the diastereomers of N-(alpha-hydroxyoctadecanoyl)-phytosphingosine, *Chem. Phys. Lipids* 133 (2005) 89-102.
- [8] M.A. Kiselev, N.Y. Ryabova, A.M. Balagurov, S. Dante, T. Hauss, J. Zbytovska, S. Wartewig, R.H.H. Neubert, New insights into the structure and hydration of a stratum corneum lipid model membrane by neutron diffraction, *Eur. Biophys. J.* 34 (2005) 1030-1040.
- [9] M.A. Kiselev, Conformation of ceramide 6 molecules and chain-flip transitions in the lipid matrix of the outermost layer of mammalian skin, the stratum corneum, *Crystallogr. Rep.* 52 (2007) 525-528.
- [10] D. Kessner, M.A. Kiselev, S. Dante, T. Hauss, P. Lersch, S. Wartewig, R.H.H. Neubert, Arrangement of ceramide [EOS] in a stratum corneum lipid model matrix: new aspects revealed by neutron diffraction studies, *Eur. Biophys. J.* 37 (2008) 989-999.
- [11] A. Schroeter, D. Kessner, M.A. Kiselev, T. Hauss, S. Dante, R.H.H. Neubert, Basic nanostructure of stratum corneum lipid matrices based on ceramides [EOS] and [AP]: a neutron diffraction study, *Biophys. J.* 97 (2009) 1104-1114.
- [12] A. Schroeter, M.A. Kiselev, T. Hauss, S. Dante, R.H.H. Neubert, Evidence of free fatty acid interdigitation in stratum corneum model membranes based on ceramide [AP] by deuterium labelling, *Biochim. Biophys. Acta, Biomembranes* 1788 (2009) 2194-2203.
- [13] M.W. de Jager, G.S. Gooris, I.P. Dolbnya, M. Ponec, J.A. Bouwstra, Modelling the stratum corneum lipid organisation with synthetic lipid mixtures: the importance of synthetic ceramide composition, *Biochim. Biophys. Acta, Biomembranes* 1664 (2004) 132-140.
- [14] M.W. de Jager, G.S. Gooris, M. Ponec, J.A. Bouwstra, Lipid mixtures prepared with well-defined synthetic ceramides closely mimic the unique stratum corneum lipid phase behavior, *J. Lipid Res.* 46 (2005) 2649-2656.
- [15] M.W. de Jager, W. Groenink, R. Bielsa i Guivernau, E. Andersson, N. Angelova, M. Ponec, J.A. Bouwstra, A novel in vitro percutaneous penetration model: evaluation of barrier properties with p-aminobenzoic Acid and two of its derivatives, *Pharm. Res.* 23 (2006) 951-960.
- [16] D. Groen, G.S. Gooris, J.A. Bouwstra, New Insights into the Stratum Corneum Lipid Organization by X-Ray Diffraction Analysis, *Biophys. J.* 97 (2009) 2242-2249.
- [17] T. Engelbrecht, T. Hauss, K. Sueß, A. Vogel, M. Roark, S.E. Feller, R.H.H. Neubert, B. Dobner, Characterisation of a new ceramide EOS species: synthesis and investigation of the thermotropic phase behaviour and influence on the bilayer architecture of stratum corneum lipid model membranes, *Soft Matter.* 7 (2011) 8998-9011.
- [18] J.A. Bouwstra, M. Ponec, The skin barrier in healthy and diseased state, *Biochim. Biophys. Acta, Biomembranes* 1758 (2006) 2080-2095.

-
- [19] H. Farwanah, R.H.H. Neubert, S. Zellmer, K. Raith, Improved procedure for the separation of major stratum corneum lipids by means of automated multiple development thin-layer chromatography, *J. Chromatogr. B: Anal. Technol. Biomed. Life Sci.* 780 (2002) 443-450.
- [20] A. Opitz, M. Wirtz, D. Melchior, A. Mehling, H. Kling, R.H.H. Neubert, Improved Method for Stratum Corneum Lipid Analysis by Automated Multiple Development HPTLC, *Chromatographia* 73 (2011) 559-565.
- [21] M. Hartmann, B.D. Hanh, H. Podhaisky, J. Wensch, J. Bodzenta, S. Wartewig, R.H.H. Neubert, A new FTIR-ATR cell for drug diffusion studies, *Analyst* 129 (2004) 902-905.
- [22] U. Guenther, I. Smirnova, R.H.H. Neubert, Hydrophilic silica aerogels as dermal drug delivery systems - Dithranol as a model drug, *Eur. J. Pharm. Biopharm.* 69 (2008) 935-942.
- [23] U. Guenther, M. Hartmann, S. Wartewig, R.H.H. Neubert, Diffusion of urea through membranes, *Diffusion Fundamentals* 4 (2006) 4.1-4.5.
- [24] A.M. Kligman, E. Christophers, Preparation of isolated sheets of human stratum corneum, *Arch. Dermatol.* 88 (1963) 702-705.
- [25] A. Ruettinger, M.A. Kiselev, T. Hauss, S. Dante, A.M. Balagurov, R.H.H. Neubert, Fatty acid interdigitation in stratum corneum model membranes: a neutron diffraction study, *Eur. Biophys. J.* 37 (2008) 759-771.

Chapter 6

SC lipid model membranes designed for studying impact of ceramide species on drug diffusion and permeation, Part II: Diffusion and permeation of model drugs

M. Ochalek ^a, H. Podhaisky ^b, H.-H. Ruettinger ^a,
J. Wohlrab ^c, R.H.H. Neubert ^a

^a *Institute of Pharmacy, Martin Luther University, Halle (Saale), Germany*

^b *Institute of Mathematics, Martin Luther University, Halle (Saale), Germany*

^c *Department of Dermatology and Venereology, Martin Luther University, Halle (Saale), Germany*

(adapted from *Eur. J. Pharm. Biopharm.* (2012) doi: 10.1016/j.ejpb.2012.06.008)

Abstract

The barrier function of two quaternary stratum corneum (SC) lipid model membranes, which were previously characterized with regard to the lipid organization, was investigated based on diffusion studies of model drugs with varying lipophilicities. Diffusion experiments of a hydrophilic drug, urea, and more lipophilic drugs than urea (i.e. caffeine, diclofenac sodium), were conducted using Franz-type diffusion cells. The amount of permeated drug was analyzed using either HPLC or CE technique. The subjects of interest in the present study were the investigation of the influence of physicochemical properties of model drugs on their diffusion and permeation through SC lipid model membranes, as well as the study of the impact of the constituents of these artificial systems (particularly ceramide species) on their barrier properties. The diffusion through both SC lipid model membranes and the human SC of the most hydrophilic model drug, urea, was faster than the permeation of the more lipophilic drugs. The slowest rate of permeation through SC lipid systems occurred in the case of caffeine. The composition of SC lipid model membranes has a significant impact on their barrier function. Model drugs diffused and permeated faster through Membrane II (presence of Cer [EOS]). In terms of the barrier properties, Membrane II is much more similar to the human SC than Membrane I.

1. Introduction

The outermost layer of the skin, the stratum corneum (SC) is considered as the main penetration barrier for topically administered drugs and other substances (e.g. water) [1]. It is composed of 10 to 25 layers of parallel to the skin surface anucleated dead cells (corneocytes) embedded in a lipid matrix and ranges from 10 to 15 μm in thickness in a dry state, however swells to several times this thickness in a fully hydrated state [2]. Since the intercellular route of transport through the normal intact SC is thought to be the most preferable one, of special interest is the organization of the SC intercellular lipid matrix [3]. In comparison to other biological membranes, the SC does not contain phospholipids. The main lipid classes in the SC intercellular lipid matrix are ceramides (Cer), free fatty acids (FFA), cholesterol (Chol) and its derivatives organized in lamellar phases [4-7]. Cer are regarded as fundamental compounds in functioning of the SC barrier [8]. To date, the existence of 12 subclasses of Cer isolated from the human SC has been reported [9]. From former studies, it is known that the constituents of the SC intercellular lipid matrix, which influence to a high degree the internal membrane structure formation and the barrier properties of the SC are: Cer [AP] (due to its head group polarity) and the acylceramide, Cer [EOS] [10-13]. In order to characterize the SC lipid organization, an approach with native SC lipids isolated from the mammalian skin was formerly used [14-18]. Nevertheless, to understand the role of each individual lipid species in the functioning and maintaining of the SC barrier, a new approach with well-defined artificial SC lipid membranes produced as oriented multilamellar systems has been introduced [11, 13, 19-21]. These studies, however, were focused on investigating the relation between lipid composition and the SC lipid system organization. No information about the SC barrier function was acquired. The lipid organization–barrier function relationship was investigated elsewhere [22-24]. The lipid systems used in those studies, however, were much more complex and consisted of a number of Cer, FFA and Chol. In such complex model systems, occurring alterations in the SC barrier function cannot be entirely attributed to one lipid, but may be a result of interactions between different subspecies of lipids. Therefore, the elucidation of the impact of each lipid compound, particularly the different ceramide species, on the diffusion and penetration of drugs for such model systems may be, in our opinion, complicated.

In the present study, the barrier properties of two quaternary lipid model membranes (composed of i.a. Cer [AP] and Cer [EOS]) were investigated. As mentioned above, use of such elementary systems facilitates studying the influence of individual lipid

species (e.g. various ceramide species), on the diffusion, penetration and permeation of drugs and other substances of interest. In our previous study, these two lipid model membranes were characterized in terms of the lipid organization using various analytical techniques (i.a. SAXD, HPTLC, ESEM, confocal Raman imaging) [25]. It was confirmed that the lipid model systems could have been prepared in a standardized way with regard to the lipid distribution and organization. Therefore, they are suitable model membranes to be tested and to be compared with the human SC in the diffusion and penetration studies. In the present study, the barrier properties of these systems were investigated by means of a comparison of diffusion and permeation of three substances with varying lipophilicities (i.e. urea, caffeine and diclofenac sodium) across SC lipid model membranes and the human SC isolated from the full thickness skin. The diffusion studies were conducted using Franz-type diffusion cells. The amount of permeated drug was analyzed using high performance liquid chromatography (HPLC) or conventional capillary electrophoresis (CE) technique. A mathematical model was developed to fit the diffusion profiles of model drugs and to estimate their diffusion coefficients.

2. Materials and methods

2.1. Materials

Synthetic Cer [EOS] and Cer [AP] were generously provided by Evonik Goldschmidt (Essen, Germany). Palmitic acid, sodium cholesteryl sulfate, caffeine, diclofenac sodium salt and urea were purchased from Sigma-Aldrich Chemie GmbH (Steinheim, Germany) and cholesterol from Sigma Chemical CO. (St. Louis, USA). Methanol, ethanol, chloroform, acetonitrile, formic acid and n-hexane were obtained from Merck (Darmstadt, Germany). Urease (from jack beans, 9.0 U mg⁻¹) was purchased from Fluka (Buchs, Switzerland). Nuclepore polycarbonate membrane filters (diameter 25 mm, pore size 50 nm) were purchased from Whatman (Kent, UK). Solvents used for the sample preparation and analytical procedures were of analytical grade.

2.2. Preparation of model lipid membranes

For the preparation of SC lipid model membranes, two compositions of a lipid mixture were used, namely: Cer [AP]/Chol/PA/ChS in the ratio 55/25/15/5 (m/m), referred to as Membrane I, and Cer [AP]/Cer [EOS]/Chol/PA in the ratio 10/23/33/33

(m/m), referred to as Membrane II. The SC lipids used for the preparation of the lipid model membranes are presented in Fig. 1. Appropriate amounts of individual lipids were dissolved in a mixture of chloroform/methanol (2/1, v/v). Following the evaporation of the organic solvents under a stream of nitrogen, the lipids were re-dissolved in a mixture of n-hexane/ethanol (2/1, v/v) at a total lipid concentration of 5 mg/ml. Automatic TLC Sampler 4 (Camag, Muttenz, Switzerland) with a specially built holder was used to apply the lipid mixtures onto porous membrane filters. The spraying of lipids was performed at a very low flow rate (80 nl/s) and under a stream of nitrogen. The sprayed area amounted to 169 mm² and the volume of lipid solution used was 100 µl. Afterward, an annealing procedure was carried out in order to enhance the multilamellar orientation of lipids and to decrease the mosaicity of samples. It consisted of a heating step (30 min at 80 °C or 70 °C in the case of Membrane I and Membrane II, respectively) and a subsequent cooling down step (to room temperature) at 100% relative humidity.

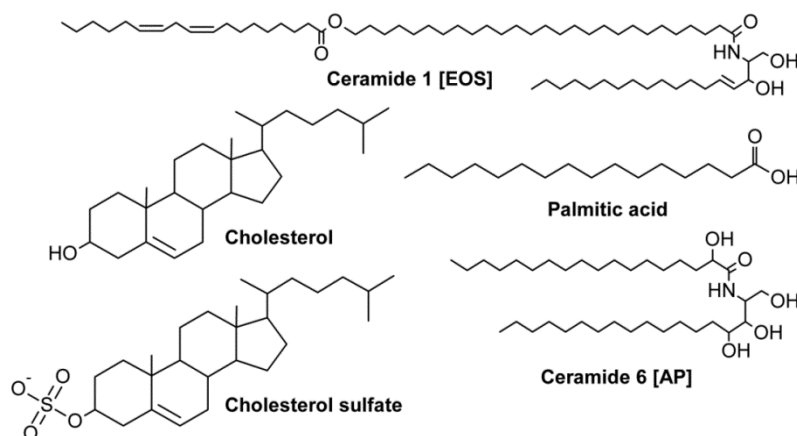


Fig. 1. Chemical structures of constituents of lipid model membranes.

2.3. Diffusion and permeation studies

In vitro diffusion and permeation experiments were carried out using Franz-type diffusion cells (Rettberg, Goettingen, Germany). As model drugs, 2% (m/m) solution of caffeine, 0.1% (m/m) solution of diclofenac sodium and 10% (m/m) solution of urea were used. The specified concentrations of model drugs were used in order to provide infinite dose conditions (i.e. the concentration of the model drug in the donor phase should not diminish significantly in the course of the experiment), as well as due to analytical reasons. Under the conditions of an infinite dose, the steady-state phase can be reached and maintained, which enables the calculation of permeability parameters [26].

Moreover, the mathematical model developed for the purpose of this study is only valid for infinite dose conditions. All solutions were prepared in phosphate-buffered saline (PBS, pH 7.4: NaCl, KCl, Na₂HPO₄ and KH₂PO₄ in water in concentrations 8.0, 0.2, 1.44 and 0.24 g/l, respectively). For diffusion experiments with urea, PBS solution without potassium ions was used (due to the analytical procedure of the urea determination in the acceptor phase). The chemical structures of model drugs are presented in Fig. 2 and their physicochemical properties are summarized in Table 1 (the pK_a and $\log P$ values were either adapted from [27, 28] or estimated using ChemAxon's Marvin software).

Table 1 Physicochemical properties of model drugs.

Parameter	Molar mass [g/mol]	$\log P$	pK_a (25 °C)
Urea	60.06	-2.11	0.18
Caffeine	194.19	-0.07	1.4
Diclofenac sodium	318.14	4.28	4.0

For all diffusion and permeation studies, the donor compartment was filled with 1 ml of the model drug solution in PBS. As the acceptor phase, approx. 5 ml of PBS (pH 7.4) were used. A magnetic bar stirred the acceptor phase throughout the time of experiments. At predetermined points in time, the samples were collected from the acceptor compartment and subsequently quantitatively analyzed using a specific analytical procedure developed for each drug. The removed volume of the acceptor phase was replaced with fresh PBS solution. All diffusion and permeation experiments were conducted under occlusive conditions (the opening of the donor compartment was closed with adhesive tape). During diffusion and permeation studies, the model membranes were kept at 32 °C by use of thermostated water baths in order to mimic the *in vivo* conditions. As model membranes, human SC and artificial lipid systems, Membrane I and Membrane II, were used. The full thickness human skin was acquired after cosmetic surgery from two Caucasian female donors (samples were taken from back, abdomen and thigh). Prior to the isolation of the SC, the subcutaneous fat tissue was dissected from the skin samples. The SC was isolated according to the method depicted by Kligman and Christophers [29]. To separate the SC from the epidermis, the skin samples were incubated in 0.1% trypsin solution (in PBS, pH 7.4) for 12–24 h at 32 °C. The isolated SC samples were stored at –26 °C until use. The protocol of this study was

approved by the ethics committee of the Martin Luther University Halle-Wittenberg (Germany).

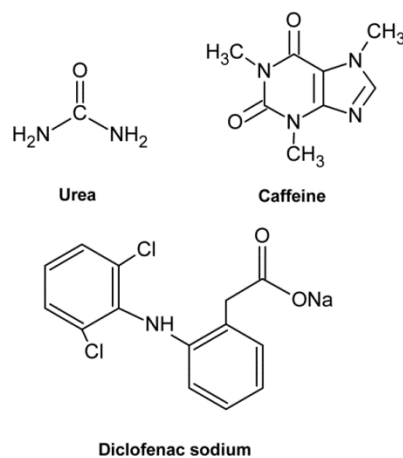


Fig. 2. Chemical structures of model drugs.

2.4. Analytics

The amount of caffeine in the acceptor compartment was analyzed by means of a HPLC method using Agilent 1100 LC System (Agilent, Waldbronn, Germany) equipped with a vacuum degasser, a binary pump, an autosampler and a diode array detector. A stationary phase used was: Eurospher 100-5-RP18 column with dimensions: 100 x 2 mm (Knauer, Berlin, Germany) maintained at a temperature of 30 °C. An isocratic mixture of water/methanol (60/40, v/v) was used as a mobile phase. The flow rate of the mobile phase amounted to 0.2 ml min⁻¹ and the injection volume of each sample was 5 µl. The detection of caffeine was performed at a wavelength of 273 nm (its maximal absorption). The limit of quantification was 0.07 µg ml⁻¹.

The quantitative analysis of diclofenac sodium was performed using the same HPLC system, as depicted earlier for the caffeine determination in the acceptor phase. Nucleosil C8 column with dimensions: 125 x 2 mm (Macherey-Nagel GmbH & Co. KG, Dueren, Germany) kept at a temperature of 30°C was used as a stationary phase. An isocratic mobile phase consisted of 0.1 % formic acid in a mixture of water/acetonitrile (50/50, v/v) and its flow rate amounted to 0.2 ml min⁻¹. 5 µl of each sample were injected into the HPLC column and the detection was carried out at a wavelength of 278 nm. The limit of quantification was 0.2 µg ml⁻¹.

The quantity of urea in the acceptor phase was investigated after an enzymatic conversion of urea to ammonium, by conventional CE with contactless conductivity detection. For diffusion studies of urea, the PBS solution without potassium ions was used. The reason for that is a similarity of ammonium and potassium ions (similar size), and hence a difficult separation of these ions by CE. To the samples taken from the acceptor compartment, an appropriate amount of 2 mg ml⁻¹ urease suspension was added. Next, the reaction mixtures were shaken for 2 hours to assure a completeness of the enzymatic conversion. Afterward, all samples were passed through 0.2 µm cellulose filters (Wicom, Heppenheim, Germany). Samples prepared in this manner were analyzed using PrinCE-C 750 CE System (Prince Technologies, Emmen, The Netherlands) with built in-house contactless conductivity detector, which in contrast to other devices of this type is equipped with a rectangular wave generator instead of a sinusoidal one (in order to improve the amplitude stability). Separations were carried out in fused-silica capillaries (CS-Chromatographie Service, Langerwehe, Germany) with 75 µm ID and 53.5 cm length (38.5 cm to detector). Capillaries were preconditioned with 1 M NaOH for 10 min and water for 10 min, and subsequently flushed with running buffer (20 mM MES/HIS buffer) for 20 min. After each run, the capillaries were rinsed with the MES/HIS buffer. In case of observed peak distortions, the flushing with 0.1 M NaOH for 5 min, water for 5 min and the MES/HIS buffer for 10 min was conducted. The separation voltage was 20 kV. The limit of quantification amounted to 0.25 µg ml⁻¹.

2.5. Mathematical model (its schematic diagram is presented in Fig. 3)

The drug concentration $u(t, x)$ within the membrane can be approximated by a solution of a linear one-dimensional diffusion equation (Fick's second law of diffusion):

$$\frac{\partial u}{\partial t} = D \frac{\partial^2 u}{\partial x^2} \quad 0 \leq x \leq L; t \geq 0 \quad (1)$$

The changes in the concentration of the model drug in the donor $u_D(t) = u(t, 0)$ and in the acceptor phase $u_A(t) = u(t, L)$ lead to the boundary conditions:

$$u'_D(t) = -\frac{D}{L_D} \frac{\partial u(t, 0)}{\partial x} \quad (2)$$

$$u'_A(t) = \frac{D}{L_A} \frac{\partial u(t, L)}{\partial x} \quad (3)$$

where $L_D = V_D/s$ and $L_A = V_A/s$ are the effective lengths of the donor and the acceptor compartment, respectively (V_D and V_A are the volumes of the donor and the acceptor phase, respectively; s is the diffusion/permeation area).

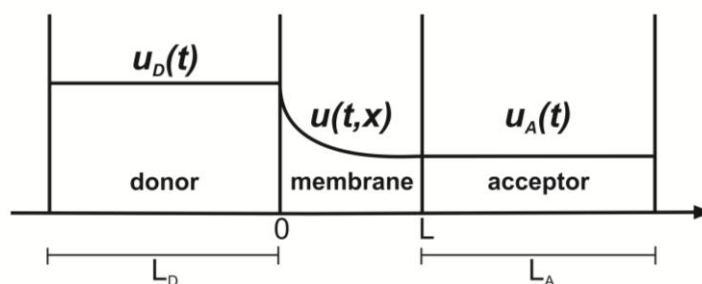


Fig. 3. A schematic diagram of the mathematical model.

The initial conditions are given by Eq. (4) and Eq. (5):

$$u(0, x) = 0 \quad x > 0 \quad (4)$$

$$u(0, 0) = u_D(0) \quad (5)$$

where $u_D(0)$ is the initial drug concentration in the donor compartment.

Replacement of the spatial derivatives in Eq. (1) by standard central differences leads to a linear system of ordinary differential equations:

$$u'_h(t) = DMu_h(t) \quad (6)$$

with a constant matrix M , where $u_h(t)$ stands for a vector of concentrations in the membrane at some (numerical) grid points. The velocity of the drug permeation through the membrane is determined by the slowest eigenmode of M corresponding to the eigenvalue λ_1 . We can therefore fit the model given by Eq. (7):

$$u_A(t) = u_\infty(1 - \exp(\gamma t)) \quad (7)$$

to the experimental data and obtain an estimate for the diffusion coefficient by: $D = \gamma/\lambda_1$. The eigenvalue λ_1 depends on the geometry (L , L_D and L_A) of the configuration. Its value can be computed using the NumPy package.

The other permeability parameters were acquired from plots of the cumulative permeated amount per cm^2 versus time. The steady-state flux (J) is the slope of the linear part of the plot, whereas the lag-time (T_L) is determined from the intercept of this linear part of the plot with the time-axis. The permeability coefficient (k_p) is computed using equation: $k_p = J/u_D(0)$.

Comparisons of the estimated permeability parameters were performed using one-way analysis of variance (ANOVA) followed by Tukey's test (*post hoc* analysis). Significance was accepted when $p < 0.05$.

3. Results and discussion

3.1. Influence of physicochemical properties of drugs on the diffusion across SC lipid model membranes

To estimate the influence of physicochemical characteristics of drugs on their diffusion through SC membranes, the diffusion and permeation of three model drugs covering a broad range of lipophilicities (Table 1) across SC lipid model membranes and the human SC were investigated. Moreover, the other important factor which can affect the rate of diffusion and permeation of substances of interest is their molecular weight. In the present study, diffusion and permeation of model drugs with varying molecular weight were examined, starting with a smallest compound (urea), a medium one (caffeine) and ending with a largest one (diclofenac sodium).

Fig. 4 shows diffusion and permeation profiles of model drugs with the model fittings across Membrane I (A), Membrane II (B) and the human SC (C). The figure clearly shows that the diffusion of urea was much faster than the permeation of caffeine and the slowest rate of permeation occurred in the case of diclofenac sodium. The relationship observed is characteristic for all membranes investigated (artificial lipid membranes and native SC). The values of steady-state flux, lag-time, permeability coefficient and diffusion coefficient are presented in Table 2.

In the present study, the impact of physicochemical properties of drugs on their diffusion and permeation behavior was investigated. Three model drugs with different lipophilicities (namely, urea with $\log P$ of -2.11 , caffeine with $\log P$ of -0.07 and diclofenac sodium with $\log P$ of 4.28 , where $\log P$ stands for \log partition coefficient value) were selected to examine the influence of the partitioning characteristics of drugs on the rate of diffusion. It is generally suggested, because of the lipophilic character of the SC intercellular matrix, that the more lipophilic a drug is, the faster should it permeate through the SC. It can be clearly seen in Fig. 4A–C that urea, which is a representative of the hydrophilic drug, diffused through both artificial lipid membranes and the human SC faster than the more lipophilic molecule, caffeine, and much faster than the most lipophilic drug, diclofenac sodium. A comparison of permeability parameters shows that the steady-state flux of urea was ~ 23 times larger than J of caffeine and ~ 194 times larger than J of diclofenac sodium in the case of Membrane I. For Membrane II, J of urea was ~ 51 -fold and ~ 849 -fold larger than the corresponding values of caffeine and diclofenac sodium, respectively. A similar relationship applies for the J values in the case

of the diffusion across the human SC, where J of urea was ~ 21 times and over 5000 times larger than the J of caffeine and diclofenac sodium, respectively. The permeability coefficient of urea in the case of Membrane I was higher than k_p of caffeine and diclofenac sodium by a factor of ~ 5 and 2, respectively. For Membrane II, k_p of urea was ~ 11 times and ~ 9 times larger than k_p of caffeine and diclofenac sodium, respectively. In the case of the human SC, k_p of urea was higher than the corresponding values of caffeine and diclofenac sodium by a factor of ~ 4 and ~ 53 , respectively. A comparison of diffusion coefficient values shows that D of urea for Membrane I was ~ 11 -fold and ~ 4 -fold larger than D of caffeine and diclofenac sodium, respectively. In the case of Membrane II, a similar relationship was observed, namely D of urea was higher than D of caffeine and diclofenac sodium by a factor of ~ 10 and ~ 8 , respectively. For the human SC, D of urea was ~ 4 times and ~ 50 times larger than D of caffeine and diclofenac sodium, respectively.

The D values in the case of permeation of caffeine and diclofenac sodium through the human SC ($0.66 \times 10^{-7} \text{ cm}^2 \text{ s}^{-1}$ and $5.4 \times 10^{-9} \text{ cm}^2 \text{ s}^{-1}$, respectively) are in good agreement with the previously published D values of caffeine ($1.4 \times 10^{-7} \text{ cm}^2 \text{ s}^{-1}$ [30], $1.03 \times 10^{-7} \text{ cm}^2 \text{ s}^{-1}$ [31]) and diclofenac in the nonionized form ($9.65 \times 10^{-9} \text{ cm}^2 \text{ s}^{-1}$ [31]). The D of urea in the case of diffusion across the human SC ($2.71 \times 10^{-7} \text{ cm}^2 \text{ s}^{-1}$) is significantly larger than previously reported D values for urea ($6.68 \times 10^{-10} \text{ cm}^2 \text{ s}^{-1}$ [32], $2.85 \times 10^{-10} \text{ cm}^2 \text{ s}^{-1}$ [33], $0.12 \times 10^{-10} \text{ cm}^2 \text{ s}^{-1}$ [25]). The reason for that is most likely the use of different instrumentation in the previous diffusion studies, namely the ATR-FTIR diffusion cell, associated with the different analytical method of urea amount determination in the acceptor phase (i.e. ATR-FTIR spectroscopy in the previous studies, HPLC in the present study). When comparing the lag-times, it can be clearly seen that the differences in the mean values of T_L in some cases are not significant. T_L of urea in the case of Membrane I was \sim twice shorter than T_L of caffeine, whereas T_L of both caffeine and diclofenac sodium and urea and diclofenac sodium were not significantly different ($\alpha = 0.05$). For Membrane II, the differences in T_L of urea and caffeine were not significant ($\alpha = 0.05$) and their values can be assumed to equal 0. On the other hand, T_L of diclofenac sodium was ~ 1.2 h and ~ 0.6 h longer than T_L of urea and caffeine, respectively. A similar relation holds for diffusion and permeation across the human SC, where, on the one hand, T_L of urea and caffeine were different, however, for both drugs had negative values which means there was no lag-time at all. T_L of diclofenac sodium was ~ 1.7 h and 0.7 h longer than T_L of urea and caffeine, respectively.

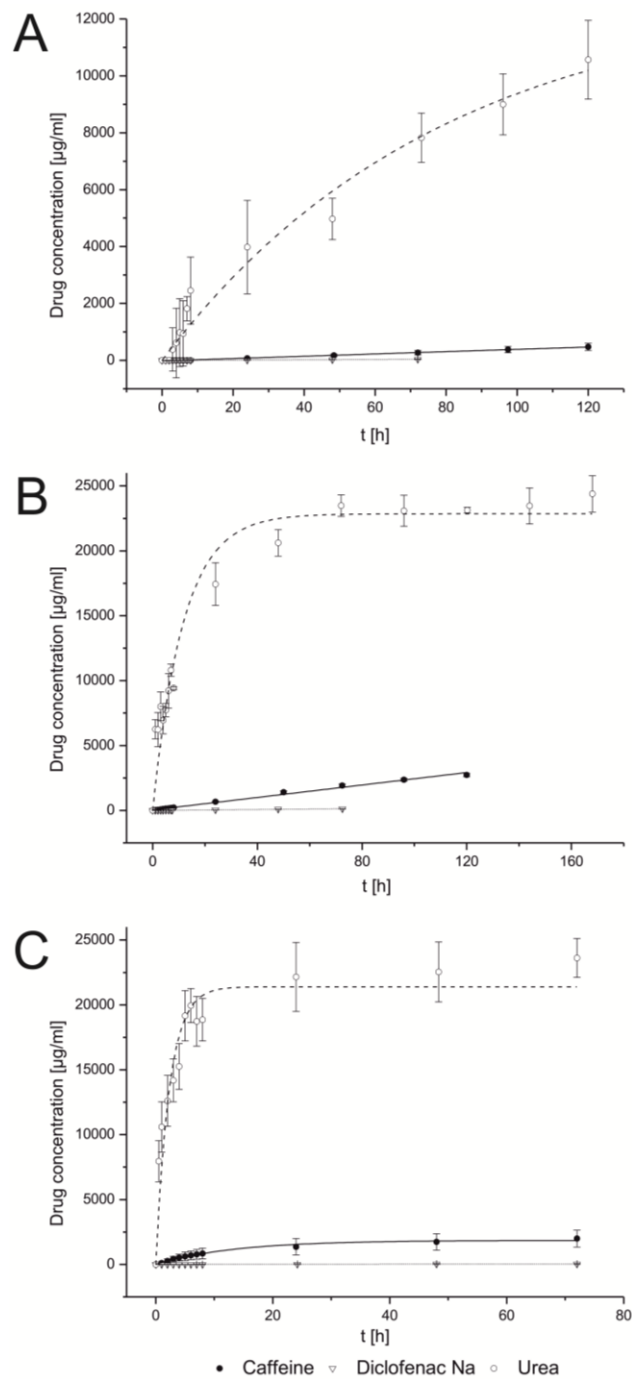


Fig. 4. Diffusion and permeation through the model lipid membranes, (A) Membrane I and (B) Membrane II, and (C) the human SC (data shown with mathematical model fittings). Error bars show the standard deviation ($n = 4$).

From the diffusion and permeation profiles of three model drugs and their permeability parameters, it can be concluded that the most hydrophilic one, urea, is characterized by the fastest diffusion through both SC lipid model membranes and the human SC. One possible explanation of this phenomenon can be the molecular weight of urea, which is much smaller when compared to the more lipophilic drugs (i.e. caffeine and

diclofenac sodium). From the Stokes-Einstein relation: $D = k_B T / (6\pi\eta r)$, where k_B is the Boltzmann's constant, T is the absolute temperature, η is the medium's viscosity and r is the radius of a spherical diffusing molecule, it is known that D of the diffusing species is inversely proportional to its radius [34]. Assuming the proportionality of the molecular weight of the molecule to its volume and taking into account the differences in the molar mass of used model drugs, the expected D values of urea, caffeine and diclofenac sodium should occur in descending order. This relation is true for urea, however it does not apply for other two model drugs in the case of SC lipid model membranes, where D and k_p values of diclofenac sodium are larger than the corresponding values of caffeine. The other possible explanation for urea's diffusion behavior can be its permeation enhancing potential. Urea is a well-known penetration enhancer for the hydrophilic pathway and its activity probably results from its keratolytic as well as hydrating properties [35-37]. The mentioned permeation enhancing activity can be responsible for the acceleration of the diffusion of urea across SC lipid model membranes and the human SC. The larger values of D and k_p of diclofenac sodium in the case of permeation across Membrane I and Membrane II, when compared to D and k_p values of caffeine, may result from their distinct partitioning characteristics. On the one hand, diclofenac sodium molecule has a larger molecular weight than caffeine molecule; on the other hand, the latter is much less lipophilic than diclofenac sodium. This results in slightly larger values of D and k_p in favor of diclofenac sodium. The larger as expected differences between the D values of caffeine and diclofenac sodium in the case of the human SC can be caused by high inter- and intra-variability of the human SC samples [1].

Table 2 Permeability parameters of urea, caffeine and diclofenac sodium – *in vitro* study.

Parameter	J [mg cm ⁻² h ⁻¹]	T_L [h]	k_p [cm h ⁻¹]	D [x 10 ⁻⁸ cm ² s ⁻¹]	
SC	42.23 ± 1.66	-1.01 ± 0.24	0.42 ± 0.02	27.14 ± 7.16	
Urea	Membrane I	1.36 ± 0.13	2.88 ± 1.13	0.014 ± 0.001	0.25 ± 0.13
	Membrane II	19.52 ± 1.53	-0.47 ± 0.50	0.20 ± 0.02	1.59 ± 0.16
SC	2.00 ± 1.12	-0.01 ± 0.15	0.10 ± 0.06	6.58 ± 4.02	
Caffeine	Membrane I	0.06 ± 0.01	5.89 ± 1.12	0.003 ± 0.001	0.023 ± 0.006
	Membrane II	0.38 ± 0.04	0.15 ± 0.26	0.019 ± 0.002	0.16 ± 0.02
SC	0.008 ± 0.004	0.73 ± 0.94	0.008 ± 0.004	0.54 ± 0.69	
Diclofenac sodium	Membrane I	0.007 ± 0.002	3.56 ± 1.69	0.007 ± 0.002	0.060 ± 0.014
	Membrane II	0.023 ± 0.001	0.77 ± 0.23	0.023 ± 0.001	0.19 ± 0.01

Permeability data represent MEAN ± SD (n = 4).

3.2. Influence of the composition of SC lipid model membranes on their barrier function

To investigate the impact of the composition of SC lipid model systems on their barrier properties, the diffusion and permeation of three model drugs across Membrane I and Membrane II were analyzed, and subsequently compared with their diffusion and permeation through the human SC.

Fig. 5 presents diffusion and permeation profiles of urea (A), caffeine (B) and diclofenac sodium (C) (and their model fittings) across SC lipid model membranes and the human SC. The values of permeability parameters of model drugs are listed in Table 2. It can be clearly seen in Fig. 5A that urea diffused faster across the human SC when compared to its diffusion through SC lipid model membranes. The slowest rate of diffusion occurred in the case of Membrane I. The steady-state flux of urea in the case of the human SC was \sim twice and \sim 31 times larger than J in the case of diffusion through Membrane II and Membrane I, respectively. The same ratio applies for a comparison of the values of the permeability coefficient of urea. In the case of diffusion across the human SC, the diffusion coefficient of urea was higher by a factor of \sim 17 and \sim 109 than D of urea for Membrane II and Membrane I, respectively. Fig. 5A clearly shows that for the diffusion profiles of urea across the human SC and Membrane II, no lag phase was observed. The values of T_L for the human SC and Membrane II are both negative and not significantly different ($\alpha = 0.05$). The lag phase of urea in the case of Membrane I, on the other hand, was well pronounced and its T_L was \sim 3.4–3.9 h longer than for the other two membranes.

A similar relationship, as presented for the diffusion of urea, was also observed in the case of permeation of caffeine across both the human SC and SC lipid model membranes (Fig. 5B). The fastest rate of permeation of caffeine occurred for the human SC and the slowest one for Membrane I. Both the steady-state flux and the permeability coefficient of caffeine in the case of the human SC were \sim 5-fold and \sim 33-fold larger than J and k_p for permeation through Membrane II and Membrane I, respectively. A comparison of diffusion coefficient values shows that D of caffeine for the human SC was \sim 41 times and \sim 286 times larger than the corresponding values in the case of permeation across Membrane II and Membrane I, respectively. The differences in the lag-times of caffeine for the human SC and Membrane II were not significant ($\alpha = 0.05$) and the values of T_L were close to 0. On the contrary, T_L of caffeine in the case of permeation across Membrane I was \sim 6 h longer than for the other membranes. Surprisingly, in the case of permeation of diclofenac sodium, the fastest rate of permeation occurred for the

experiments with Membrane II. The permeation profiles of diclofenac sodium across the human SC and Membrane I are similar (Fig. 5C). Their similarity is emphasized by the same values of J and k_p for these two membranes ($\alpha = 0.05$). The values of J and k_p of diclofenac sodium in the case of permeation through Membrane II were higher than for the other membranes by a factor of ~ 3 . The differences in the values of the diffusion coefficient of diclofenac sodium in the case of diffusion across the human SC and both Membrane I and Membrane II were not significant ($\alpha = 0.05$). On the other hand, D of diclofenac sodium for Membrane II was ~ 3 times larger than D for Membrane I. The lag-time of diclofenac sodium in the case of Membrane II was slightly longer than T_L for the human SC. The longest lag phase occurred in the case of permeation across Membrane I (i.e. ~ 2.8 h longer T_L than for the other membranes).

Based on the results presented, it can be assumed that the composition of SC lipid model membranes influences to a high degree their barrier properties. A comparison of diffusion and permeation profiles, as well as the permeability parameters, of model drugs across SC lipid model membranes and the human SC leads to the conclusion that, in terms of the barrier function, Membrane II is much more similar to the human SC than Membrane I. The most unequivocal evidence confirming this theory is the comparison of T_L values of model drugs in the case of diffusion and permeation across the human SC and Membrane II, which are either very much alike (for diclofenac sodium) or the same (for urea and caffeine; $\alpha = 0.05$). The other permeability parameters of model drugs, except for J and k_p values in the case of permeation of diclofenac sodium across Membrane I and the human SC, also point at higher degree of similarity of the barrier function of Membrane II and the human SC. A possible explanation for this phenomenon can be the different lipid composition, hence the distinct lipid organization, of SC lipid model membranes. From the previous studies on the lipid organization [12, 19, 25, 38], it is known that the polar Cer [AP] (four OH-groups within the head group) is responsible for the formation of a very stable system with a periodicity of $\sim 45\text{--}46$ Å (Membrane I). The ability of short-chain Cer (e.g. Cer [AP]) to exist in the fully extended as well as the hairpin conformation (transformation from one to the other conformation by the chain-flip transition) is of major importance for the elucidation of the lipid arrangement within SC lipid model membranes. Cer [AP] in the fully extended conformation keeps the lipid bilayers together and can be considered as an armature (“armature reinforcement model”, [12]).

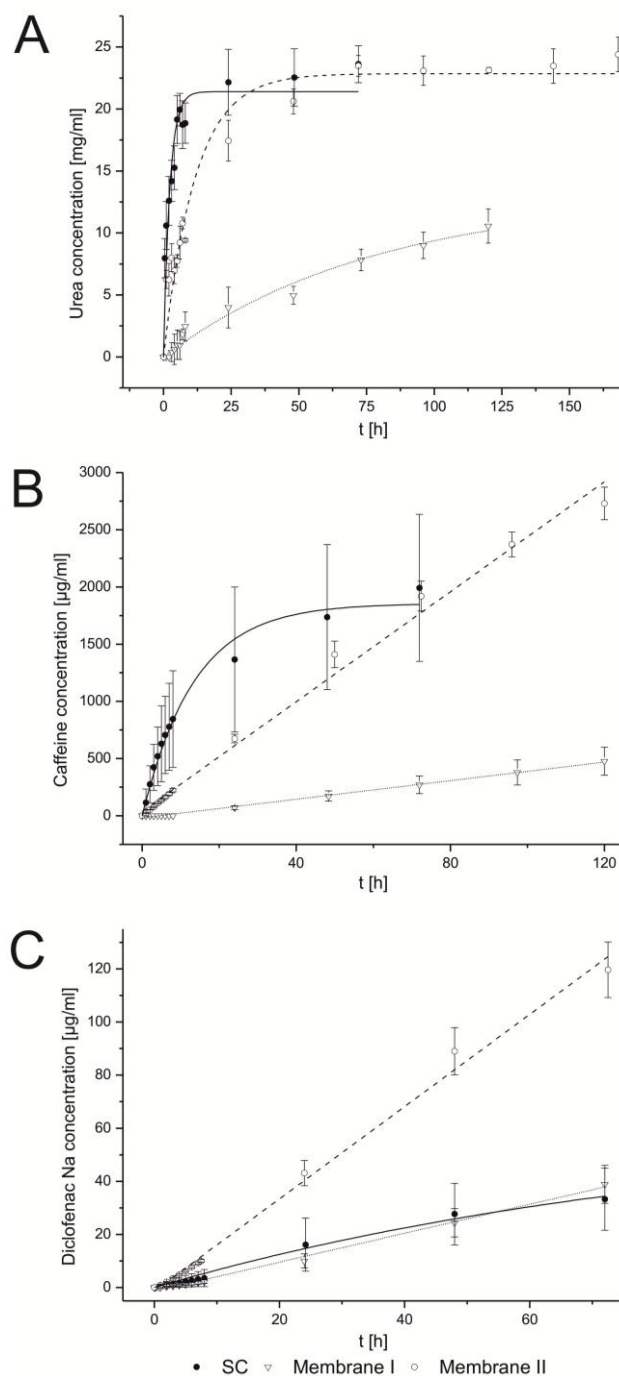


Fig. 5. Diffusion and permeation profiles of (A) urea, (B) caffeine and (C) diclofenac sodium (across model lipid membranes and human SC) and their model fittings. Error bars show the standard deviation ($n = 4$).

The presence of Cer [EOS] within the lipid system (Membrane II) does not influence significantly the lipid organization in terms of the periodicity of the lamellar phase (~ 46 Å, [19, 25]). This finding leads to the conclusion that the long-chain Cer [EOS] is forced to fit into the membrane created by Cer [AP] with its long alkyl chain traversing the bilayer and expanding into the adjacent layer [19]. This phenomenon, however, can lead to a relaxation within the lipid assembly, i.e. the lipids within the lipid systems are not

arranged so tight as it was in the case of Membrane I. This assumption finds its confirmation in the results of diffusion and permeation studies of model drugs through Membrane I and Membrane II. The model drugs diffused and permeated faster across Membrane II, which is considered to be much more similar to the human SC, than Membrane I, with regard to the barrier function.

4. Conclusions

Diffusion and permeation studies of three model drugs with varying lipophilicities (urea, caffeine and diclofenac sodium) were conducted in order to acquire information on both the impact of physicochemical properties of drugs on their diffusion and permeation across SC lipid model membranes and the influence of the constituents of these systems (in particular the different ceramide species) on their barrier function. Firstly, the fastest diffusion through both SC lipid model membranes and the human SC occurred in the case of the most hydrophilic model drug, urea. This can be attributed to its smallest molecular weight, as well as its permeation enhancing potential for the hydrophilic pathway (hence the acceleration of the process of diffusion). The differences in the permeation rates of caffeine and diclofenac sodium can be explained by their distinct partitioning properties. The most lipophilic drug, diclofenac sodium, permeated faster across lipophilic SC model membranes than caffeine (larger values of D and k_p in the case of diclofenac sodium). Secondly, the composition of SC lipid membranes has a significant impact on their barrier properties. With regard to the barrier function, Membrane II is much more similar to the human SC than Membrane I. In the presence of Cer [EOS] (as in Membrane II) the lipids within the SC model systems are not arranged so tight as it is in the case of Membrane I, which results in the faster diffusion and permeation of model drugs across Membrane II (similar diffusion profiles of model drugs through Membrane II and the human SC).

Acknowledgements

The financial support for Michal Ochalek provided by the “Graduiertenförderung des Landes Sachsen-Anhalt” is gratefully appreciated.

References

- [1] P.W. Wertz, B. van den Bergh, The physical, chemical and functional properties of lipids in the skin and other biological barriers, *Chem. Phys. Lipids* 91 (1998) 85-96.
- [2] J.A. Bouwstra, A. de Graaff, G.S. Gooris, J. Nijssse, J.W. Wiechers, A.C. van Aelst, Water distribution and related morphology in human stratum corneum at different hydration levels, *J. Invest. Dermatol.* 120 (2003) 750-758.
- [3] M.L. Williams, P.M. Elias, The extracellular matrix of stratum corneum: role of lipids in normal and pathological function, *Crit. Rev. Ther. Drug Carrier Syst.* 3 (1987) 95-122.
- [4] P.W. Wertz, M.C. Miethke, S.A. Long, J.S. Strauss, D.T. Downing, The composition of the ceramides from human stratum corneum and from comedones, *J. Invest. Dermatol.* 84 (1985) 410-412.
- [5] N.Y. Schurer, G. Plewig, P.M. Elias, Stratum corneum lipid function, *Dermatologica* 183 (1991) 77-94.
- [6] K.J. Robson, M.E. Stewart, S. Michelsen, N.D. Lazo, D.T. Downing, 6-Hydroxy-4-sphingenine in human epidermal ceramides, *J. Lipid Res.* 35 (1994) 2060-2068.
- [7] Y. Masukawa, H. Narita, E. Shimizu, N. Kondo, Y. Sugai, T. Oba, R. Homma, J. Ishikawa, Y. Takagi, T. Kitahara, Y. Takema, K. Kita, Characterization of overall ceramide species in human stratum corneum, *J. Lipid Res.* 49 (2008) 1466-1476.
- [8] L. Coderch, O. Lopez, A. de la Maza, J.L. Parra, Ceramides and skin function, *Am. J. Clin. Dermatol.* 4 (2003) 107-129.
- [9] J. van Smeden, L. Hoppel, R. van der Heijden, T. Hankemeier, R.J. Vreeken, J.A. Bouwstra, LC/MS analysis of stratum corneum lipids: ceramide profiling and discovery, *J. Lipid Res.* 52 (2011) 1211-1221.
- [10] S. Raudenkolb, S. Wartewig, R.H.H. Neubert, Polymorphism of ceramide 6: A vibrational spectroscopic and X-ray powder diffraction investigation of the diastereomers of N-(alpha-hydroxyoctadecanoyl)-phytosphingosine, *Chem. Phys. Lipids* 133 (2005) 89-102.
- [11] M.A. Kiselev, N.Y. Ryabova, A.M. Balagurov, S. Dante, T. Hauss, J. Zbytovska, S. Wartewig, R.H.H. Neubert, New insights into the structure and hydration of a stratum corneum lipid model membrane by neutron diffraction, *Eur. Biophys. J.* 34 (2005) 1030-1040.
- [12] M.A. Kiselev, Conformation of ceramide 6 molecules and chain-flip transitions in the lipid matrix of the outermost layer of mammalian skin, the stratum corneum, *Crystallogr. Rep.* 52 (2007) 525-528.
- [13] D. Kessner, M.A. Kiselev, S. Dante, T. Hauss, P. Lersch, S. Wartewig, R.H.H. Neubert, Arrangement of ceramide [EOS] in a stratum corneum lipid model matrix: new aspects revealed by neutron diffraction studies, *Eur. Biophys. J.* 37 (2008) 989-999.
- [14] S.H. White, D. Mirejovsky, G.I. King, Structure of lamellar lipid domains and corneocyte envelopes of murine stratum corneum. An X-ray diffraction study, *Biochemistry* 27 (1988) 3725-3732.
- [15] B. Ongpipattanakul, M.L. Francoeur, R.O. Potts, Polymorphism in stratum corneum lipids, *Biochim. Biophys. Acta, Biomembranes* 1190 (1994) 115-122.
- [16] T.J. McIntosh, M.E. Stewart, D.T. Downing, X-ray diffraction analysis of isolated skin lipids: reconstitution of intercellular lipid domains, *Biochemistry* 35 (1996) 3649-3653.
- [17] J.A. Bouwstra, G.S. Gooris, K. Cheng, A. Weerheim, W. Bras, M. Ponc, Phase behavior of isolated skin lipids, *J. Lipid Res.* 37 (1996) 999-1011.
- [18] T.J. McIntosh, Organization of skin stratum corneum extracellular lamellae: diffraction evidence for asymmetric distribution of cholesterol, *Biophys. J.* 85 (2003) 1675-1681.
- [19] A. Schroeter, D. Kessner, M.A. Kiselev, T. Hauss, S. Dante, R.H.H. Neubert, Basic nanostructure of stratum corneum lipid matrices based on ceramides [EOS] and [AP]: a neutron diffraction study, *Biophys. J.* 97 (2009) 1104-1114.

- [20] A. Schroeter, M.A. Kiselev, T. Hauss, S. Dante, R.H.H. Neubert, Evidence of free fatty acid interdigitation in stratum corneum model membranes based on ceramide [AP] by deuterium labelling, *Biochim. Biophys. Acta, Biomembranes* 1788 (2009) 2194-2203.
- [21] T. Engelbrecht, T. Hauss, K. Sueß, A. Vogel, M. Roark, S.E. Feller, R.H.H. Neubert, B. Dobner, Characterisation of a new ceramide EOS species: synthesis and investigation of the thermotropic phase behaviour and influence on the bilayer architecture of stratum corneum lipid model membranes, *Soft Matter* 7 (2011) 8998-9011.
- [22] M.W. de Jager, W. Groenink, R. Bielsa i Guivernau, E. Andersson, N. Angelova, M. Ponec, J.A. Bouwstra, A novel in vitro percutaneous penetration model: evaluation of barrier properties with p-aminobenzoic acid and two of its derivatives, *Pharm. Res.* 23 (2006) 951-960.
- [23] D. Groen, G.S. Gooris, M. Ponec, J.A. Bouwstra, Two new methods for preparing a unique stratum corneum substitute, *Biochim. Biophys. Acta, Biomembranes* 1778 (2008) 2421-2429.
- [24] D. Groen, D.S. Poole, G.S. Gooris, J.A. Bouwstra, Investigating the barrier function of skin lipid models with varying compositions, *Eur. J. Pharm. Biopharm.* 79 (2011) 334-342.
- [25] M. Ochalek, S. Heissler, J. Wohlrab, R.H.H. Neubert, Characterization of lipid model membranes designed for studying impact of ceramide species on drug diffusion and penetration, *Eur. J. Pharm. Biopharm.* 81 (2012) 113-120.
- [26] OECD (2004), Guidance Document for the Conduct of Skin Absorption Studies, OECD Series on Testing and Assessment, No. 28, OECD Publishing. doi: 10.1787/9789264078796-en.
- [27] T. Khazaenia, F. Jamali, A comparison of gastrointestinal permeability induced by diclofenac-phospholipid complex with diclofenac acid and its sodium salt, *J. Pharm. Pharm. Sci.* 6 (2003) 352-359.
- [28] A. Kokate, X. Li, B. Jasti, Effect of drug lipophilicity and ionization on permeability across the buccal mucosa: a technical note, *AAPS PharmSciTech.* 9 (2008) 501-504.
- [29] A.M. Kligman, E. Christophers, Preparation of isolated sheets of human stratum corneum, *Arch. Dermatol.* 88 (1963) 702-705.
- [30] S. Hansen, A. Henning, A. Naegel, M. Heisig, G. Wittum, D. Neumann, K.-H. Kostka, J. Zbytovska, C.-M. Lehr, U.F. Schaefer, In-silico model of skin penetration based on experimentally determined input parameters. Part I: Experimental determination of partition and diffusion coefficients, *Eur. J. Pharm. Biopharm.* 68 (2008) 352-367.
- [31] M.E. Johnson, D. Blankschtein, R. Langer, Evaluation of Solute Permeation Through the Stratum Corneum: Lateral Bilayer Diffusion as the Primary Transport Mechanism, *J. Pharm. Sci.* 86 (1997) 1162-1172.
- [32] M. Hartmann, B.D. Hanh, H. Podhaisky, J. Wensch, J. Bodzenta, S. Wartewig, R.H.H. Neubert, A new FTIR-ATR cell for drug diffusion studies, *Analyst* 129 (2004) 902-905.
- [33] U. Guenther, M. Hartmann, S. Wartewig, R.H.H. Neubert, Diffusion of urea through membranes, *Diffusion Fundamentals* 4 (2006) 4.1-4.5.
- [34] W.J. McAuley, K.T. Mader, J. Tetteh, M.E. Lane, J. Hadgraft, Simultaneous monitoring of drug and solvent diffusion across a model membrane using ATR-FTIR spectroscopy, *Eur. J. Pharm. Sci.* 38 (2009) 378-383.
- [35] A.C. Williams, B.W. Barry, Penetration enhancers, *Adv. Drug Deliver. Rev.* 56 (2004) 603-618.
- [36] H.Y. Thong, H. Zhai, H.I. Maibach, Percutaneous penetration enhancers: an overview, *Skin Pharmacol. Physiol.* 20 (2007) 272-282.
- [37] H. Trommer, R.H.H. Neubert, Overcoming the stratum corneum: the modulation of skin penetration. A review, *Skin Pharmacol. Physiol.* 19 (2006) 106-121.
- [38] D. Kessner, A. Ruettinger, M.A. Kiselev, S. Wartewig, R.H.H. Neubert, Properties of Ceramides and Their Impact on the Stratum Corneum Structure: Part 2: Stratum Corneum Lipid Model Systems, *Skin Pharmacol. Physiol.* 21 (2008) 58-74.

Chapter 7

SC lipid model membranes designed for studying impact of ceramide species on drug diffusion and permeation, Part III: Influence of penetration enhancer on diffusion and permeation of model drugs

M. Ochalek ^a, H. Podhaisky ^b, H.-H. Ruettinger ^a,
R.H.H. Neubert ^a, J. Wohlrab ^c

^a Institute of Pharmacy, Martin Luther University, Halle (Saale), Germany

^b Institute of Mathematics, Martin Luther University, Halle (Saale), Germany

^c Department of Dermatology and Venereology, Martin Luther University, Halle (Saale), Germany

(adapted from *Int. J. Pharm.* (2012) doi: 10.1016/j.ijpharm.2012.06.044)

Abstract

The impact of the lipophilic penetration enhancer, oleic acid (OA), on the barrier properties of stratum corneum (SC) lipid model membranes was investigated based on diffusion and permeation studies of model drugs covering a broad range of lipophilicities. Diffusion and permeation experiments of urea, caffeine and diclofenac sodium were conducted using Franz-type diffusion cells. HPLC and capillary electrophoresis techniques were employed to analyze the amount of permeated drug. An incorporation of OA to the SC lipid model membranes did not change the relation between the diffusion and permeation behavior of model drugs presented previously for SC lipid model membranes without OA. The fastest rate of diffusion through SC lipid model membranes occurred in the case of the most hydrophilic drug, urea. In the case of permeation studies of caffeine and diclofenac sodium across SC lipid model systems, the permeability parameters were either equal or slightly larger in favor of the most lipophilic drug, diclofenac sodium. OA had a pronounced impact on the barrier properties of SC lipid model membranes. It caused the impairment of the barrier function of the SC lipid model membrane with Cer [AP] (phytosphingosine-based ceramide), however, surprisingly improved the barrier properties of the SC lipid model system with Cer [EOS] (sphingosine-based acylceramide).

1. Introduction

The outermost layer of the skin, the stratum corneum (SC) constitutes the main penetration barrier for topically administered drugs and other substances (e.g. water) (Wertz and van den Bergh, 1998). It consists of parallel to the skin surface anucleated dead cells (corneocytes) that are embedded in a lipid matrix (Elias, 1983). The intercellular route of transport through the normal intact SC is thought to be the most preferable one (Williams and Elias, 1987). Therefore, the organization of the SC intercellular lipid matrix is of special interest. The SC intercellular lipid matrix does not contain phospholipids, contrary to other biological barriers (e.g. cell membranes). It is mainly composed of ceramides (Cer), free fatty acids (FFA), cholesterol (Chol) and its derivatives (e.g. cholesterol sulfate, ChS) that are organized in lamellar phases (Masukawa et al., 2008; Robson et al., 1994; Schurer et al., 1991; Wertz et al., 1985). Cer, FFA and Chol make up approx. 50%, 10% and 25% of the SC lipid mass, respectively, with ChS comprising about 5% of the total Chol (Weerheim and Ponec, 2001; Wertz, 2000). FFA found in the SC are mainly saturated, straight-chained species. Their chain lengths range from 16 through 30 carbons and the most abundant species are C22:0, C24:0 and C26:0 (Weerheim and Ponec, 2001; Wertz and van den Bergh, 1998). A key role in the functioning of the SC barrier play Cer (Coderch et al., 2003). Recent study reported the existence of 12 subclasses of Cer isolated from the human SC (van Smeden et al., 2011). In order to investigate the SC lipid organization, native SC lipids isolated from the mammalian skin were used in former studies (Bouwstra et al., 1996; McIntosh, 2003; McIntosh et al., 1996; Ongpipattanakul et al., 1994; White et al., 1988). Nevertheless, to elucidate the role of each lipid species in the functioning and maintaining of the SC barrier, a new approach with well-defined artificial SC lipid systems produced as oriented multilamellar membranes has been recently introduced (Engelbrecht et al., 2011a; Kessner et al., 2008; Kiselev, 2007; Kiselev et al., 2005; Raudenkolb et al., 2005; Schroeter et al., 2009a; Schroeter et al., 2009b). The use of such systems can help to overcome obstacles like the poor availability of human skin and the high inter- and intra-variability of the human SC samples. In these studies, it was found that the short chain and polar phytosphingosine-based Cer [AP] and the acylceramide, Cer [EOS], influence to a high degree the internal membrane structure formation and the barrier properties of the SC. However, the focus in these studies was placed on the relation between the lipid composition and the SC lipid system organization, and no information about the SC barrier function was obtained. The lipid organization–barrier function relationship was

investigated elsewhere (de Jager et al., 2006; Groen et al., 2011). However, lipid systems used there were much more complex and were composed of a number of Cer, FFA and Chol. The use of such complex model membranes does not allow to assign alterations occurring in the SC barrier function just to one lipid. On the contrary, they might result from interactions between different subspecies of lipids. The investigation of the influence of each lipid constituent (in particular the Cer species) on the diffusion and permeation of drugs across such model systems may be hampered.

The process of drug diffusion and permeation across the SC can be modulated. The facilitation of the drug administration into deeper skin layers or to the systemic circulation is desired in the treatment of many diseases. There are a number of mechanisms of the temporary impairment of the SC barrier function and they have been extensively reviewed (Trommer and Neubert, 2006). In addition to physical methods (e.g. phonophoresis, iontophoresis), a chemical penetration enhancement plays a crucial role in the modulation of the SC penetration (Walker and Smith, 1996; Williams and Barry, 2004). The enhancement of the drug penetration into the SC or the permeation through the SC is proven for a number of chemical substances called penetration enhancers. However, their exact mechanism of action is not yet fully explained. *cis*-9-octadecenoic acid (oleic acid, OA) belongs to the group of well-studied penetration enhancers (Francoeur et al., 1990; Walker and Hadgraft, 1991). Francoeur et al. (1990) found that following skin treatment with OA, the penetration of piroxicam was significantly increased. This phenomenon was ascribed to a direct perturbing effects of OA on the SC lipids, as well as a formation of phase-separated fluid domains in the presence of OA. Similar findings were reported elsewhere (Naik et al., 1995; Rowat et al., 2006; Tanojo et al., 1997). A number of studies on the effects of the OA action on the phospholipid-based systems were also carried out (Funari et al., 2003; Prades et al., 2003; Separovic and Gawrisch, 1996). It was found in these studies that the double bond of OA substantially influenced the molecular arrangement of lipid alkyl chains and hence the lipid bilayer arrangement. As a consequence, an increased chain disorder was produced. The model lipid system composed of Cer [AP], Chol, PA, ChS and OA was investigated by means of small angle X-ray scattering (Zbytovska et al., 2009) and neutron scattering (Engelbrecht et al., 2011b). These studies confirmed the OA mode of action described earlier.

In the present study, the barrier properties of two quaternary lipid model membranes (composed of i.a. Cer [AP] and Cer [EOS]) with additionally incorporated OA were investigated. In our previous studies, two lipid model membranes (Membrane I and Membrane II, see Table 1) were, firstly, characterized in terms of the lipid organization

using numerous analytical techniques (Ochalek et al., 2012a) and, secondly, the impact of their composition on the barrier function was examined by conducting diffusion and permeation studies of three model drugs (Ochalek et al., 2012b). The results of the first study showed that regarding the lipid distribution and organization, the SC lipid model membranes were prepared in a standardized way. Moreover, it was confirmed in the second study that the composition of SC lipid model systems had a significant impact on their barrier function. The objective of the present study was to investigate the impact of the penetration enhancer, OA, on the barrier properties of SC lipid model membranes. As stated previously, the use of simple, but well-defined artificial SC lipid systems elucidates its investigation. It was analyzed by means of a comparison of diffusion and permeation of three model drugs that cover a broad range of lipophilicities (i.e. urea, caffeine and diclofenac sodium) across SC lipid model membranes with integrated OA. The studies were carried out using Franz-type diffusion cells. Analytical procedures, HPLC and capillary electrophoresis (CE), were employed to analyze the amount of permeated drug through SC lipid model membranes. A mathematical model was used in order to estimate diffusion coefficients of the model drugs.

2. Materials and methods

2.1. Materials

Synthetic Cer [EOS] and Cer [AP] were generously provided by Evonik Goldschmidt (Essen, Germany). Palmitic acid (PA), oleic acid, sodium cholesteryl sulfate, caffeine, diclofenac sodium salt and urea were obtained from Sigma-Aldrich Chemie GmbH (Steinheim, Germany) and cholesterol from Sigma Chemical CO. (St. Louis, USA). Methanol, ethanol, chloroform, acetonitrile, formic acid and n-hexane were purchased from Merck (Darmstadt, Germany). Urease (from jack beans, 9.0 U mg⁻¹) was purchased from Fluka (Buchs, Switzerland). Nuclepore polycarbonate membrane filters (diameter 25 mm, pore size 50 nm) were obtained from Whatman (Kent, UK). Solvents used for the sample preparation and analytical procedures were of analytical grade.

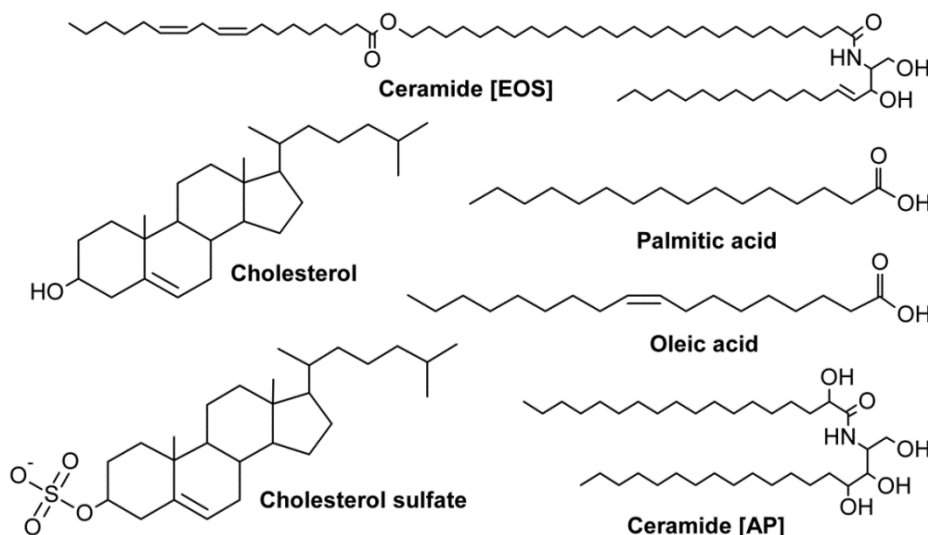


Fig. 1. Chemical structures of constituents of SC lipid model membranes.

2.2. Preparation of SC model lipid membranes with oleic acid

The SC lipid model membranes were prepared according to the method described earlier (Ochalek et al., 2012a). Briefly, appropriate amounts of individual lipids (Table 1) were dissolved in a mixture of chloroform/methanol (2/1, v/v). A distinguishing factor from the previously used SC lipid model membranes (Membrane I and Membrane II) was a presence of a lipophilic penetration enhancer, OA (10%, mass percentage – also known as m/m), in currently used SC lipid model membranes (Membrane Ia and Membrane IIa). The chemical structures of lipids used for the preparation of SC lipid model membranes are presented in Fig. 1. Following the evaporation of chloroform and methanol under a stream of nitrogen (because of the incompatibility of chloroform and Nuclepore polycarbonate filters), the lipids were re-dissolved in a mixture of n-hexane/ethanol (2/1, v/v) at a total lipid concentration of 5 mg/ml. The lipid mixtures were applied onto porous membrane filters using Automatic TLC Sampler 4 (Camag, Muttenz, Switzerland) with a specially built holder at a very low flow rate (80 nl/s) and under a stream of nitrogen. 100 μl of a lipid solution were sprayed on the filter area of 169 mm^2 . In order to enhance the multilamellar orientation of lipids and to decrease the mosaicity of samples, an annealing procedure was performed subsequently. It consisted of a heating step (30 min at 80 °C or 70 °C in the case of Membrane Ia and Membrane IIa, respectively) and a subsequent cooling down step (to room temperature) at 100% relative humidity. SC lipid model membranes prepared in this manner were, afterward, a subject to diffusion and permeation studies.

Table 1 Composition of SC lipid model membranes.

Model membrane	Composition	Ratio (m/m)
Membrane I ^a	Cer [AP]/Chol/PA/ChS	55/25/15/5
Membrane II ^a	Cer [AP]/Cer [EOS]/Chol/PA	10/23/33/33
Membrane Ia	Cer [AP]/Chol/PA/ChS/OA	49.5/22.5/13.5/4.5/10
Membrane IIa	Cer [AP]/Cer [EOS]/Chol/PA/OA	9/20.7/29.7/29.7/10

^a Membrane I and Membrane II were investigated in a previous study (Ochalek et al., 2012b).

2.3. Diffusion and permeation studies

In order to perform *in vitro* diffusion and permeation experiments, Franz-type diffusion cells (Rettberg, Goettingen, Germany) were used. 10% (m/m) solution of urea, 2% (m/m) solution of caffeine and 0.1% (m/m) solution of diclofenac sodium were used as model drugs. Drug solutions were prepared in phosphate-buffered saline (PBS, pH 7.4: NaCl, KCl, Na₂HPO₄ and KH₂PO₄ in water in concentrations 8.0, 0.2, 1.44 and 0.24 g/l, respectively). In the case of urea, PBS solution without potassium ions was used (owing to the analytical technique of the urea determination in samples taken from the acceptor compartment). Model drugs used in the study are shown in Fig. 2. Their physicochemical properties are presented in Table 2. The pK_a and $\log P$ values, where $\log P$ stands for log partition coefficient value, were either found in the literature (Khazaeinia and Jamali, 2003; Kokate et al., 2008) or calculated using ChemAxon's Marvin software. The $\log D$ values (log distribution coefficient values) were calculated using equation: $\log D = \log P + \log[1/(1 + 10^x)]$, where $x = pH - pK_a$ or $pH + pK_a$ in the case of acids and bases, respectively (Scherrer and Howard, 1977). As can be seen in Table 2, the $\log D$ values of urea and caffeine equal their $\log P$ values. The reason for this was neutral (unionized) character of these two drugs at pH used in the study, contrary to diclofenac sodium which was mostly ionized in these conditions (negatively charged diclofenac ions). For all diffusion and permeation studies, the donor phase consisted of 1 ml of the model drug solution in PBS. The acceptor compartment was filled with approx. 5 ml of PBS (pH 7.4) that were stirred by use of a magnetic bar. The samples from the acceptor compartment were collected at predetermined points in time. Subsequently, a quantitative analysis of collected samples was carried out using a specific analytical routine developed for each model drug. The reduced volume of the acceptor phase was supplemented with the fresh PBS solution after each sample collection. All diffusion and

permeation experiments were performed under occlusive conditions, provided by sealing the opening of the donor compartment with an adhesive tape. In order to mimic the *in vivo* conditions, the temperature inside the diffusion cells was maintained at 32 °C by use of thermostated water baths. The artificial SC lipid systems with the incorporated penetration enhancer, OA, (Membrane Ia and Membrane IIa) were used as model membranes in diffusion and permeation studies.

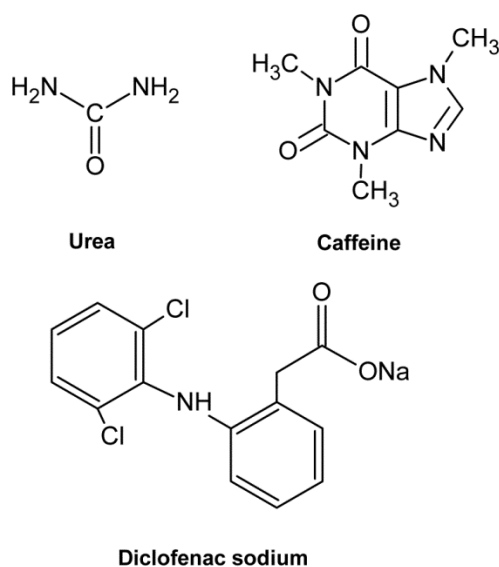


Fig. 2. Chemical structures of model drugs.

Table 2 Physicochemical properties of model drugs

Drug	Molar mass [g/mol]	log <i>P</i>	log <i>D</i> _{7.4} ^a	p <i>K</i> _a (25 °C)
Urea	60.06	-2.11	-2.11	0.18
Caffeine	194.19	-0.07	-0.07	1.4
Diclofenac sodium	318.14	4.28 ^b	0.88	4.0

^a values of log distribution coefficients at pH = 7.4

^b log *P* value of the uncharged drug form

2.4. HPLC and CE assays; data modeling

The concentration of drugs in the samples collected from the acceptor compartment was determined using either HPLC or CE technique (Ochalek et al., 2012b).

The HPLC method was developed to analyze the quantity of caffeine in the receptor compartment. The Agilent 1100 LC System (Agilent, Waldbronn, Germany) equipped with

a vacuum degasser, a binary pump, an autosampler and a diode array detector was used in this study. Separations were carried out in a Eurospher 100-5-RP18 column with dimensions: 100 x 2 mm (Knauer, Berlin, Germany) kept at a temperature of 30 °C. As a mobile phase, an isocratic mixture of water/methanol (60/40, v/v) was used, at a flow rate of 0.2 ml min⁻¹. The injection volume of each sample amounted to 5 µl. The detection of caffeine was carried out at a wavelength of 273 nm and its limit of quantification amounted to 0.07 µg ml⁻¹.

The amount of diclofenac sodium in the receptor phase was found using the same HPLC system, as described in the case of caffeine determination. As a stationary phase, Nucleosil C8 column with dimensions: 125 x 2 mm (Macherey–Nagel GmbH & Co. KG, Dueren, Germany) was used. 0.1 % formic acid in a mixture of water/acetonitrile (50/50, v/v) with a flow rate of 0.2 ml min⁻¹ was applied as a mobile phase. 5 µl of each sample were injected into the HPLC column maintained at a temperature of 30 °C. The detection was performed at a wavelength of 278 nm and the limit of quantification of diclofenac sodium amounted to 0.2 µg ml⁻¹.

A conventional CE with contactless conductivity detection method was developed to quantitatively analyze the urea samples taken from the receptor phase. The samples were examined after an enzymatic conversion of urea to ammonium. This procedure was described in detail in our previous study (Ochalek et al., 2012b). Briefly, 2 mg ml⁻¹ urease suspension was added to the samples collected from the receptor compartment. In order to guarantee a completeness of the enzymatic conversion, the mixtures were shaken for 2 hours, subsequently. Next, the samples were filtrated using 0.2 µm cellulose filters (Wicom, Heppenheim, Germany). To determine the ammonium amount and hence the urea concentration in the acceptor phase, PrinCE-C 750 CE System (Prince Technologies, Emmen, The Netherlands) was used. In order to improve the amplitude stability, the built in-house contactless conductivity detector was equipped with a rectangular wave generator instead of a sinusoidal one, contrary to other devices of this type. Fused-silica capillaries (CS-Chromatographie Service, Langerwehe, Germany) with 75 µm ID and 50.8 cm length (35.3 cm to detector) were preconditioned with 1 M NaOH for 10 min and water for 10 min, and subsequently rinsed with running buffer (20 mM MES/HIS buffer) for 20 min. The capillaries were flushed with the MES/HIS buffer after each run. The additional rinsing with 0.1 M NaOH for 5 min, water for 5 min and the MES/HIS buffer for 10 min was performed, when peak deformations were observed. The separation voltage amounted to 20 kV. The limit of quantification was 0.25 µg ml⁻¹. As mentioned earlier, in the case of diffusion studies of urea, the PBS solution without potassium ions was used

because of a similarity of ammonium and potassium ions (similar size), and hence a difficult separation of these ions by CE.

To calculate diffusion coefficients of model drugs, a mathematical model was developed. Its detailed description was presented previously (Ochalek et al., 2012b). For simplicity reasons, the potential interaction between diclofenac ions and FFA ions from the lipid model membranes was not taken into account in the mathematical data modeling. In accordance with the Fick's second law of diffusion, the drug concentration $u(t, x)$ within the model membrane can be approximated by a solution of a linear one-dimensional diffusion equation:

$$\frac{\partial u}{\partial t} = D \frac{\partial^2 u}{\partial x^2} \quad 0 \leq x \leq L; t \geq 0 \quad (1)$$

where L is the membrane thickness. Fitting appropriate initial and boundary conditions to Eq. (1) and replacing the spatial derivatives by standard central differences led to a linear system of ordinary differential equations with a constant matrix M . Taking into account that the velocity of the drug permeation through the membrane is determined by the slowest eigenmode of M corresponding to the eigenvalue λ_1 , one can fit the model given by:

$$u_A(t) = u_\infty(1 - \exp(\gamma t)) \quad (2)$$

to the experimental data and acquire an estimate for the diffusion coefficient by: $D = \gamma/\lambda_1$.

In order to obtain other permeability parameters, the cumulative permeated amount of model drugs per cm^2 was plotted as a function of time. The slope of the linear part of the plot was taken as the steady-state flux (J) and its intercept with the time-axis was the lag-time (T_L). The permeability coefficient (k_p) was calculated as a quotient of the flux and the initial drug concentration in the donor compartment.

The estimated permeability parameters were compared using one-way analysis of variance (ANOVA) with Tukey's test as *post hoc* analysis. Significance was accepted when $p < 0.05$. In cases when the compared parameters were not normally distributed or the variances were not equal, a nonparametric Kruskal-Wallis ANOVA test was performed (a level of significance was set at $p < 0.05$).

3. Results and discussion

3.1. Diffusion and permeation of model drugs through SC lipid model membranes in the presence of the penetration enhancer, OA

Diffusion and permeation studies of three model drugs with varying lipophilicities (Table 2) across SC lipid model membranes with incorporated OA (10%, m/m) were performed in order to investigate the impact of the penetration enhancer on their diffusion and permeation profiles.

Fig. 3 displays diffusion and permeation profiles of model drugs with the mathematical model fittings across Membrane Ia (A) and Membrane IIa (B). It can be clearly seen in the figure that in the case of both SC lipid model systems, the diffusion of urea was faster than the permeation of caffeine and diclofenac sodium. Moreover, the slowest rate of permeation was characteristic for the latter. The values of steady-state flux (J), lag-time (T_L), permeability coefficient (k_p) and diffusion coefficient (D) are listed in Table 3. In the case of Membrane Ia (Fig. 3A), the J values amounted to 10.65 ± 1.33 , 0.24 ± 0.07 and 0.017 ± 0.003 $\text{mg cm}^{-2} \text{h}^{-1}$ for urea, caffeine and diclofenac sodium, respectively. The corresponding T_L values for urea, caffeine and diclofenac sodium amounted to -0.37 ± 0.27 , 0.18 ± 0.22 and 0.19 ± 0.09 h, and the k_p values were 0.11 ± 0.01 , 0.012 ± 0.004 and 0.017 ± 0.003 cm h^{-1} , respectively. The D values amounted to 5.44 ± 2.55 , 0.09 ± 0.02 and $0.16 \pm 0.04 \times 10^{-8}$ $\text{cm}^2 \text{s}^{-1}$ in the case of urea, caffeine and diclofenac sodium, respectively. The diffusion and permeation profiles of model drugs across Membrane IIa are presented in Fig. 3B. The J values in the case of urea, caffeine and diclofenac sodium amounted to 9.54 ± 1.52 , 0.20 ± 0.06 and 0.013 ± 0.002 $\text{mg cm}^{-2} \text{h}^{-1}$, and the T_L values were -0.77 ± 0.17 , -0.24 ± 0.13 and -0.14 ± 0.03 h, respectively. The k_p values amounted to 0.095 ± 0.015 , 0.010 ± 0.003 and 0.013 ± 0.002 cm h^{-1} , and the values of D were 12.83 ± 8.37 , 0.16 ± 0.15 and $0.21 \pm 0.04 \times 10^{-8}$ $\text{cm}^2 \text{s}^{-1}$ for urea, caffeine and diclofenac sodium, respectively.

In our previous study, the influence of physicochemical properties of model drugs on their diffusion and permeation behavior was examined (Ochalek et al., 2012b). Three model drugs covering a broad range of lipophilicities (log D values of model drugs at pH = 7.4 amounted to -2.11 , -0.07 and 0.88 for urea, caffeine and diclofenac sodium, respectively) and characterized by a different molecular weight were chosen to investigate the impact of the partitioning characteristics of drugs on the rate of diffusion. It was found that the most hydrophilic drug, urea, diffused through both artificial lipid

membranes (Membrane I and Membrane II) and the human SC faster than the more lipophilic molecule, caffeine, and much faster than the most lipophilic drug, diclofenac sodium. The fastest rate of diffusion in the case of urea was explained by its smallest molecular weight, when compared to the more lipophilic drugs, as well as its permeation enhancing potential for the hydrophilic pathway. When comparing the permeation behavior of caffeine and diclofenac sodium, two factors have to be taken into account. On the one hand, caffeine is characterized by a smaller molecular weight than the latter; on the other hand, diclofenac sodium is more lipophilic than caffeine and appears mostly in an ionized form. Altogether, it resulted in slightly larger values of k_p and D in favor of diclofenac sodium.

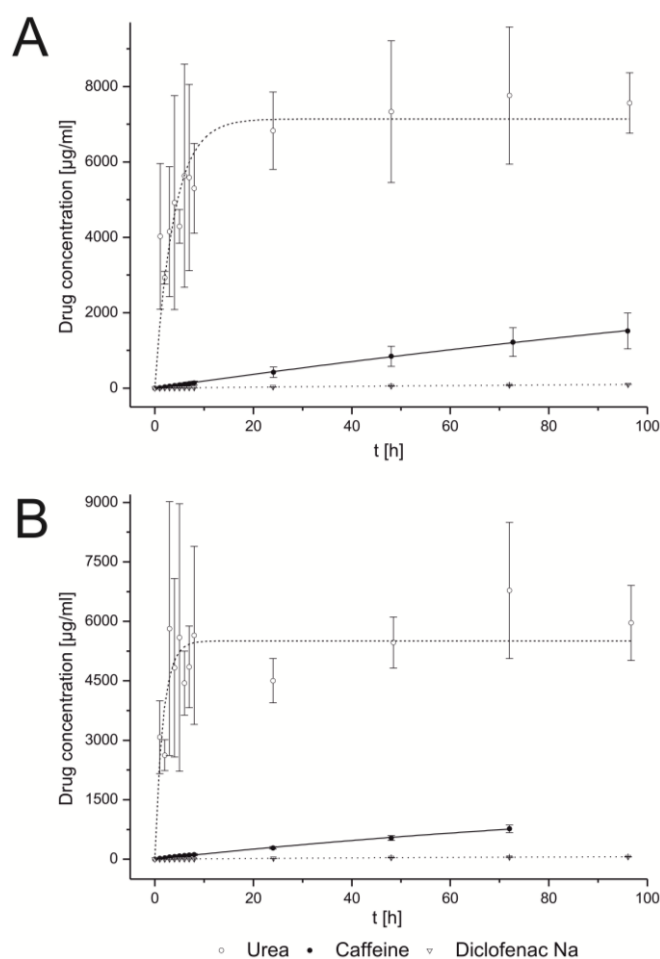


Fig. 3. Diffusion and permeation through the model lipid membranes, (A) Membrane Ia and (B) Membrane IIa (data shown with mathematical model fittings). Error bars show the standard deviation (n = 4).

Interestingly, an addition of 10% (m/m) of the lipophilic penetration enhancer, OA, did not change the relation observed earlier for the SC lipid model membranes devoid of

OA. A comparison of permeability parameters shows that the J of urea was ~ 44 times larger than J of caffeine and ~ 627 times larger than J of diclofenac sodium in the case of Membrane Ia. A similar relationship applies for the J values in the case of the diffusion across Membrane IIa, where J of urea was ~ 48 times and ~ 734 times larger than the J of caffeine and diclofenac sodium, respectively. The k_p of urea in the case of Membrane Ia was higher than k_p of caffeine and diclofenac sodium by a factor of ~ 9 and ~ 7 , respectively. For Membrane IIa, k_p of urea was ~ 10 times and ~ 7 times larger than k_p of caffeine and diclofenac sodium, respectively. However, in the case of both SC lipid model membranes, the k_p values of caffeine and diclofenac sodium were not significantly different ($\alpha = 0.05$).

Table 3 Permeability parameters of urea, caffeine and diclofenac sodium – *in vitro* study.

Drug/Parameter	J [mg cm ⁻² h ⁻¹]	T_L [h]	k_p [cm h ⁻¹]	D [x 10 ⁻⁸ cm ² s ⁻¹]
SC ^a	42.23 ± 1.66	-1.01 ± 0.24	0.42 ± 0.02	27.14 ± 7.16
Membrane I ^a	1.36 ± 0.13	2.88 ± 1.13	0.014 ± 0.001	0.25 ± 0.13
Urea				
Membrane II ^a	19.52 ± 1.53	-0.47 ± 0.50	0.20 ± 0.02	1.59 ± 0.16
Membrane Ia	10.65 ± 1.33	-0.37 ± 0.27	0.11 ± 0.01	5.44 ± 2.55
Membrane IIa	9.54 ± 1.52	-0.77 ± 0.17	0.095 ± 0.015	12.83 ± 8.37
SC ^a	2.00 ± 1.12	-0.01 ± 0.15	0.10 ± 0.06	6.58 ± 4.02
Membrane I ^a	0.06 ± 0.01	5.89 ± 1.12	0.003 ± 0.001	0.023 ± 0.006
Caffeine				
Membrane II ^a	0.38 ± 0.04	0.15 ± 0.26	0.019 ± 0.002	0.16 ± 0.02
Membrane Ia	0.24 ± 0.07	0.18 ± 0.22	0.012 ± 0.004	0.09 ± 0.02
Membrane IIa	0.20 ± 0.06	-0.24 ± 0.13	0.010 ± 0.003	0.16 ± 0.15
SC ^a	0.008 ± 0.004	0.73 ± 0.94	0.008 ± 0.004	0.54 ± 0.69
Membrane I ^a	0.007 ± 0.002	3.56 ± 1.69	0.007 ± 0.002	0.060 ± 0.014
Diclofenac sodium				
Membrane II ^a	0.023 ± 0.001	0.77 ± 0.23	0.023 ± 0.001	0.19 ± 0.01
Membrane Ia	0.017 ± 0.003	0.19 ± 0.09	0.017 ± 0.003	0.16 ± 0.04
Membrane IIa	0.013 ± 0.002	-0.14 ± 0.03	0.013 ± 0.002	0.21 ± 0.04

Permeability data represent MEAN ± SD (n = 4).

^a J , T_L , k_p and D values for the human SC, Membrane I and Membrane II were obtained in a previous study (Ochalek et al., 2012b).

A comparison of D values shows that D of urea for Membrane Ia was ~ 60 -fold and ~ 34 -fold higher than D of caffeine and diclofenac sodium, respectively. In the case of Membrane IIa, a similar relationship was observed. Namely, D of urea was larger than D of caffeine and diclofenac sodium by a factor of ~ 80 and ~ 61 , respectively, whereas the

D values of caffeine and diclofenac sodium were not significantly different ($\alpha = 0.05$). T_L of caffeine and diclofenac sodium in the case of Membrane Ia were not significantly different ($\alpha = 0.05$), and were slightly longer than T_L of urea, which can be assumed to equal 0 (a negative value). For Membrane IIa, the differences in T_L of caffeine and diclofenac sodium were not significant ($\alpha = 0.05$) and their values, as well as T_L of urea, can be assumed to equal 0. As mentioned above, in the case of SC lipid model membranes with incorporated OA, the same relation was observed as for the systems devoid of OA. The most hydrophilic substance, urea, was characterized by the fastest rate of diffusion through both SC lipid model membranes (Membrane Ia and Membrane IIa). When comparing the permeability parameters of caffeine and diclofenac sodium for both SC lipid model systems, the values of D , k_p and T_L were either equal or slightly higher in favor of the most lipophilic drug, diclofenac sodium. The reasons for such diffusion and permeation behavior of model drugs were described earlier. The incorporation of OA into the SC lipid model membranes changed the diffusion and permeation behavior of model drugs to the same extent. As a consequence, a similar relation holds for diffusion and permeation of model drugs across SC lipid model membranes with and without OA.

3.2. Influence of the penetration enhancer, OA, on the barrier function of two SC lipid model membranes

To investigate the impact of the penetration enhancer on the barrier properties of SC lipid model systems, the diffusion and permeation studies of three model drugs across Membrane Ia and Membrane IIa were carried out. Subsequently, the results of these studies were compared with the outcomes of the previously performed diffusion and permeation experiments through the SC lipid model membranes devoid of OA (Membrane I and Membrane II) and the human SC (Ochalek et al., 2012b).

Fig. 4 displays diffusion and permeation profiles of urea (A), caffeine (B) and diclofenac sodium (C), with mathematical model fittings, across SC lipid model membranes and the human SC. The permeability parameters of model drugs for all membranes used in the diffusion and permeation studies are presented in Table 3.

In the case of diffusion of urea through Membrane Ia and Membrane IIa (Fig. 4A), diffusion profiles were much alike. Moreover, the values of J , k_p and D of urea were not significantly different ($\alpha = 0.05$) for Membrane Ia and Membrane IIa. The T_L values of urea for both SC lipid model membranes with OA were negative, and hence can be assumed to equal 0. On the other hand, when comparing diffusion profiles and

permeability parameters of urea for SC lipid model membranes with and devoid of OA, one can notice clear differences. J of urea in the case of Membrane Ia was ~ 8 times larger than J in the case of diffusion through Membrane I. For Membrane IIa, the J value of urea was ~ 2 times smaller than J in the case of Membrane II. The same ratios apply for a comparison of the k_p values of urea (between Membrane Ia and Membrane I, and Membrane IIa and Membrane II). In the case of diffusion through Membrane Ia, the D value of urea was higher by a factor of ~ 22 than D of urea for Membrane I, and for Membrane IIa ~ 8 -fold larger than D of urea for Membrane II. As can be seen in Fig. 4A, for the diffusion profiles of urea across the human SC and all SC lipid model membranes but Membrane I, no lag phase was observed. The values of T_L for the human SC, Membrane II, Membrane Ia and Membrane IIa were negative (i.e. can be assumed to equal 0). Moreover, T_L of urea for Membrane IIa and Membrane II, as well as for Membrane IIa and SC, were not significantly different ($\alpha = 0.05$). In the case of Membrane I, T_L of urea was well pronounced and was ~ 3.3 h longer than for Membrane Ia. The other permeability parameters in the case of diffusion of urea across the human SC were considerably larger than for all SC model lipid membranes. A similar relation as described for the diffusion of urea holds also for the permeation of caffeine across both the human SC and SC lipid model membranes (Fig. 4B). In the case of permeation of caffeine through Membrane Ia and Membrane IIa, the values of J , k_p and D were not significantly different ($\alpha = 0.05$). Both J and k_p values of caffeine in the case of permeation across Membrane Ia were 4-fold larger than J and k_p for permeation through Membrane I, and in the case of Membrane IIa ~ 2 -fold smaller than for Membrane II. A comparison of D values shows that D of caffeine for Membrane Ia was ~ 4 times larger than the corresponding value in the case of permeation across Membrane I, and in the case of Membrane IIa and Membrane II, the D values were not significantly different ($\alpha = 0.05$). The T_L values of caffeine for the SC, Membrane II, Membrane Ia and Membrane IIa were close to 0. The differences in T_L of caffeine for Membrane Ia and Membrane II, Membrane Ia and the human SC, and Membrane IIa and the human SC were not significant ($\alpha = 0.05$). T_L of caffeine in the case of permeation across Membrane I was ~ 5.7 h longer than for Membrane Ia. The J , k_p and D values of caffeine in the case of permeation through the human SC were considerably larger than for all SC model lipid membranes. The permeation profiles of diclofenac sodium across the human SC and SC lipid model membranes are shown in Fig. 4C. For the permeation of diclofenac sodium across Membrane Ia and Membrane IIa, the values of J , k_p and D were not significantly different ($\alpha = 0.05$). The J and k_p values of diclofenac sodium in the case of permeation through

Membrane Ia were higher than for Membrane I by a factor of ~ 2 , and for Membrane IIa ~ 2 times smaller than for Membrane II. The differences in the D values of diclofenac sodium for the human SC and all SC lipid model membranes were not significant at the 0.05 level. The T_L of diclofenac sodium in the case of Membrane Ia was close to 0 and ~ 3.4 h shorter than T_L for Membrane I. For Membrane IIa, T_L can be assumed to equal 0 and was ~ 0.9 h shorter than in the case of Membrane II.

The penetration enhancer, OA, had a pronounced impact on the barrier properties of SC lipid model membranes. A comparison of diffusion and permeation profiles, as well as the permeability parameters, of model drugs acquired for the diffusion/permeation across SC lipid model membranes with and without OA leads to the conclusion that the presence of OA weakened the barrier function of Membrane I, however, surprisingly demonstrated an opposite effect on Membrane II. The influence of OA on the bilayer structure of SC model lipid membranes was investigated by Engelbrecht et al. (2011b). In their neutron diffraction studies, a lipid membrane composed of Cer [AP], Chol, PA, ChS and 10% (m/m) OA (i.e. Membrane Ia), was used. It was confirmed by use of deuterated OA that the unsaturated FFA was incorporated into lipid bilayers of SC lipid model membranes. It was also found that OA did not induce a change in a lamellar periodicity of the SC lipid model membrane. However, on the other hand, OA caused increased alkyl chain disorder and disturbed the lamellar assembly of lipids within bilayers of SC lipid model membranes. The perturbations observed were most likely caused by the presence of the *cis* double bond within OA molecules. These findings are confirmed by the results of the present study. Because of the impairment of the barrier function of Membrane Ia due to the presence of the penetration enhancer, diffusion and permeation of model drugs occurred more rapidly than for the SC lipid model membrane without OA (Membrane I). The values of J , k_p and D for the diffusion and permeation of drugs through Membrane Ia were considerably higher than for Membrane I, hence pointed at Membrane Ia as a SC lipid model membrane with weaker barrier. The most noticeable evidence confirming its weaker barrier properties were differences in T_L values between Membrane Ia and Membrane I. While for Membrane Ia, they were either 0 or close to 0, in the case of Membrane I, the lag phase was well marked (amounted to $\sim 3\text{--}6$ h for diffusion and permeation studies of model drugs used). To the best of our knowledge, in the case of Membrane IIa (composed of i.a. Cer [AP] and Cer [EOS]), no studies on the bilayer structure and the impact of the penetration enhancer on its barrier function were carried out.

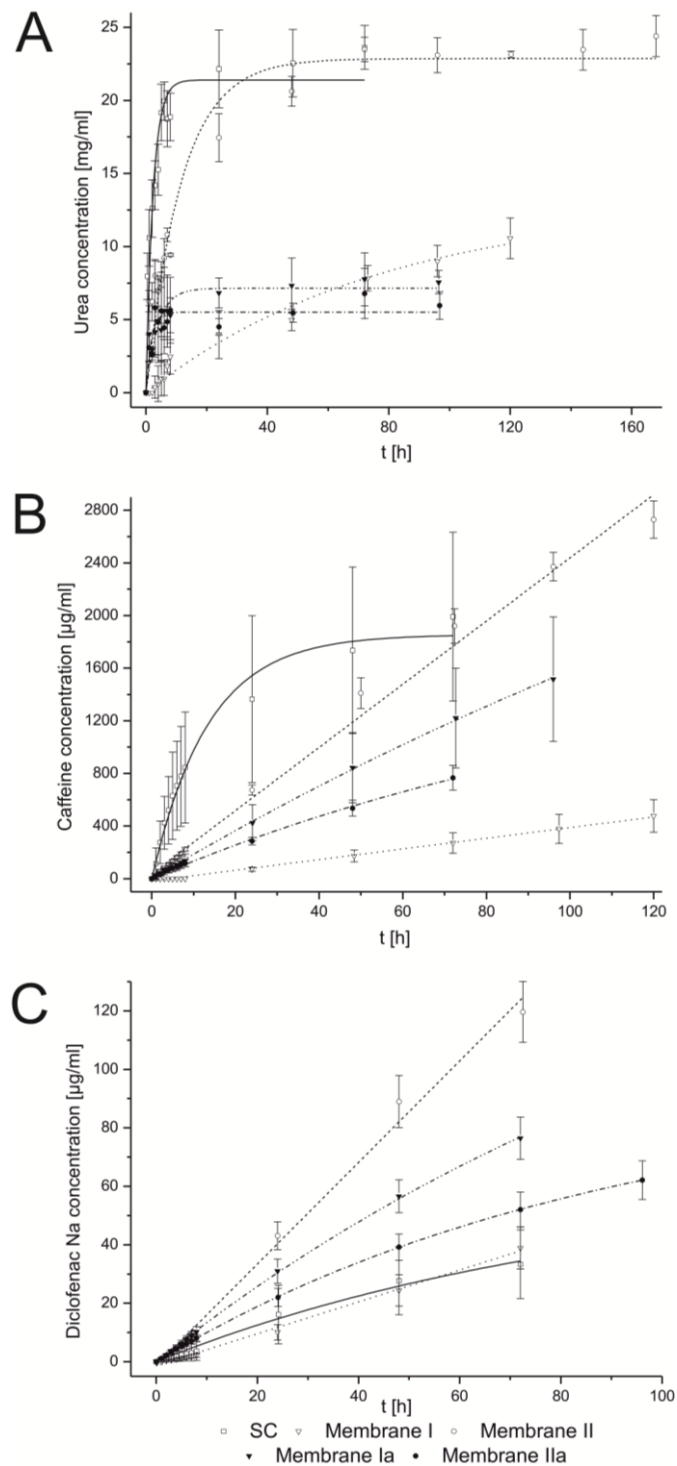


Fig. 4. Diffusion and permeation profiles of (A) urea, (B) caffeine and (C) diclofenac sodium (across model lipid membranes and human SC) and their model fittings. Error bars show the standard deviation ($n = 4$). The diffusion and permeation profiles for the SC, Membrane I and Membrane II were presented previously (Ochalek et al., 2012b).

Therefore, it was not possible to relate directly the distinct barrier properties of Membrane IIa to the changes in its lipid organization. However, the results of the present study clearly indicate that Membrane IIa has stronger barrier properties than Membrane

II. The lower values of J and k_p were characteristic for Membrane IIa. A comparison of D values shows that for permeation of caffeine and diclofenac sodium through Membrane IIa and Membrane II, D values were equal ($\alpha = 0.05$); and for diffusion of urea, D in the case of Membrane IIa was even larger than for Membrane II. Surprisingly, T_L values of model drugs for Membrane IIa were either equal ($\alpha = 0.05$) or even slightly shorter than for Membrane II. The reason why Membrane IIa despite the presence of the penetration enhancer had stronger barrier properties, is most likely the different lipid composition, hence the distinct lipid organization, of SC lipid model membranes. Membrane IIa contained a considerable amount of Cer [EOS] and only 9% (m/m) of Cer [AP]. The long-chain ceramide, Cer [EOS], is normally forced to fit into the membrane created by Cer [AP] and its long alkyl chain traverses the lipid bilayer and expands into the adjacent layer (Schroeter et al., 2009a). The presence of OA within this membrane probably improved the lamellar ordering of SC lipids. A possible explanation for that can be a possession of the *cis* double bond by OA molecule, which can more easily fit to the lipid bilayer where a ceramide with two *cis* double bonds (namely Cer [EOS]) is also present. Therefore, in the case of Membrane IIa, OA did not cause perturbations to the lamellar assembly of lipids within bilayers of this SC lipid model membrane. The lipids within Membrane IIa were arranged slightly tighter than in the case of Membrane II.

4. Conclusions

Diffusion and permeation studies of three model drugs covering a broad range of lipophilicities (urea, caffeine and diclofenac sodium) were performed to investigate the influence of physicochemical properties of drugs on their diffusion and permeation across SC lipid model membranes in the presence of the lipophilic penetration enhancer, OA, as well as to examine the impact of the penetration enhancer on the barrier properties of SC lipid model membranes. Firstly, an addition of 10% (m/m) of OA to the SC lipid model membranes did not influence the relation between the diffusion and permeation behavior of model drugs presented previously for SC lipid model membranes devoid of the penetration enhancer. The fastest rate of diffusion through both SC lipid model membranes (Membrane Ia and Membrane IIa) occurred in the case of the most hydrophilic drug, urea. For permeation studies of caffeine and diclofenac sodium across both SC lipid model systems, the D , k_p and T_L values were either equal or slightly higher in favor of the most lipophilic drug, diclofenac sodium. Secondly, the impact of the lipophilic penetration enhancer, OA, on the barrier function of SC lipid model membranes was

analyzed. OA caused the impairment of the barrier function of Membrane I (confirmed by the studies on Membrane Ia), however, surprisingly increased the barrier properties of Membrane II (easily visible when comparing diffusion and permeation profiles of model drugs across Membrane II and Membrane IIa). Based on the results presented, it can be assumed that OA within Membrane IIa improved the lamellar ordering of SC lipids. The *cis* double bond of OA can more easily fit to the lipid bilayer where two other *cis* double bonds coming from Cer [EOS] are present. As a consequence, the chain disorder of lipids within bilayers of Membrane IIa was reduced. It resulted in the improvement of the barrier function of the SC lipid model membrane (with Cer [EOS]) in the presence of OA.

Acknowledgements

The financial support for Michal Ochalek provided by the Institute of Applied Dermatopharmacy (IADP) of the Martin Luther University Halle-Wittenberg is gratefully appreciated. The authors would like to express their gratitude to Dr. A. Schroeter for her invaluable advice and comments on the structure of SC lipid model membranes.

References

- Bouwstra, J.A., Gooris, G.S., Cheng, K., Weerheim, A., Bras, W., Ponc, M., 1996. Phase behavior of isolated skin lipids. *J. Lipid Res.* 37, 999-1011.
- Coderch, L., Lopez, O., de la Maza, A., Parra, J.L., 2003. Ceramides and skin function. *Am. J. Clin. Dermatol.* 4, 107-129.
- de Jager, M.W., Groenink, W., Bielsa i Guivernau, R., Andersson, E., Angelova, N., Ponc, M., Bouwstra, J.A., 2006. A novel in vitro percutaneous penetration model: evaluation of barrier properties with p-aminobenzoic acid and two of its derivatives. *Pharm. Res.* 23, 951-960.
- Elias, P.M., 1983. Epidermal lipids, barrier function, and desquamation. *J. Invest. Dermatol.* 80, 44s-49s.
- Engelbrecht, T., Hauss, T., Sueß, K., Vogel, A., Roark, M., Feller, S.E., Neubert, R.H.H., Dobner, B., 2011a. Characterisation of a new ceramide EOS species: synthesis and investigation of the thermotropic phase behaviour and influence on the bilayer architecture of stratum corneum lipid model membranes. *Soft Matter* 7, 8998-9011.
- Engelbrecht, T.N., Schroeter, A., Hauss, T., Neubert, R.H.H., 2011b. Lipophilic penetration enhancers and their impact to the bilayer structure of stratum corneum lipid model membranes: Neutron diffraction studies based on the example Oleic Acid. *Biochim. Biophys. Acta, Biomembranes* 1808, 2798-2806.
- Francoeur, M.L., Golden, G.M., Potts, R.O., 1990. Oleic acid: its effects on stratum corneum in relation to (trans)dermal drug delivery. *Pharm. Res.* 7, 621-627.
- Funari, S.S., Barcelo, F., Escriba, P.V., 2003. Effects of oleic acid and its congeners, elaidic and stearic acids, on the structural properties of phosphatidylethanolamine membranes. *J. Lipid Res.* 44, 567-575.
- Groen, D., Poole, D.S., Gooris, G.S., Bouwstra, J.A., 2011. Investigating the barrier function of skin lipid models with varying compositions. *Eur. J. Pharm. Biopharm.* 79, 334-342.

- Kessner, D., Kiselev, M.A., Dante, S., Hauss, T., Lersch, P., Wartewig, S., Neubert, R.H.H., 2008. Arrangement of ceramide [EOS] in a stratum corneum lipid model matrix: new aspects revealed by neutron diffraction studies. *Eur. Biophys. J.* 37, 989-999.
- Khazaeinia, T., Jamali, F., 2003. A comparison of gastrointestinal permeability induced by diclofenac-phospholipid complex with diclofenac acid and its sodium salt. *J. Pharm. Pharm. Sci.* 6, 352-359.
- Kiselev, M.A., 2007. Conformation of ceramide 6 molecules and chain-flip transitions in the lipid matrix of the outermost layer of mammalian skin, the stratum corneum. *Crystallogr. Rep.* 52, 525-528.
- Kiselev, M.A., Ryabova, N.Y., Balagurov, A.M., Dante, S., Hauss, T., Zbytovska, J., Wartewig, S., Neubert, R.H.H., 2005. New insights into the structure and hydration of a stratum corneum lipid model membrane by neutron diffraction. *Eur. Biophys. J.* 34, 1030-1040.
- Kokate, A., Li, X., Jasti, B., 2008. Effect of drug lipophilicity and ionization on permeability across the buccal mucosa: a technical note. *AAPS PharmSciTech.* 9, 501-504.
- Masukawa, Y., Narita, H., Shimizu, E., Kondo, N., Sugai, Y., Oba, T., Homma, R., Ishikawa, J., Takagi, Y., Kitahara, T., Takema, Y., Kita, K., 2008. Characterization of overall ceramide species in human stratum corneum. *J. Lipid Res.* 49, 1466-1476.
- McIntosh, T.J., 2003. Organization of skin stratum corneum extracellular lamellae: diffraction evidence for asymmetric distribution of cholesterol. *Biophys. J.* 85, 1675-1681.
- McIntosh, T.J., Stewart, M.E., Downing, D.T., 1996. X-ray diffraction analysis of isolated skin lipids: reconstitution of intercellular lipid domains. *Biochemistry* 35, 3649-3653.
- Naik, A., Pechtold, L.A.R.M., Potts, R.O., Guy, R.H., 1995. Mechanism of oleic acid-induced skin penetration enhancement in vivo in humans. *J. Control. Release* 37, 299-306.
- Ochalek, M., Heissler, S., Wohlrab, J., Neubert, R.H.H., 2012a. Characterization of lipid model membranes designed for studying impact of ceramide species on drug diffusion and penetration. *Eur. J. Pharm. Biopharm.* 81, 113-120.
- Ochalek, M., Podhaisky, H., Ruettinger, H.-H., Wohlrab, J., Neubert, R.H.H., 2012b. SC lipid model membranes designed for studying impact of ceramide species on drug diffusion and permeation, Part II: Diffusion and permeation of model drugs. *Eur. J. Pharm. Biopharm.*, doi: 10.1016/j.ejpb.2012.06.008.
- Ongpipattanakul, B., Francoeur, M.L., Potts, R.O., 1994. Polymorphism in stratum corneum lipids. *Biochim. Biophys. Acta, Biomembranes* 1190, 115-122.
- Prades, J., Funari, S.S., Escriba, P.V., Barcelo, F., 2003. Effects of unsaturated fatty acids and triacylglycerols on phosphatidylethanolamine membrane structure. *J. Lipid Res.* 44, 1720-1727.
- Raudenkolb, S., Wartewig, S., Neubert, R.H.H., 2005. Polymorphism of ceramide 6: A vibrational spectroscopic and X-ray powder diffraction investigation of the diastereomers of N-(alpha-hydroxyoctadecanoyl)-phytosphingosine. *Chem. Phys. Lipids* 133, 89-102.
- Robson, K.J., Stewart, M.E., Michelsen, S., Lazo, N.D., Downing, D.T., 1994. 6-Hydroxy-4-sphinganine in human epidermal ceramides. *J. Lipid Res.* 35, 2060-2068.
- Rowat, A.C., Kitson, N., Thewalt, J.L., 2006. Interactions of oleic acid and model stratum corneum membranes as seen by ²H NMR. *Int. J. Pharm.* 307, 225-231.
- Scherrer, R.A., Howard, S.M., 1977. Use of distribution coefficients in quantitative structure-activity relationships. *J. Med. Chem.* 20, 53-58.
- Schroeter, A., Kessner, D., Kiselev, M.A., Hauss, T., Dante, S., Neubert, R.H.H., 2009a. Basic nanostructure of stratum corneum lipid matrices based on ceramides [EOS] and [AP]: a neutron diffraction study. *Biophys. J.* 97, 1104-1114.
- Schroeter, A., Kiselev, M.A., Hauss, T., Dante, S., Neubert, R.H.H., 2009b. Evidence of free fatty acid interdigitation in stratum corneum model membranes based on ceramide [AP] by deuterium labelling. *Biochim. Biophys. Acta, Biomembranes* 1788, 2194-2203.
- Schurer, N.Y., Plewig, G., Elias, P.M., 1991. Stratum corneum lipid function. *Dermatologica* 183, 77-94.

- Separovic, F., Gawrisch, K., 1996. Effect of unsaturation on the chain order of phosphatidylcholines in a dioleoylphosphatidylethanolamine matrix. *Biophys. J.* 71, 274-282.
- Tanojo, H., Geest, A.B.-v., Bouwstra, J.A., Junginger, H.E., Bodde, H.E., 1997. In vitro human skin barrier perturbation by oleic acid: Thermal analysis and freeze fracture electron microscopy studies. *Thermochimica Acta* 293, 77-85.
- Trommer, H., Neubert, R.H.H., 2006. Overcoming the stratum corneum: the modulation of skin penetration. A review. *Skin Pharmacol. Physiol.* 19, 106-121.
- van Smeden, J., Hoppel, L., van der Heijden, R., Hankemeier, T., Vreeken, R.J., Bouwstra, J.A., 2011. LC/MS analysis of stratum corneum lipids: ceramide profiling and discovery. *J. Lipid Res.* 52, 1211-1221.
- Walker, M., Hadgraft, J., 1991. Oleic-Acid - a Membrane Fluidizer or Fluid within the Membrane. *Int. J. Pharm.* 71, R1-R4.
- Walker, R.B., Smith, E.W., 1996. The role of percutaneous penetration enhancers. *Adv. Drug Deliver. Rev.* 18, 295-301.
- Weerheim, A., Ponc, M., 2001. Determination of stratum corneum lipid profile by tape stripping in combination with high-performance thin-layer chromatography. *Arch. Dermatol. Res.* 293, 191-199.
- Wertz, P.W., 2000. Lipids and barrier function of the skin. *Acta Derm. Venereol. Suppl.* 208, 7-11.
- Wertz, P.W., Miethke, M.C., Long, S.A., Strauss, J.S., Downing, D.T., 1985. The composition of the ceramides from human stratum corneum and from comedones. *J. Invest. Dermatol.* 84, 410-412.
- Wertz, P.W., van den Bergh, B., 1998. The physical, chemical and functional properties of lipids in the skin and other biological barriers. *Chem. Phys. Lipids* 91, 85-96.
- White, S.H., Mirejovsky, D., King, G.I., 1988. Structure of lamellar lipid domains and corneocyte envelopes of murine stratum corneum. An X-ray diffraction study. *Biochemistry* 27, 3725-3732.
- Williams, A.C., Barry, B.W., 2004. Penetration enhancers. *Adv. Drug Deliver. Rev.* 56, 603-618.
- Williams, M.L., Elias, P.M., 1987. The extracellular matrix of stratum corneum: role of lipids in normal and pathological function. *Crit. Rev. Ther. Drug Carrier Syst.* 3, 95-122.
- Zbytovska, J., Vavrova, K., Kiselev, M.A., Lessieur, P., Wartewig, S., Neubert, R.H.H., 2009. The effects of transdermal permeation enhancers on thermotropic phase behaviour of a stratum corneum lipid model. *Colloids Surf., A* 351, 30-37.

8 Summary and perspectives

The molecular organization of the SC intercellular lipid matrix and its barrier function are still vigorously discussed. There are several theoretical models of the SC lipid matrix organization, however, none of them fully explains all structural aspects of the human SC lipid organization. A better understanding of the interactions between different classes of SC lipids is of great importance for the elucidation of the influence of the SC lipid matrix components on the SC barrier function. In the first studies on the SC organization and function, native SC lipids isolated from the mammalian skin and/or lipid model membranes created from the extracted SC lipids were used [1-9]. However, the complexity of such systems limits the possibility to relate differences in the SC lipid composition to changes in the SC molecular organization and function. Therefore, well-defined artificial SC lipid model membranes were used within the framework of this thesis. The SC lipid model membranes composed of synthetic SC lipids offer many advantages over the native ones. One can avoid problems like the limited availability and high inter- and intra-individual variability of native SC membranes [10]. The most important advantage of such systems seems to be that their composition can be systematically modified. It offers a lot of possibilities to investigate and elucidate the role of each individual lipid species in the SC intercellular nanostructure of the lipid matrix and the SC barrier function on a previously unavailable level. This new approach allows also to study the impact of the penetration enhancer on the SC lipid organization on a molecular level, and hence to relate the alterations in the SC intercellular lipid organization to the change in the SC barrier function. Based on such studies, one can extrapolate the results obtained in the *in vitro* experiments to the *in vivo* situation. The main objective of this thesis was to get a better insight into the SC intercellular lipid matrix composition/organization–barrier function relationship based on the investigations of simple, artificial SC lipid model membranes composed i.a. of Cer [AP] and Cer [EOS].

Firstly, a preparation method of synthetic SC lipid model membranes on a porous substrate was developed (Chapter 5). The successful conduct of this step was of major importance for the subsequent diffusion and permeation studies of model drugs. In order to investigate the barrier properties of SC lipid model systems, the lipid mixture has to be deposited in a standardized way on the substrate that does not affect the rate of diffusion/permeation of model drugs (i.e. does not show any barrier properties). The Nuclepore polycarbonate membrane filters turned out to be a perfect solution. In the

second step, the SC lipid model membranes prepared on the polycarbonate filters were characterized by means of various analytical techniques like SAXD, HPTLC, ESEM, confocal Raman imaging and ATR-FTIR spectroscopy. It was confirmed that the SC lipid model membranes (Cer [AP]/Chol/PA/ChS in the m/m ratio of 55/25/15/5, and Cer [AP]/Cer [EOS]/Chol/PA in the m/m ratio of 10/23/33/33) prepared using the preparation method described were reproducible and of good quality. The microscopic techniques, polarization microscopy and ESEM, confirmed that the lipids deposited on the polycarbonate filter formed a continuous lipid layer covering the whole sprayed area of the filter. The results of the HPTLC and confocal Raman imaging studies showed that the individual lipid species were distributed uniformly on the filter. The SAXD confirmed that the lipids within the SC lipid model systems formed the lamellar structure with two present lamellar phases, however, the LPP was not observed. The probable reason of the absence of the LPP was the simplicity of the lipid model membranes used in this project, which were composed of only four individual lipid species and/or the absence or too low concentration of Cer [EOS]. The diffusion experiments of a small hydrophilic compound, urea, revealed that the SC lipid model membrane composed of Cer [AP], Chol, PA and ChS showed very strong barrier properties, even stronger than the isolated human SC. This effect was explained by the very simplistic composition of the lipid model membrane, when compared to a very complex structure of the native SC. This result created also the question concerning the importance of the LPP for the proper barrier function. It was concluded that the proposed approach with simple lipid model systems can be applied in order to study the SC intercellular lipid matrix composition/organization–barrier function relationship.

To gain insights into the relation between the composition/organization of the SC lipid model membranes and their barrier function, diffusion and permeation studies of model drugs across the artificial and native SC membranes were performed (Chapter 6). In these studies, three model drugs covering a broad range of lipophilicities (urea, caffeine and diclofenac sodium) were used to acquire information on both the influence of physicochemical properties of drugs on their diffusion and permeation across SC lipid model membranes and the impact of the components of these systems (particularly the different ceramide species) on their barrier function. The results of these studies showed that the fastest diffusion through both SC lipid model membranes and the human SC occurred in the case of the most hydrophilic model drug, urea. This outcome was attributed to the smallest molecular weight of urea (in comparison to the other model drugs), as well as its permeation enhancing potential for the hydrophilic pathway (hence

the acceleration of the process of diffusion). On the other hand, the most lipophilic drug (diclofenac sodium) permeated faster across lipophilic SC model membranes than caffeine, which was confirmed by larger values of D and k_p in the case of diclofenac sodium. The differences in the permeation rates of caffeine and diclofenac sodium can be explained by their distinct partitioning properties. Furthermore, it was demonstrated that the composition of SC lipid membranes had a significant impact on their barrier properties. With regard to the barrier function, the SC lipid model membrane containing Cer [AP] and Cer [EOS] was much more similar to the human SC than the SC lipid model membrane containing only Cer [AP]. In the presence of Cer [EOS], the lipids within the SC model systems were not arranged so tight as it is in the case of the SC lipid model membrane consisting of Cer [AP], Chol, PA and ChS. It resulted in the faster diffusion and permeation of model drugs across the membrane with Cer [AP] and Cer [EOS].

The final objective of this thesis was the investigation of the impact of the penetration enhancer on the barrier properties of the SC lipid model membranes (Chapter 7). It was demonstrated that the addition of OA to the SC lipid model membranes did not influence the relation between the diffusion and permeation behavior of model drugs presented previously for SC lipid model membranes devoid of the penetration enhancer. The fastest rate of diffusion through both SC lipid model membranes occurred in the case of urea. In the case of permeation studies of caffeine and diclofenac sodium across both SC lipid model systems, the D , k_p and T_L values were either equal or slightly higher in favor of the most lipophilic drug, diclofenac sodium. In this study, the influence of the lipophilic penetration enhancer (OA) on the barrier function of SC lipid model membranes was also examined. It was found that OA caused the impairment of the barrier function of the SC lipid model membrane containing Cer [AP], however, surprisingly improved the barrier properties of the SC lipid model membrane with Cer [AP] and Cer [EOS]. It was concluded that OA within the SC lipid model membrane containing Cer [AP] and Cer [EOS] improved the lamellar ordering of SC lipids. The reason for that is most likely the presence of the *cis* double bond in OA molecule, which can more easily fit to the lipid bilayer where two other *cis* double bonds coming from Cer [EOS] are present. In result, the chain disorder of lipids within bilayers of this SC lipid model membrane was reduced, hence the barrier function of the SC lipid model membrane with Cer [AP] and Cer [EOS], in the presence of OA, was enhanced.

In summary, the results presented in this thesis show that well-defined synthetic SC lipid model membranes can be used successfully in studies on the impact of individual SC lipid components on the SC barrier function. Within the framework of this thesis, the

roles of short-chain Cer [AP] and long-chain acylceramide, Cer [EOS], in the SC organization and barrier function were investigated. As mentioned previously, one of the main advantages of the simplistic SC lipid model membranes described is the possibility to modify their composition systematically. In future studies, one can use the SC lipid model systems that differ from each other in the ratio of the SC lipid constituents and/or in their composition. From such studies, one can gain further insights into the importance of each lipid subclass in the proper membrane organization and barrier function. Furthermore, other model drugs, with different molecular weights and lipophilicities, can be used in future diffusion and permeation studies in order to confirm the results obtained in this work describing the impact of the physicochemical properties of model drugs on their diffusion/permeation behavior. Finally, the SC lipid model membranes proved to be a perfect system to investigate the mode of action of penetration enhancers at the molecular level. Therefore, the influence of other penetration enhancers on the SC intercellular lipid matrix organization and its barrier properties can be examined in future studies.

References

- [1] S.H. White, D. Mirejovsky, G.I. King, Structure of lamellar lipid domains and corneocyte envelopes of murine stratum corneum. An X-ray diffraction study, *Biochemistry* 27 (1988) 3725-3732.
- [2] B. Ongpipattanakul, M.L. Francoeur, R.O. Potts, Polymorphism in stratum corneum lipids, *Biochim. Biophys. Acta, Biomembranes*. 1190 (1994) 115-122.
- [3] T.J. McIntosh, M.E. Stewart, D.T. Downing, X-ray diffraction analysis of isolated skin lipids: reconstitution of intercellular lipid domains, *Biochemistry* 35 (1996) 3649-3653.
- [4] J.A. Bouwstra, G.S. Gooris, K. Cheng, A. Weerheim, W. Bras, M. Ponec, Phase behavior of isolated skin lipids, *J. Lipid Res.* 37 (1996) 999-1011.
- [5] T.J. McIntosh, Organization of skin stratum corneum extracellular lamellae: diffraction evidence for asymmetric distribution of cholesterol, *Biophys. J.* 85 (2003) 1675-1681.
- [6] J.A. Bouwstra, G.S. Gooris, J.A. van der Spek, W. Bras, Structural investigations of human stratum corneum by small-angle X-ray scattering, *J. Invest. Dermatol.* 97 (1991) 1005-1012.
- [7] J.A. Bouwstra, G.S. Gooris, F.E. Dubbelaar, A.M. Weerheim, A.P. Ijzerman, M. Ponec, Role of ceramide 1 in the molecular organization of the stratum corneum lipids, *J. Lipid Res.* 39 (1998) 186-196.
- [8] S.E. Friberg, D.W. Osborne, Interaction of a Model Epidermal Lipid with a Vegetable Oil Adduct, *J. Disper. Sci. Technol.* 8 (1987) 249-258.
- [9] D. Kuempel, D.C. Swartzendruber, C.A. Squier, P.W. Wertz, In vitro reconstitution of stratum corneum lipid lamellae, *Biochim. Biophys. Acta* 1372 (1998) 135-140.
- [10] J.A. Bouwstra, F.E. Dubbelaar, G.S. Gooris, M. Ponec, The lipid organisation in the skin barrier, *Acta Derm. Venereol. Suppl.* 208 (2000) 23-30.

9 Zusammenfassung und Ausblick

Die molekulare Organisation von der SC interzellulären Lipidmatrix und ihre Barrierefunktion werden lebhaft diskutiert. Es gibt mehrere theoretische Modelle der SC-Lipidmatrixorganisation, aber keines von ihnen erläutert völlig alle strukturellen Aspekte der Organisation von humanem SC. Ein besseres Verständnis von Interaktionen zwischen den verschiedenen Klassen von SC-Lipiden ist von großer Bedeutung für die Aufklärung des Einflusses von SC-Lipidmatrixkomponenten auf die Barrierefunktion des SC. In den ersten Studien über die SC-Organisation und Funktion wurden native, aus der Säugerhaut isolierte SC-Lipide und/oder Lipid-Modellmembranen eingesetzt, die aus den extrahierten SC-Lipiden präpariert wurden [1-9]. Die Komplexität solcher Systeme begrenzt die Möglichkeit, die Unterschiede in der SC-Lipidzusammensetzung auf Veränderungen in der molekularen Organisation und Funktion des SC zu beziehen. Daher wurden definierte künstliche SC-Lipidmodellmembranen im Rahmen der vorliegenden Arbeit verwendet. Die SC-Lipidmodellmembranen aus synthetischen SC-Lipiden bieten viele Vorteile gegenüber den nativen Membranen. Man kann Probleme, wie die begrenzte Verfügbarkeit und hohe inter- und intra-individuelle Variabilität von nativen SC-Membranen vermeiden [10]. Der wichtigste Vorteil solcher Systeme scheint zu sein, dass ihre Zusammensetzung systematisch modifiziert werden kann. Sie bieten viele Möglichkeiten, um die Rolle der einzelnen Lipidspezies hinsichtlich der interzellulären Nanostruktur der Lipidmatrix und der Barrierefunktion des SC auf einer Ebene zu untersuchen und zu erläutern, wie das bisher nicht möglich war. Diese neue Einstellung ermöglicht auch, den Einfluss der Penetrationsmodulatoren auf die SC-Lipidorganisation auf molekularer Ebene zu untersuchen, und damit die Veränderungen der interzellulären Lipidorganisation des SC in Beziehung zu Änderungen der SC-Barrierefunktion zu setzen. Basierend auf solchen Studien kann man die erhaltenen Ergebnisse aus den *in vitro*-Experimente zur *in vivo*-Situation extrapolieren. Das Hauptziel der vorliegenden Arbeit war es, einen besseren Einblick in die Beziehung der interzellulären Lipidmatrixzusammensetzung/Organisation zur Barrierefunktion zu bekommen, basierend auf den Untersuchungen an einfachen, künstlichen SC-Lipidmodellmembranen, die unter anderem Cer [AP] und Cer [EOS] enthielten.

Es wurde erstens ein Herstellungsverfahren von synthetischen SC-Lipidmodellmembranen auf einem porösen Substrat entwickelt (Kapitel 5). Die erfolgreiche Durchführung dieses Schrittes war von großer Bedeutung für die nachfolgenden

Diffusions- und Permeationsstudien von Modellarzneistoffen. Um die Barriereigenschaften der SC-Lipidmodellsysteme zu untersuchen, muss die Lipidmischung auf dem Substrat so standardisiert präpariert werden, dass sie keinen Einfluss auf die Geschwindigkeit der Diffusion/Permeation von Modellarzneistoffen hat (d.h. dass sie keine Barriereigenschaften zeigt). Die Nuclepore-Membranfilter aus Polykarbonat erwiesen sich als perfekte Lösung. Im zweiten Schritt wurden die SC-Lipidmodellmembranen auf den Filtern aus Polykarbonat hergestellt und mittels verschiedenen analytischen Methoden wie SAXD, HPTLC, ESEM, konfokale Raman Imaging und ATR-FTIR-Spektroskopie charakterisiert. Es wurde bestätigt, dass die SC-Lipidmodellmembranen (Cer [AP]/Chol/PA/ChS im m/m Verhältnis von 55/25/15/5, und Cer [AP]/Cer [EOS]/Chol/PA im m/m Verhältnis von 10/23/33/33) unter Verwendung des beschriebenen Herstellungsverfahrens reproduzierbar und von guter Qualität herstellbar waren. Die mikroskopischen Techniken, Polarisationsmikroskopie und ESEM, bestätigten, dass die Lipide eine kontinuierliche Lipidschicht auf der gesamten bearbeiteten Oberfläche des Filters aus Polykarbonat bildeten. Die Ergebnisse der HPTLC und der konfokalen Raman Imaging Studien zeigten, dass die einzelnen Lipidspezies homogen auf dem Filter verteilt wurden. Die SAXD-Studien bestätigten, dass die Lipide in den SC-Lipidmodellsystemen Nanostrukturen mit zwei lamellaren Phasen ausgebildet haben. Eine LPP wurde jedoch nicht beobachtet. Die Gründe für das Fehlen der LPP waren wahrscheinlich die Einfachheit der in diesem Projekt verwendeten Lipidmodellmembranen, die nur aus vier Lipidspezies bestanden und/oder das Fehlen bzw. die zu geringe Konzentration von Cer [EOS]. Die Diffusionsexperimente mit der kleinen hydrophilen Substanz (Harnstoff) ergaben, dass die SC-Lipidmodellmembran, die Cer [AP], Chol, PA und ChS enthielt, sehr starke Barriereigenschaften zeigte, sogar stärkere als das isolierte humane SC. Dieser Effekt wurde durch die sehr vereinfachte Zusammensetzung der Lipid-Modellmembran, verglichen mit der sehr komplexen Struktur des nativen SC, erklärt. Dieses Ergebnis stellte auch die Bedeutung der LPP für die ordnungsgemäße Barrierefunktion des SC in Frage. Es wurde festgestellt, dass die vorgeschlagene Einstellung mit einfachen Lipidmodellsystemen angewendet werden kann, um die Relation der Zusammensetzung der interzellulären Lipidmatrix zur Barrierefunktion des SC zu untersuchen.

Um Einblicke in die Beziehung zwischen der Komposition/Organisation von SC-Lipidmodellmembranen und ihrer Barrierefunktion zu erhalten, wurden Diffusions- und Permeationsstudien von Modellarzneistoffen durch die künstlichen und nativen SC-Membranen durchgeführt (Kapitel 6). In diesen Studien wurden drei Modellarzneistoffe

mit verschiedener Lipophilie (Harnstoff, Koffein und Diclofenac-Natrium) verwendet, um Informationen sowohl über den Einfluss der physikalisch-chemischen Eigenschaften dieser Arzneistoffe auf ihre Diffusion und Permeation durch SC-Lipidmodellmembranen als auch über die Auswirkungen von den Komponenten dieser Lipidmembranen (vor allem den verschiedenen Ceramid-Klassen) auf ihre Barrierefunktion zu erhalten. Die Ergebnisse dieser Studien zeigten, dass die schnellste Diffusion durch beide SC-Lipidmodellmembranen und das humane SC im Fall vom hydrophilsten Modellarzneistoff (Harnstoff) aufgetreten ist. Dieses Ergebnis wurde dem kleinen Molekulargewicht von Harnstoff (im Vergleich zu den anderen Modellarzneistoffen) sowie seinem diffusionsverstärkenden Potential hinsichtlich des hydrophilen Weges (daher die Beschleunigung der Diffusion) zugeschrieben. Der lipophilste Arzneistoff (Diclofenac-Natrium) durchdrang dagegen schneller als Koffein die lipophilen SC-Modellmembranen. Dies wurde durch größere Werte von D und k_p für Diclofenac-Natrium bestätigt. Die Unterschiede in den Permeationsraten von Koffein und Diclofenac-Natrium können durch ihre unterschiedliche Lipophilie erklärt werden. Es wurde weiterhin gezeigt, dass die Zusammensetzung der SC-Lipidmembranen eine signifikante Auswirkung auf die Barriereigenschaften hat. In Bezug auf die Barrierefunktion, war die SC-Lipidmodellmembran mit Cer [AP] und Cer [EOS] dem humanen SC weitaus ähnlicher als die SC-Lipidmodellmembran nur mit Cer [AP]. In Anwesenheit von Cer [EOS] wurden die Lipide der SC-Modellsysteme nicht so eng angeordnet, wie im Falle der SC-Lipidmodellmembran, die Cer [AP], Chol, PA und ChS enthielt. Das führte zur schnelleren Diffusion und Permeation der Modellarzneistoffe durch die Membran mit Cer [AP] und Cer [EOS].

Das abschließende Ziel dieser Arbeit war die Untersuchung des Einflusses von Penetrationsmodulatoren auf die Barriereigenschaften der SC-Lipidmodellmembranen (Kapitel 7). Es wurde gezeigt, dass die Zugabe von Ölsäure (OA) zu den SC-Lipidmodellmembranen keinen Einfluss auf das Diffusions- und Permeationsverhalten der Modellarzneistoffe hatte. Die schnellste Diffusion durch beide SC-Lipidmodellmembranen ist im Fall von Harnstoff aufgetreten. Bei Permeationsstudien von Koffein und Diclofenac-Natrium durch beide SC-Lipidmodellsysteme waren die Werte von D , k_p und T_L entweder gleich oder etwas höher für den lipophilsten Wirkstoff, Diclofenac-Natrium. In dieser Studie wurde der Einfluss des lipophilen Penetrationsmodulators (OA) auf die Barrierefunktion der SC-Lipidmodellmembranen untersucht. Es wurde festgestellt, dass OA eine Reduktion der Barrierefunktion der SC-Lipidmodellmembran mit Cer [AP] verursacht hat, jedoch die Barriereigenschaften der SC-Lipidmodellmembran mit Cer

[AP] und Cer [EOS] überraschend verstärkt hat. Daraus wurde geschlossen, dass OA die lamellare Anordnung der SC-Lipide innerhalb der SC-Lipidmodellmembran mit Cer [AP] und Cer [EOS] verbessert hat. Der Grund dafür ist wahrscheinlich die Anwesenheit der *cis*-Doppelbindung im OA-Molekül, die sich leichter an die Lipiddoppelschicht anpassen kann, wo zwei weitere *cis*-Doppelbindungen von Cer [EOS] vorhanden sind. Deshalb wurde die Kettenstörung von Lipiden in Doppelschichten vom SC-Lipidmodellmembran reduziert. Die Barrierefunktion der SC-Lipidmodellmembran mit Cer [AP] und Cer [EOS] wurde somit in Anwesenheit von OA verstärkt.

Zusammenfassend lässt sich feststellen, dass die in der vorliegenden Arbeit präsentierten definierten synthetischen SC-Lipidmodellmembranen in Studien über die Auswirkungen der einzelnen SC-Lipidkomponenten auf die SC-Barrierefunktion erfolgreich eingesetzt werden können. Im Rahmen dieser Arbeit wurde der Einfluss des kurzkettigen Cer [AP] und des langkettigen Acylceramids, Cer [EOS], auf die Organisation und Barrierefunktion des SC untersucht. Wie bereits erwähnt, ist der wesentliche Vorteil der beschriebenen vereinfachten SC-Lipidmodellmembranen in der Möglichkeit zu sehen, die Zusammensetzung der Membranen systematisch zu modifizieren. Man kann in künftigen Studien die SC-Lipidmodellsysteme nutzen, um sowohl das Verhältnis der SC-Lipidbestandteile als auch ihre Zusammensetzung zu variieren. Aus solchen Studien können weitere Einblicke in die Bedeutung der einzelnen Lipidklassen für die Membranorganisation und Barrierefunktion des SC gewonnen werden. Weiterhin können andere Modellarzneistoffe mit unterschiedlichen Molekulargewichten und unterschiedlicher Lipophilie in künftigen Diffusions- und Permeationsstudien eingesetzt werden, um die Ergebnisse dieser Arbeit hinsichtlich des Einflusses der physikalisch-chemischen Eigenschaften der Modellarzneistoffe auf ihr Diffusions-/Permeationsverhalten zu bestätigen. Folglich scheinen die SC-Lipidmodellmembranen ein perfektes System zu sein, um den Wirkungsmechanismus von Penetrationsmodulatoren auf molekularer Ebene zu untersuchen. Daher kann in künftigen Studien der Einfluss weiterer Penetrationsmodulatoren auf die interzelluläre Lipidmatrixorganisation und die Barriereigenschaften des SC untersucht werden.

Literaturverzeichnis

- [1] S.H. White, D. Mirejovsky, G.I. King, Structure of lamellar lipid domains and corneocyte envelopes of murine stratum corneum. An X-ray diffraction study, *Biochemistry* 27 (1988) 3725-3732.
- [2] B. Ongpipattanakul, M.L. Francoeur, R.O. Potts, Polymorphism in stratum corneum lipids, *Biochim. Biophys. Acta, Biomembranes*. 1190 (1994) 115-122.

-
- [3] T.J. McIntosh, M.E. Stewart, D.T. Downing, X-ray diffraction analysis of isolated skin lipids: reconstitution of intercellular lipid domains, *Biochemistry* 35 (1996) 3649-3653.
- [4] J.A. Bouwstra, G.S. Gooris, K. Cheng, A. Weerheim, W. Bras, M. Ponec, Phase behavior of isolated skin lipids, *J. Lipid Res.* 37 (1996) 999-1011.
- [5] T.J. McIntosh, Organization of skin stratum corneum extracellular lamellae: diffraction evidence for asymmetric distribution of cholesterol, *Biophys. J.* 85 (2003) 1675-1681.
- [6] J.A. Bouwstra, G.S. Gooris, J.A. van der Spek, W. Bras, Structural investigations of human stratum corneum by small-angle X-ray scattering, *J. Invest. Dermatol.* 97 (1991) 1005-1012.
- [7] J.A. Bouwstra, G.S. Gooris, F.E. Dubbelaar, A.M. Weerheim, A.P. Ijzerman, M. Ponec, Role of ceramide 1 in the molecular organization of the stratum corneum lipids, *J. Lipid Res.* 39 (1998) 186-196.
- [8] S.E. Friberg, D.W. Osborne, Interaction of a Model Epidermal Lipid with a Vegetable Oil Adduct, *J. Disper. Sci. Technol.* 8 (1987) 249-258.
- [9] D. Kuempel, D.C. Swartzendruber, C.A. Squier, P.W. Wertz, In vitro reconstitution of stratum corneum lipid lamellae, *Biochim. Biophys. Acta* 1372 (1998) 135-140.
- [10] J.A. Bouwstra, F.E. Dubbelaar, G.S. Gooris, M. Ponec, The lipid organisation in the skin barrier, *Acta Derm. Venereol. Suppl.* 208 (2000) 23-30.

List of Publications

Research articles

- ◆ M. Ochalek, S. Heissler, J. Wohlrab, R.H.H Neubert, Characterization of lipid model membranes designed for studying impact of ceramide species on drug diffusion and penetration, *Eur. J. Pharm. Biopharm.* 81 (2012) 113–120.
- ◆ M. Ochalek, H. Podhaisky, H.-H. Ruettinger, J. Wohlrab, R.H.H. Neubert, SC lipid model membranes designed for studying impact of ceramide species on drug diffusion and permeation, Part II: Diffusion and permeation of model drugs, *Eur. J. Pharm. Biopharm.* (2012) doi: 10.1016/j.ejpb.2012.06.008.
- ◆ M. Ochalek, H. Podhaisky, H.-H. Ruettinger, R.H.H. Neubert, J. Wohlrab, SC lipid model membranes designed for studying impact of ceramide species on drug diffusion and permeation, Part III: Influence of penetration enhancer on diffusion and permeation of model drugs, *Int. J. Pharm.* (2012) doi: 10.1016/j.ijpharm.2012.06.044.

Poster presentations

- ◆ M. Ochalek, Z.J. Kokot, R.H.H. Neubert,
Influence of ceramide [AP] on the structure of lipid model membranes mimicking the stratum corneum, *5th Polish-German Symposium*, Poznan, Poland, 2009
- ◆ M. Ochalek, R.H.H. Neubert,
Diffusion of urea through the artificial and native membranes, *7th World Meeting on Pharmaceutics, Biopharmaceutics and Pharmaceutical Technology*, La Valetta, Malta, 2010

- ◆ M. Ochalek, R.H.H. Neubert,
Diffusion of model drugs through artificial and native stratum corneum membranes,
6th Polish-German Symposium, Duesseldorf, Germany, 2011

- ◆ M. Ochalek, S. Heissler, J. Wohlrab, R.H.H. Neubert,
Characterization of artificial lipid model membranes mimicking human stratum
corneum intercellular lipid matrix, *12th Gordon Research Conference on Barrier
Function of Mammalian Skin*, Waterville Valley, NH, USA, 2011

Acknowledgements

I would like to thank all people who contributed to this thesis, in particular my advisor Prof. Dr. rer. nat. habil. Dr. h.c. Reinhard Neubert for the possibility to conduct my PhD study in his working group at the Martin Luther University Halle-Wittenberg and for providing a very interesting subject of my PhD thesis. Without his willingness to help, guidance and patience, this work could not have been completed.

I would like to express my deepest gratitude to Prof. Dr. Johannes Wohlrab for providing human skin samples, as well as careful reading of my manuscripts.

I am truly indebted and thankful to Prof. Dr. Hans-Hermann Ruettinger and Stefan Heissler (Institute of Functional Interfaces, Karlsruhe Institute of Technology, Eggenstein-Leopoldshafen, Germany) for the help and assistance with the capillary electrophoresis and confocal Raman imaging measurements, respectively.

I would like to show my gratitude to Dr. Helmut Podhaisky for his help in the development of the diffusion mathematical model and fruitful discussions on this subject.

I am obliged to Dr. Annett Schroeter and Dr. Yahya Mrestani for their support and openness to discussions throughout my PhD study.

I am also grateful to Manuela Woigk and Heike Rudolf for a technical assistance with the HPLC and ATR-FTIR spectroscopy experiments, respectively, and to Dieter Reese for a construction of the ATR-FTIR diffusion cell.

Many thanks to all colleagues from the “Biopharmacy” group for providing a friendly working atmosphere and their support during my stay in Halle.

Finally, I would like to thank my family, especially my parents and my sisters, as well as my friends. Their support, encouragement and trust gave me strength and motivation to get this work done.

Curriculum vitae

Personal details

Name: Michal Ochalek
Born: 05.03.1984 in Szamocin, Poland
Nationality: Polish

Education

1998–2002 Maria Sklodowska-Curie High School, Pila, Poland
29.05.2002 A-levels at Maria Sklodowska-Curie High School, Pila, Poland
2002–2003 Dentistry studies at the Poznan University of Medical Sciences, Poznan, Poland
2003–2008 Pharmacy studies at the Poznan University of Medical Sciences, Poznan, Poland
03/2008–08/2008 Conduct of the experimental part of the Master thesis in the group of Prof. Dr. Dr. h.c. R.H.H. Neubert, Martin Luther University Halle-Wittenberg, Halle, Germany
15.09.2008 Defense of the Master thesis: "Synthesis of N-(α -hydroxy-behenoyl)phytosphingosine, its stereochemical separation and investigation by using ATR-FTIR spectroscopy and small angle X-ray diffraction" at the Poznan University of Medical Sciences, Poznan, Poland, Degree: MSc. Pharm.
10/2008–04/2009 Practical training at the "Herbia" Pharmacy, Poznan, Poland
12.05.2009 Approbation as a pharmacist, Poznan University of Medical Sciences, Poznan, Poland

Professional experience

04/2009–07/2012 PhD student in the group of Prof. Dr. Dr. h.c. R.H.H. Neubert, Department of Pharmaceutical Technology and Biopharmacy, Institute of Pharmacy, Martin Luther University Halle-Wittenberg, Halle, Germany

Eidesstattliche Erklärung

Hiermit erkläre ich gemäß § 5 Absatz 2b der Promotionsordnung der Naturwissenschaftlichen Fakultät I (Biowissenschaften) der Martin-Luther-Universität Halle-Wittenberg, dass ich die Ergebnisse der vorliegenden Dissertationsarbeit

**Barrier properties of stratum corneum lipid model membranes
based on ceramide [AP] and [EOS]**

am Institut für Pharmazeutische Technologie und Biopharmazie der Martin-Luther-Universität Halle-Wittenberg selbständig und ohne fremde Hilfe erarbeitet und verfasst habe. Ferner habe ich nur die in der Dissertation angegebenen Literaturstellen und Hilfsmittel verwendet und die entnommenen und benutzten Literaturstellen auch als solche kenntlich gemacht. Weiterhin habe ich die vorliegende Arbeit bisher keiner anderen Prüfungsbehörde vorgelegt.

Halle (Saale), im Juni 2012

Michal Ochalek